TAMPEREEN TEKNILLINEN YLIOPISTO
TAMPERE UNIVERSITY OF TECHNOLOGY

NIKO KORHONEN

TENSILE CAPACITY OF THE GROOVED STEEL PIPE PILE

Master`s thesis

Examiner: Professor Tim Länsivaara

The examiner and topic of thesis is approved on 31 October 2017

ABSTRACT

NIKO KORHONEN: Tensile capacity of the grooved steel pipe pile
Tampere University of Technology
Master of Science Thesis, 92 pages, 16 Appendix pages
October 2017
Master's Degree Programme in Civil Engineering
Major: Municipal Engineering
Examiner: Professor Tim Länsivaara

Keywords: tensile force, steel pipe pile, tension pile, tensile capacity, bond strength

Anchors are often used to resist tensile forces on tall and narrow structures where steel pipe piles are used to restrain compressive force. It has been studied that by grooving the steel pipe pile and by drilling and grouting the pile to the bedrock it could also resist tensile forces. The grooved tensile pipe pile could thus replace the anchors and increase the cost-effectiveness of the design.

This master`s thesis was funded by SSAB and is based on the previous research "The tensile capacity of steel pipe piles drilled into the bedrock" published in 2015. In this research grooved steel pipe piles drilled and grouted into the bedrock to resist tensile forces are studied by literature review and field test. The main focus was to develop the design of grooved tensile steel pipe pile, implement theory on the field test and compare the results to previous studies. This research can be divided in two parts. In the first part instructions and theory concerning tensile piles are studied by literature review. In the second part grooved tensile steel pipe pile design are tested by the field test.

From the literature review it was found that the material properties, size of the annulus, size of the reamer, friction and mechanical interlocking affects to the bond strength and design of the grooved tensile pipe pile. With the aid of the literature review and previous research the design was modified by increasing the wall thickness of the pile and by selecting oversized reamer for some of the piles. Otherwise similar grooved tensile pipe pile design was used in the loading test as in previous studies.

In this research the piles were tested from the ground level in construction like situation. The achieved bond strength stayed between 0.24 to 0.88 MPa. The highest tensile capacity was 3068 kN. Failure was assumed to happen on steel to grout surface. The highest values were obtained on piles with wider annulus between rock and pile surface. It is assumed that this enabled a better flushing and grouting resulting in higher capacity. Therefore base on the tested piles, the RDs 220/12.5 pile with grooves and 273 mm ring bit is recommended to be used as tensile pile.

Results were finally compared to the present instructions and previous studies. It was found that capacity of the grooved tensile pipe pile was over five times higher than it is allowed to use for the design according to present instructions.

TIIVISTELMÄ

NIKO KORHONEN: Uritetun paalun vetokapasiteetti
Tampereen teknillinen yliopisto
Diplomityö, 92 sivua, 16 liitesivua
Lokakuu 2017
Rakennustekniikan diplomi-insinöörin tutkinto-ohjelma
Pääaine: Infrarakenteet
Tarkastaja: professori Tim Länsivaara

Avainsanat: vetopaalu, putkipaalu, vetokapasiteetti, tartuntalujuus

Ankkureita on usein käytetty kapeissa ja korkeissa rakennuksissa vastustamaan perustuksiin kohdistuvia vetovoimia. Näissä rakennuksissa käytetään myös teräsputkipaaluja vastustamaan puristusvoimia. On tutkittu, että uritetulla teräsputkipaalulla voitaisiin ottaa vastaan vetovoimia, jolloin teräsputkipaalut voisivat korvata ankkurit ja perustusrakenteesta saataisiin kustannustehokkaampi ratkaisu.

Tämä diplomityö on SSAB:n toimeksianto ja jatkotutkimus vuonna 2015 tehdylle diplomityölle “Kallioon porattujen teräsputkipaalujen vetokapasiteetti”. Tässä diplomityössä tutkitaan uritetun putkipaalun vetokapasiteettia kirjallisuus- ja kenttätutkimuksella. Tutkimuksen tavoitteena oli kehittää ja testata SSAB:n uritettua vetopaalumallia kenttätutkimuksella, sekä vertailla tuloksia edellisiin tutkimuksiin ja nykyiseen ohjeistukseen. Tutkimus voidaan jakaa kahteen osaan. Ensimmäisessä osassa vetopaaluihin liittyvää ohjeistusta ja teoriaa käsitellään kirjallisuuskatsauksella. Toisessa osassa uritettua vetopaalua testataan kenttätutkimuksella.

Kirjallisuustutkimuksessa havaittiin materiaaliominaisuuksien, kalliorakovälin ja avartimen koon ja kitkan, sekä pintojen välisen mekaanisen sidoksen vaikuttavan tartuntalujuuteen. Kirjallisuuskatsauksen ja edellisen tutkimuksen pohjalta uritettua vetopaalumallia muutettiin edelliseen tutkimukseen nähden lisäämällä paalujen seinämävahvuutta ja käyttämällä ylikoon avarrinta osalla paaluista.

Vetokokeessa paalut koestettiin suoraan maakerroksen päältä työmaaolosuhteissa. Tutkimuksessa saavutetut tartuntalujuudet olivat 0,24 ja 0,88 MPa väliltä. Suurin saavutettu vetokapasiteetti oli 3068 kN. Murto pääteltiin tapahtuvan paalun ja laastin tartuntapinnalta. Tuloksiin perustuen paalun huuhtelu ja injektointi prosessi oletettiin onnistuvan parhaiten ylikoon avartimella, jonka vuoksi tällä paalumallilla saatiin myös parhaat tulokset. Tämän tutkimuksen testatuista paaluista RDs220/12.5 paalu 273 mm avartimella on suositeltu vetopaalumalli.

Tutkimuksen tuloksia verrattiin lopuksi tämän hetken vetopaaluohjeistukseen. Tutkimuksen pohjalta tasaisiin paaluihin perustuvassa nykyisessä Liikenneviraston ohjeet rajoittavat uritetun putkipaalun vetokapasiteetin käyttöä. Tässä tutkimuksessa saavutettiin yli viisi kertaa suurempi kapasiteetti kuin Liikenneviraston ohjeistuksessa on sallittua käyttää vetopaalumitoituksessa.

FOREWORD

This thesis was delivered by the designer and consultant company Pöyry to order from SSAB. I would like to thank the whole SSAB Company for the order and for opportunity to work on such interesting subject.

Special thanks to the head organizers for this research Antti Perälä from SSAB and Jouko Lehtonen from Pöyry for support and opportunity to study as interesting subject as steel pipe piles. I personally learned much from the study and I hope it will bring forth the research and design of the tensile steel pipe pile.

Niko Korhonen

Tampere, 31.10.2017

TABLE OF CONTENTS

LIST OF FIGURES

LIST OF TABLES

LIST OF SYMBOLS AND ABBREVIATIONS

SSAB	Swedish steel pipe pile manufacturer
NCCI 7	Instruction for the geotechnical design of bridges by the Eurocode 7
w/c	Water to cement ratio
DTH	Down the hole hammer drilling method
GL	Geotechnical class
CC	Consequence class
PTL	Piling work class
A_s	Cross-section area of the steel [mm^2]
$A_{s;j}$	Area of the pile sheath [m^2]
c_u	Closed shear strength of the soil [kPa]
D	Depth of the drill hole in the bedrock [m]
d	Diameter of the drill hole [m]
E	Elastic modulus of the material [MPa]
E_a	Elastic modulus of the steel [MPa]
E_a	Elastic modulus of the grout [MPa]
f_{ctk}	Characteristic tensile strength [MPa]
$F_{t;d}$	Design load for tension
f_y	Yield strength of the steel material [N/mm^2]
k_b	Coefficient of adhesion on the pile surface
L	Original length of the steel
ΔL	Change in length of the steel [m],
L_{min}	Minimum drilling depth [m].
L_{cr}	Critical drilling depth
N_{Rd}	Tensile capacity [N]
$q_{s;j;k}$	Pile sheath friction resistance [kPa]
$R_{s;k}$	Geotechnical resistance of the pile sheath [kN]
$R_{t;k}$	Characteristic tensile resistance [kN]
$q_{b;k}$	Geotechnical end resistance of the pile [MPa]
σ_{cyl}	Compressive strength of the bedrock [MPa]
$\tau_{s;k}$	Characteristic bond strength between concrete or grout and the bedrock [MPa]
$\sigma`$	Effective axial stress on the pile surface
α	Adhesion factor
$\gamma_{s;t}$	Partial factor of tensile resistance [MPa]
γ	Unit weight of the rock [kN/m^3]
Φ	Angle of the rock cone [°]
γ_{M0}	Material factor of safety
ε	Strain of the steel

1. INTRODUCTION

1.1 The background of the study

This research is an assignment from the Swedish steel manufacturer SSAB to study drilled steel pipe pile under tensile force and to develop its tensile capacity. This study is follow-up research for the Sirèn`s (2015) Master`s thesis "The tensile capacity of steel pipe piles drilled into the bedrock". In the previous research was found that the grooved surface improves tensile capacity of the steel pipe pile. In experimental field test they could not load all piles to the failure, thus real tensile capacity of the piles could not be determined. The research left some questions and therefore needed to be continued.

In this research tensile capacity of the grooved pipe pile is investigated and compared to previous studies. In previous studies by Sirèn (2015) and Ahomies (2014), tensile capacity of the steel pipe piles was studied by literature review and the field test. In the study of Ahomies piles were installed trough soil layer but the overburden soil layer was excavated before testing. In the study by Sirèn piles were installed and tested on an exposed bedrock surface. In this study the field test is done above the soil layer and drilled through the soil layer into the bedrock to adapt real construction like site conditions. Thus, the effect of the soil layer to tensile capacity is also investigated.

1.2 Objectives and limitations

The research method for the study a literature review and an experimental field-test. The focus is to investigate problems encountered in the previous researches and investigate factors affecting the pile bond capacity. Challenge and focus for the research is to study which attributes affect the tensile capacity and how the overburden soil layer affects the system. Therefore, the objective is to get reliable information of the tensile capacity of the grooved pipe pile which is drilled through soil layer and grouted into the bedrock and compare it to theory.

Schedule related goals are to finish the literature review during spring 2017 and execute the field test in summer of 2017. Hopefully there is something interesting to show for the SSAB steel pipe pile day in 2018 in designer and contractor point of view.

Proper testing method is designed for testing tensile capacity of the grooved steel pipe pile. This research does not include structural design of the test structure. Research focuses only piles with diameter under 300 mm, which are also called as micropiles.

1.3 Lay-out of the report

Thesis consists of six main chapters, which can be united into two coherent whole, the theory and the experimental part of the research. Theory consists of the general information behind the pile design, design of the tensile piles, its guidelines and instructions according to Eurocode and the review of the previous studies. The experimental part includes the field test and results of the test. Finally, the conclusion is made and further actions for the research are presented.

The first chapter of the research is introduction chapter where the research and its methods, objectives and limitations are presented. In the second chapter, the general information of the RD and RDs pile design and installation processes are presented. The chapters mainly focus on SSAB`s RD pile design and its elements, drilling methods and installation through a soil layer into the bedrock.

The third chapter of the research presents the tension pile design according to EN design standards. Also other factors that affect the tensile capacity are presented. The fourth chapter consists of literature review where factors affecting tensile capacity are studied. These factors and their effects to the grooved pile design are discussed.

The fifth chapter of the research is the experimental part of the study. In this chapter the experimental part of the research is presented. The results of the test is presented and discussed in the sixth chapter. Conclusions of the research are made and further actions are presented if necessary. Summary of the research is presented in the seventh chapter of the research.

2. STEEL PIPE PILE AS TENSION PILE

2.1 Introduction

According to Tomlinson *et al.* (2008, p. 305) vertical tension piles are used in where piles need to restrain uplifting forces caused by structure over the pile or conditions around the pile. In example if building, bridge, chimney, ship docking station or gas pipeline is vulnerable to strong winds or any other horizontal forces it may cause uplifting force to the pile. Sometimes ground conditions can cause the uplifting force. Swelling of the soil layer can also be the cause of uplifting force in certain countries.

The simplest way to resist uplift forces is to drive a pile long enough to take load of forces in shaft friction. In cases where the soil is cohesive or the soil layer is shallow enough and it is economical to reach the bedrock, the pile can be anchored to the rock. If the soil layer is very deep, uplift forces may be restrained by adding dead weight to the pile to overcome the load. Usually it is not recommended and economical to add dead weight to overcome the uplift forces. The weight also acts as a compressive load to the structure and can cause settlements to the surrounding soil. Additional uplift resistance can be achieved by extending the base of the pile. (Tomlinson 2008, p.308)

According to Tomlinson *et al.* (2008, p. 308) anchors which are grouted into the bedrock in the form of bars, tubes, or cables are the most economical choice to provide required uplift force. In Finland, these methods are also widely used. Ahomies (2014) suggested if the pile can restrain tensile forces in certain situations it may be cheaper than taking tensile forces by anchor. This is due to extra work phase in anchor installation. Therefore this study focuses on taking the tensile force with grooved steel pipe pile as an option for anchoring.

The base procedure of installing the pile to the bedrock through a soil layer and using it as a tension pile is by drilling a hole for the pile, placing the pile into the hole and grouting the annulus between pile and bedrock to create a bond which can endure the tension force. These procedures which can be seen in Figure 1 must be studied through in order to understand the base mechanism of using the drilled and grouted steel pipe pile as a tension pile.

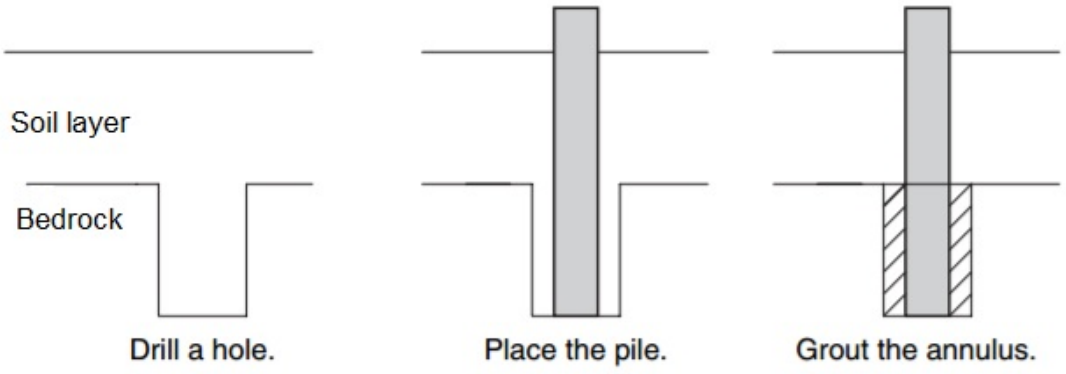

Figure 1. *Drilling and grouting the pile into the bedrock (Rajapakse 2005)*

As the two previous studies by Ahomies (2014) and Siren (2015) this research focuses on steel manufacturer SSAB`s RD piles which are drilled through the soil into the bedrock and grouted. RD piles are drilled pipe piles from global steel manufacturer SSAB. In this research the installation of the pile and pile design is studied to develop more versatile solution for foundation to resist tensile forces.

2.2 The RD steel pipe pile

The basic structure of the RD pile can be seen in Figure 2. The pile consists of a pipe pile elements which connect each other with splices. The splices can be either external threaded sleeves or elements can be welded together. The structure also includes bearing plate, casing shoe and the ring bit. The whole pile structure is CE0 certified. When the piles are delivered, the customer receives a material quality certificate to ensure the quality of the batch. (SSAB 2016, pp. 4–10)

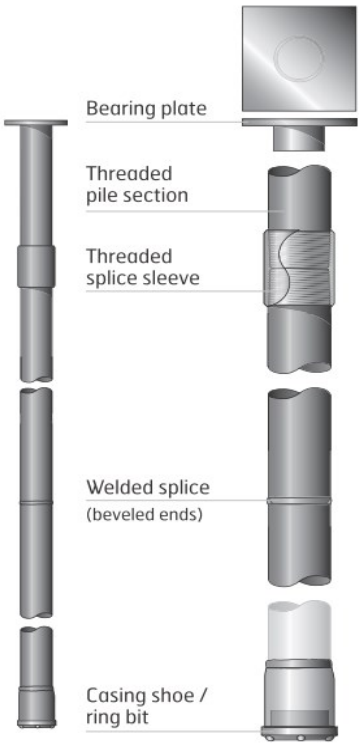

Figure 2. *RD Steel pipe pile (SSAB 2016, p.9)*

The design follows the European standards SFS-EN 14199 and SFS-EN 1536 and can be divided to the following classes by its size. Drilled micro pile is considered to have diameter of 30 to 300 mm and bore pile is considered to have diameter over 300 mm. This study focuses on the micropiles.

SSAB has two brands for their drilled steel pipe piles, RD and RDs. The RD pile is made from the steel S440J2H and the RDs pile is made from the high yielding steel grade S550J2H. (SSAB 2016, p. 9) According to standards steel is considered high-strength steel when its yield strength class is over 500 MPa (SFS-EN 14199).

One of the most important parts of the pile is a ring bit at the end of the pile. The ring bit is a combination of a casing shoe and a reamer. The casing shoe is meant to transfer the forces between the pile and the bedrock. It also widens the tip of the pile so that it prevents pile from entering to the soil by sharing the pressure to the wider surface. The

second part of the ring bit is the reamer. While drilling reamer rotates and widens the drill hole thus it has lower friction on the surface while installing the pile. The reamer is also used to make wide annulus between the soil or bedrock and the pile which will be grouted afterwards. Grouting attaches the pile to bedrock so that it can resist tensile forces.

Ring bits can also be either solitary ring bits or fixed ring bits. The difference of these is that the reamer is either fixed to the casing shoe and therefore to the pile or totally separate. The casing shoe is welded to the pile. In the study by Ahomies (2014) different ring bits was tested. In the study the breakage of the joint between the pile and the grout was brittle with the solitary ring bits and tougher with the fixed ring bit. Thus the ring bit should be integrated to the pile when it is meant to resist tensile forces.

Drilled RD piles are extended with the welded splice or the threaded splice sleeve. According to manufacturer the sleeves meet the requirements from the Finnish piling instruction PO-2011 and Eurocode SFS-EN 1993-5 National Annex. A tensile strength for the splice is at least 50% of the compressive strength of the pile when the installation is done per SSAB design and installation manual (SSAB 2016). If the pile is continued by welding the properties of the pile remain the same if the welding is done according to instructions. The requirements for welding are presented in SFS-EN ISO 5817 and SFS-EN ISO 3834-4. Usually when the weld is carefully done by the professional and the mechanical properties of the weld is right for the steel used, the quality of the weld is accounted as good enough. Also NDT test can be made to ensure quality of the weld.

2.3 The RD pile installation

2.3.1 Drilling methods

The pile installation is done by the drilling through the soil layer into the bedrock or other hard layer under the soil. For the installation, proper equipment is needed to drill the pile through the soil. The general requirements are presented in the Finnish piling instructions (RIL 254-2016) and the main idea is the following.

The drilling rig which is used for the drilling should have the proper properties that it can be used at construction site safely and reliably. The drilling equipment is based on either a top hammer or a down-the-hole (DTH) hammer based equipment. With both methods either concentric or eccentric drilling method can be used. The flushing can be done with air, water or other drilling fluid. The drill cutting is flushed through drilling bit and through the pile up to the surface. A part of the drill cutting mixes with the surrounding soil and part of the cutting gets flushed along the outer surface. (RIL 254-2016, pp. 210–211) The drilling method and the system are presented in Figure 3.

On top hammer based equipment the stroke is focused on the top of the drill rod which is also drilled at the same time. Thus energy from the blow is directed to the casing shoe at the end of the pile by the drilling rod. Energy from the stroke diminishes along the drilling rod and therefore is less when number of joints and the length of the rod increases. The greatest installation length with this method is around 30–50m depending on the soil layer. The length is deeper with the soft cohesive soil layers. Top hammer based drilling equipment is usually hydraulic or pneumatic. The rods and the hydraulic rotary are included in the equipment. With the pneumatic hammer the number of strokes per minute can be around 1600–3400 and with the hydraulic hammer 2000–4000. This drilling method is suitable for the pile size diameter under 200 mm. (RIL 254-2016, p. 210)

DTH based equipment differs mainly only one way from the top hammer method. Energy from blow of the hammer is directed to casing shoe at the end of the pile. The drilling rod is attached to the DTH hammer with the guide sleeve which is attached to the drilling bit by the shank adapter. The blow is directed via guide device to the chasing shoe same time as the rotary unit at the top of the pile rotates the rods and pile is pulled to the soil. This method is suitable for the pile diameter to the 1200 mm (Perälä 2017. The length of the pile does not have special effect to the drilling capacity and this is why it can be used for longer piles. (RIL 254-2016, p. 211)

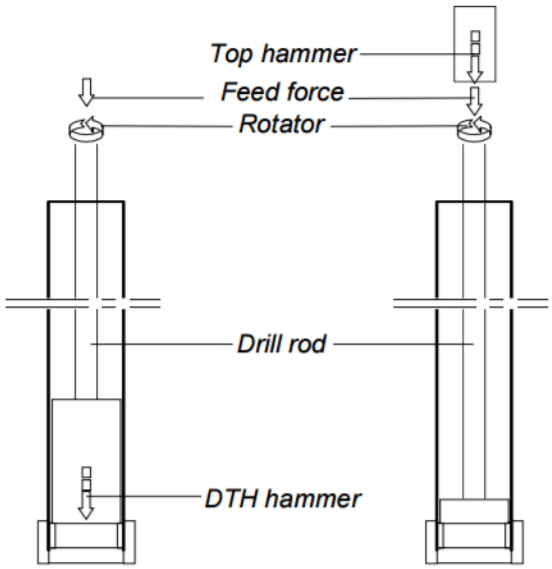

Figure 3. *Top hammer and DTH drilling configuration (Finnish road administration 2003)*

There are two mainly used drilling methods, the eccentric drilling method and the concentric drilling method. In the eccentric drilling method which can be seen in Figure 4 a pilot bit and integrated reamer bit is used. In this method an eccentric reamer bit widens the drilling hole made by the pilot bit. The method makes the hole larger than the pile. While drilling, the pile is pulled into the soil by the drill bit and the casing shoe which is

welded to the pile casing. When the target depth is reached, the drill bit, rods and the hammer can be lifted from the pile. Eccentric drilling method leaves always a little shelf which dimensions are determined by the used drilling bit. (RIL 254-2016, p.212)

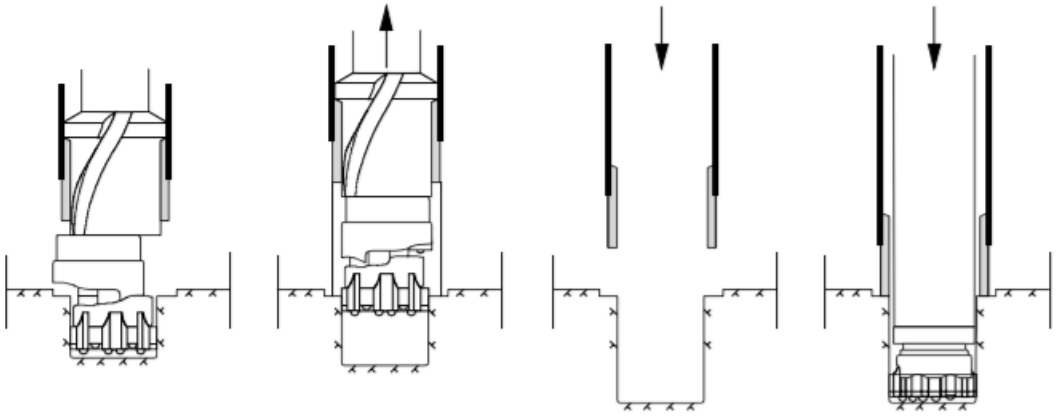

Figure 4. *Eccentric drilling method (Finnish road administration 2003)*

In concentric drilling method, which can be seen in Figure 5, the reamer (the ring bit) is part of the pile. It can be fixed or unattached to the head of the casing. During drilling the pilot bit is locked to the ring bit and it rotates and widens the drilling hole. After drilling the pilot is rotated backwards and can be lifted from the pile. Thus, the pilot bit can be changed and continued as rock drilling. Concentric drilling generally produces more straight drill holes and is more reliable and faster. When the ring bit is not attached to the casing it requires lower torque and thus is more common. (RIL 254-2016, p. 212–213) According to Finnish road Administration guide (2003) the grouted piles are always drilled by the concentric drilling method.

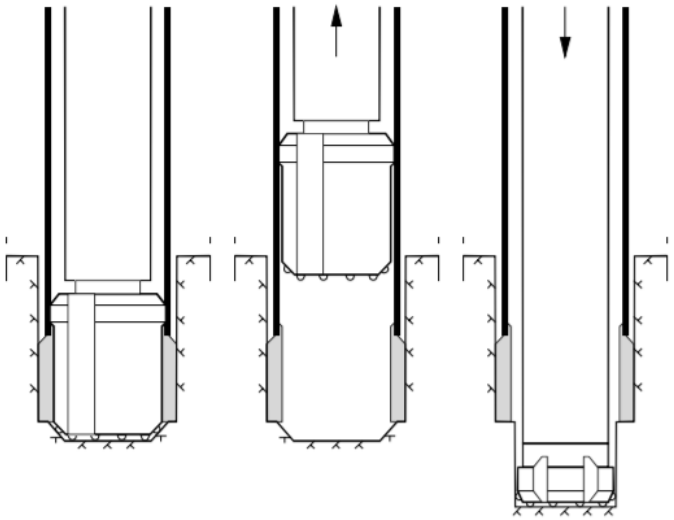

Figure 5. *Concentric drilling method (Finnish road administration 2003)*

The drilling may disturb the fine grades soil around the pile and therefore it may increase the pore water pressure and decrease the soil strength. This effect may be limited by selecting proper flushing or grouting pressure and slower drilling speed. It is highly important to notice especially sand or silty soils which may therefore results in settlements. (Finnish road administration 2003).

When drilling, flushing agents as air, water, bentonite, polymers or slurry may be used. The flushing causes disturbance of the soil and should not remove more soil from the ground than the volume of casing or should not consume more water than is fed into the ground. When water is used for flushing with top hammer the water pressure should generally be at least 20 bar and the water supply rate 20 l/min to keep the flushing holes clear in the drill bit (Finnish road administration 2003).

2.3.2 Flushing and grouting

After the pile is drilled into the bedrock, concrete or mortar is used to fill the annulus between the pile and the bedrock. The mortar hardens and creates a stiff connection with the bedrock and the pile due to adhesion. Thus the joint can resist torque, compressive and tensile forces. Instructions for grouting can be found for micropiles from standards SFS-EN 14199 (2015) and SFS-EN 12715 (2001). Finnish transportation agency guides in their instructions of geotechnical design (Liikennevirasto 2017, Appendix 8) to use the latter.

Before grouting a pile needs to be flushed in order to clean the annulus between the steel pipe and the bedrock. According to NCCI7 the volume of water used for the flushing should be at least 5 times the volume of annulus and at least 300 liter to ensure proper quality. Grouting should be done immediately after flushing to prevent the drill cuttings and soil to fall down in to the annulus (Liikennevirasto 2017, Appendix 8).

Grout is also used to protect the pile from corrosion. Usually the pile is designed to last 5-100 years' service life depending its usage and surroundings. Thus the pile usually has sacrificial layer of steel to last its lifetime without losing its properties. Sacrificial layer cannot be used on bond length of the pile. When the pile is grouted, there have to be sufficient layer of grout due to cracking of mortar to protect the pile from corrosion. If the corrosion develops under the grouted layer it can impair the bond between the pile and the mortar. When selecting grouting material, the exposure class from standard SFS-EN 206-1 (2016) should be taken into account, especially with the aggressive soils. According to Finnish piling instructions (RIL 254-2016, p.119) the thickness of outer protective layer for the bond length of grouted micropile should be at least of 20 mm and for mortar minimum of 35 mm. The protective layer thickness of the grout varies between 20–40 mm depending on the environment circumstances. Concrete also creates an alkaline oxide layer on the pile surface to protect the pile from corrosion (Leppänen 1992).

According to EN standards (SFS-EN 14199 2015, SFS-EN 12715 2001) grouting should be planned according to application used and ground conditions at the site. Although water to cement ratio should not be more than 0.55 and the compressive strength of the grout should be at least class C25/30. There are multiple methods for grouting as seen in Figure 6 but fundamentally there is no limiting factors how it is done expect the application where it is used. Common methods for grouting micropiles are listed in appendices in SFS EN-14199 (2015). These methods are filling, concreting, single step grouting or multiple steps grouting through casing, bearing element, tube-à-manchettes, special valves or tubes. The main idea is to fill the annulus or/and the pile with the cement based grout to achieve required needs. The name of the substance change based on the grain size of the base material. Usually less than 2 mm grain size cement based mixture is referred as grout and under 4 mm grain size cement based mixture is referred as mortar. These are known as concrete like materials.

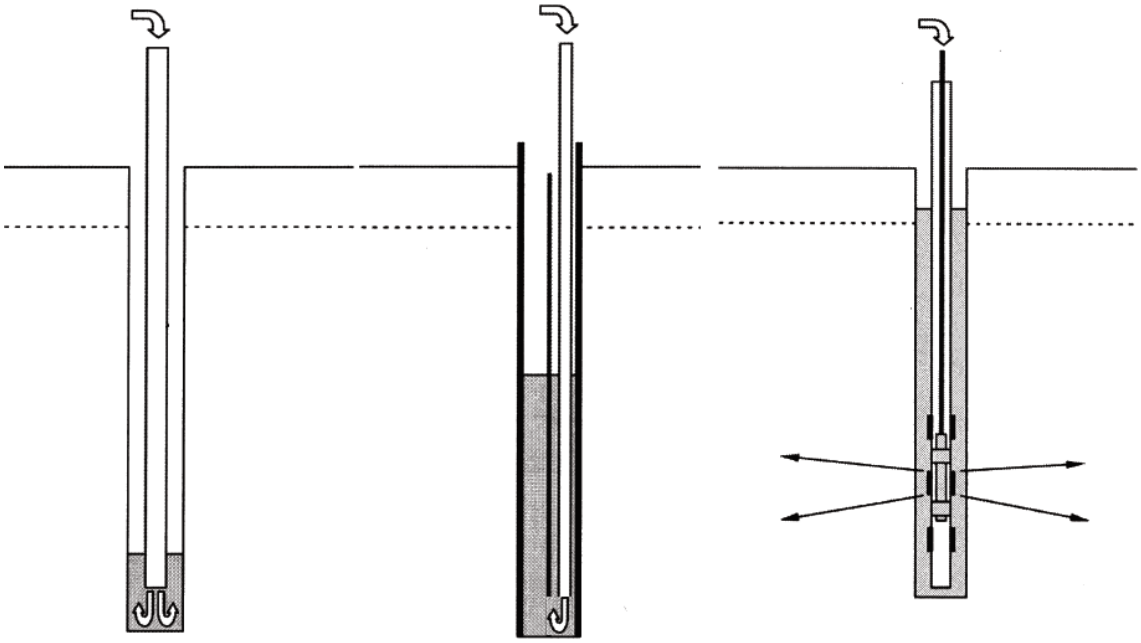

Figure 6. *Different grouting methods (modified from SFS-EN 14199)*

Ahomies (2014) investigated different grouting methods and came to result that single stage tube-à-manchette grouting is proper method for a drilled and grouted steel pipe pile. Siren (2015) came to same conclusion. This method is used also in this research. In single stage method, fine grained cement substance is grouted through tube-à-manchette. The manchette is let down to the pile and a packer is tighten to seal the pipe pile. Material is grouted through smaller steel pipe and the packer to the bottom of the pile. At the bottom of the pile are 4 grouting holes drilled through the pile sheath so that the grout can spread into the annulus between the bedrock and the pile. The annulus is grouted thoroughly the whole bond length.

The quality of the grouting should be controlled during the work. The quality of the grout can be controlled by testing the grout. Instructions for testing are based on routine tests at the construction site. The test includes density test at the mixer, viscosity test and bleed test at the construction site. Also compressive strength should be tested at least 2 sets of 3 samples after 7 day period per site. The quality of the grouting can also be tested by borehole testing or pregrouting to avoid the loss of grout and to get required cover for the bearing element. (SFS-EN 14199 2015, Annex C)

According to NCCI 7 (Liikennevirasto 2017) during grouting the mass of the grout should be at least 3 times the volume of the annulus. If grouting valves are not in use and the grout can fall back to the pile and the pile is not filled with grout or concrete the volume of the pile should be included in calculation. The grout should be expendable mass and the water/cement ratio should be according to instructions of the producer. The process should be documented so that any deflections could be seen.

3. DESIGN OF TENTION PILES ACCORDING TO STANDARDS

3.1 Introduction

In Finland design of the piles for civil engineering is based on the Eurocode design system, National annexes for Eurocodes and act of Ministry of the Environment. In addition European application standards for specific products should be followed. When design is based on this system the main technical requirements for design in earth and foundation engineering is fulfilled. Other instructions such as Finnish piling instructions follow these standards and give more detailed instructions for the use of civil engineering. (RIL 254-2016, p. 27)

In road and railroad construction works the design is controlled under Finnish Transport Agency. The agency has made series of instructions which follow EN standards. One of these instructions is NCCI 7 (Liikennevirasto 2017) which is application directive for the Eurocode 7 Geotechnical design.

The structural design and geotechnical design is based on the Eurocode design system. The main idea of the design follows partial safety factor method which is described in Eurocode 0 (SFS-EN 1990) Basis of structural design. Standard also refers to other Eurocodes as Eurocode 1 (SFS-EN 1991) Action on structures, Eurocode 2 (SFS EN-1992) Design of concrete structures, Eurocode 3 (SFS-EN 1993-1-1) steel structures and Eurocode 7 (SFS-EN 1997-1) Geotechnical design which are used for the design. Different countries have their own national annexes which can make corrections for the Eurocode based on the differences between countries.

Structural design of piles is to be made according to Eurocode design standards. For steel pipe piles, design should be done according to Eurocode 3 (SFS-EN 1993) steel structures. All the piling materials and parts should also be CE certified. The pile should be able to resist the affecting forces through its life time. These forces are loads dating from the time of the installation, operation-time loads and loads caused by the environment.

The piling work class has been made to ensure that the pile structure can endure the stresses and forces during its lifetime. In Finland there are three piling work classes PTL1–PTL3. The manufacturers of the piles ensure that the pile meet the structural requirements of the specific class. In addition to the stresses in piling work, the conditions of the site should be taken into account in pile structural design when selecting piling

work class. The site conditions are determined by the consequence classes CC1–CC3 from the SFS-EN 1990 national annex and by the geotechnical classes GL1–GL3. Thus from the Table 1 can be seen the lowest piling class to be used for the specific geotechnical class and consequence class combinations. (RIL 254-2016, p. 102)

Table 1. *Piling work classes in usual construction work (translated RIL 254-2016, p. 102)*

Geotechnical class	Consequence class		
	CC1	CC2	CC3
GL1	PTL1…(PTL3)	PTL2…(PTL3)	PTL2…(PTL3)
GL2	PTL1…(PTL3)	PTL2…(PTL3)	PTL3
GL3	PTL2…(PTL3)	PTL2…(PTL3)	PTL3

The risks for failure or malfunction of the structure are always involved when the structures are designed. Thus Eurocode 0 (SFS EN-1990 2006) defines three consequence classes (CC) CC1 – CC3. Consequence class 3 (CC3) is a class for structures which have really high consequences for loss of human life, economic, social or environmental consequences if failure occurs. These types of structures could be public buildings or example concert hall where consequences for failure are high. Consequence class 2 (CC2) is a class for structures which have medium consequences for loss of human life, economic, social or environmental consequences are considerable. These types of structures could be office buildings, other public buildings and residential buildings. Consequence class 1 (CC1) is a class for low consequence for human life and economic, social or environmental consequences are small. Consequence class affects structural design of piles and to the selection of piling work class.

Geotechnical class is used when defining the design properties for the construction site. The geotechnical classes are divided in to three classes which determine how demanding the site conditions are, thus how demanding the pile design is. In the geotechnical class 1 (GL1) belong structures which not cause major risks and the basic requirements for the design can be fulfilled by the experience of the similar conditions and the qualitative geotechnical investigations. Thus soil is usually bedrock, moraine or coarse grain soil. In geotechnical class 2 (GL2) includes structures which require more investigations, soundings and analysis based on the geotechnical parameters. These structures are not affected by unusual or exceptional ground conditions or forces. Usually when the structure is a building where people work or live as permanent basis and it requires piling, it belongs at least to this class. Geotechnical class 3 belong structures which are not included in GL1 or GL2 and major risks are involved, the structure is unusual or the ground conditions are challenging. Eurocode 7 (SFS-EN 1997 2014) gives instructions and certain outlines for the design with geotechnical classes therefore it should be included in the design documents. Usually structures which may need piling belong to geotechnical class 2 or 3. (RIL 254-2016, p. 37–39)

3.2 Geotechnical design of the tension pile according to Eurocodes and national instructions

3.2.1 Introduction

According to Eurocode 7 (SFS-EN 1997-1 2014) when designing tensile piles its resistance should be greater than affecting axial tensile force. Thus two failure mechanisms should be covered:

- Pile pull-out from the soil or bedrock,
- The rise of the soil block in and around the pile or pile group.

If the pile is drilled into the bedrock the failure mechanism can be accounted as failure of the bedrock around the pile. In this research the singular piles are drilled into the bedrock and thus this failure mechanism is covered.

3.2.2 Drilled and grouted pipe pile

According to Finnish piling instructions (RIL 254-2016, p. 72) shaft resistance of pile which is drilled and grouted into the bedrock can be used to resist tensile forces. After the bedrock is reached the drilling is continued into the bedrock. A drill hole is cleaned by flushing and after filled with grout, mortar or concrete. Contact between bedrock and a pile is assured by drilling the pile for distance of three times diameter of the pile into the bedrock. If bedrock surface is inclined pile should be drilled over four times the diameter into the bedrock. The pile must be drilled at least 0.5 m into the non-fractured bedrock. With fractured bedrock the drilled pile should be drilled deeper or grouted into bedrock to ensure a rigid contact. The bedrock is seen as firm when it does not have cracks or have only few tight cracks and the rock is not weathered. When a pile is drilled and grouted into the bedrock and shaft resistance is used to resist tensile forces drilling depth should be minimum 3 m if the properties of the bedrock are not determined (RIL 254-2016, p.86). According to NCCI7 (Liikennevirasto 2017, p. 56) minimum drilling depth is 2 m or 3 times diameter of the pile if the pile is a tensile pile.

With eccentric drilling method the eccentric reamer will leave a gap between the bedrock and the pipe pile thus the contact therefore should be verified. After drilling the proper contact is assured by the end blows with the drill hammer to top of the pile. When drilling a pipe pile with casing shoe or ring bit these add-ons widen the area of the pile tip and thus when is drilled into the bedrock the actions affect the whole area of the pile tip and transfers the effects to the bedrock.

When piles are supported by the firm bedrock, base resistance of the pile is not usually the limiting factor. Usually the limiting factor is the structural resistance of the pile. The pile is considered to be supported by the bedrock when the soil survey or other ob-

servations support the notion. Characteristic value for geotechnical resistance referring to Finnish piling instructions (RIL 254-2016, p. 70) can be calculated with Equation:

$$q_{b;k} = \frac{7 * \sigma_{cyl}}{d^{0,2}} \quad (1)$$

Where $q_{b;k}$ is geotechnical end resistance of the pile [MPa],

σ_{cyl} is compressive strength of the Finnish bedrock which is usually 150-300 MPa (Rantamäki *et al.* 2009, p 19),

d is diameter of the drilled piles [cm].

If a pile is drilled into the bedrock its shaft resistance can be used in geotechnical design. If so, the pile should be drilled into the bedrock and the drill hole should be cleaned and filled with concrete, mortar or grout. As the concrete hardens it will attach the pile to the rock. According to Finnish piling instructions (RIL 254-2016, p. 72) the geotechnical resistance of the pile shaft can therefore be calculated with Equation:

$$R_{s;k} = \pi * d * D * \tau_{s;k} \quad (2)$$

Where $R_{s;k}$ is geotechnical resistance of the pile shaft [kN],

d is diameter of the drill hole [m],

D is depth of the drill hole in the bedrock [m],

$\tau_{s;k}$ is characteristic bond strength between concrete or grout and the bedrock [MPa].

According to Equation the shaft resistance is basically dependent on the bond strength of the concrete and the surface area of the pile. The bond strength between steel pipe pile and the grout can be calculated using Equation (RIL 254-2016, p. 73):

$$\tau_{s;k} = k_b f_{ctk} \quad (3)$$

Where k_b is coefficient of adhesion on the pile surface

- which is for smooth surface 0.7
- and for grooved surface 2.0,

f_{ctk} is characteristic tensile strength of the concrete or grout [MPa].

From Equation *(3)* can be seen that the surface profile has major role for the coefficient of adhesion on pile surface. Thus by modifying the profile the bond strength can be increased on the pile surface. Shaft resistance can also be raised by using grout with high-

er strength or by increasing the effective surface area of the pile. Relation for the higher class of grout and its tensile strength and the average adhesive bond strength between rock and the grout can be seen in Table 2. The characteristic tensile strength of a 5% fractal is used in the Table 2 (SFS-EN 1992, p. 30).

Table 2. *The characteristics tensile strength of the grout. (Modified from RIL 254-2016, p. 73)*

The strength class of concrete/mortar/grout	The characteristic tensile strength of concrete/mortar/grout f_{ctk} [MPa]	The characteristic bond strength between rock and the concrete/mortar/grout $\tau_{s;k}$ [MPa]
C20/25	1.50	0.50 - 1.00
C25/30	1.80	0.55 - 1.10
C30/37	2.00	0.60 - 1.20
C35/45	2.20	0.65 - 1.30
C40/50	2.50	0.70 - 1.40
C45/55	2.70	0.75 - 1.50

3.2.3 Tensile resistance of the pile in a soil layer

Tensile resistance of a pile in coarse grain soil layer can be determined by Equation (4) where it is dependent of the pile surface area and characteristic value of the pile shaft friction $q_{s;j;k}$ which can be calculated from the soil properties (SFS-EN 1997 2014, p.77):

$$R_{t;k} = \Sigma A_{s;j} * q_{s;j;k} \quad (4)$$

Where $R_{t;k}$ is the tensile resistance of the pile in a soil layer [kN],

$A_{s;j}$ is the area of the pile shaft [m^2],

$q_{s;j;k}$ is the pile shaft friction resistance [kPa].

In the coarse grain soils shaft friction resistance in an individual soil layer can be calculated by Equation:

$$q_{s;i} = \sigma`_{v;i} K_s * \tan \varphi_a \quad (5)$$

Where $\sigma`$ is effective axial stress on the pile surface [MPa],

$K_s * tan\ \varphi_a$ is the bond strength friction factor which can be determined from the Figure 4.4 Finnish piling instructions (RIL 254-2016, p.66)

$K_s * tan\ \varphi_a$ is determined by relation on the soil friction factor and pile type. The factor is lower with the drilled piles. In the fine grained soils bond strength q_s is determined by

the adhesion of the soil and the undrained shear strength of the soil as seen from Equation:

$$q_s = \alpha * c_u \quad (6)$$

Where c_u is undrained shear strength of the soil [kPa].

α is adhesion factor and can be determined from Figure 4.5 Finnish piling instruction manual (RIL 254-2016, p.68),

If there is coarse grained soil over the fine grained soil the coarse grained part of the bond strength should not be taken into account due to effect of negative skin friction. Also the bond strength from the fine grained soil should not be taken into account under tensile load in the short term situation. The development of the adhesion can take several months thus it is recommended to take it into account only in long term situations if so (RIL 254-2016, p. 67). According to Finnish transportation agency instructions (Liikennevirasto 2017, p. 56) a pile tensile resistance in cohesive soil layers can be used only with short term loads which are not cyclic.

3.2.4 Tensile capacity determined by the load test and the soil survey

Load tests for the piles should be made whenever there is no comparable experience for the usage of the tensile piles in similar situations or there is other uncertainty about design of the pile. The load test is used to evaluate the design of the pile foundation. The static load test is used with the tension piles and the piles are loaded until the failure. When the piles are under tensile load at least 2% of the piles should be tested. The load tests are used especially in very demanding conditions in GL3 (RIL 254-2016).

The design values by the Eurocode 7 (SFS-EN 1997-1) for the capacity of tensile pile are derived by Equation:

$$R_{t;d} = \frac{R_{t;k}}{\gamma_{s;t}} \quad (7)$$

Where $R_{t;k}$ is the characteristic tensile resistance [kN],

$\gamma_{s;t}$ is partial factor of tensile resistance which can be determined from the Table 3.

Table 3. *Factor of safety for tensile resistance (RIL 254-2016, p.83)*

Resistance	Entry	Value
Short term loading	$\gamma_{s;t}$	1.35
Long term loading	$\gamma_{s;t}$	1.5

The characteristic value for tensile resistance can be determined by the load test. More than 2% of the piles should be tested with the static loading test. The minimum and average tensile resistance is then calculated and divided with the correlation factor ξ_1 or ξ_2 from the Table 4. These values take into account the changes by the act of Ministry of the Environment (Ympäristöministeriö 2016) and are therefore higher than originally in Eurocode 7.

Table 4. *Correlation factor for static loading test (RIL 254-2016, p.83)*

ξ when n=	1	2	3/50%	4	5/100%
ξ_1	1.75	1.63	1.50	1.38	1.25
ξ_2	1.75	1.50	1.31	1.25	1.25

From these values the lowest is chosen to represent the characteristic value for the tensile resistance as shown in the Equation 8.

$$R_{t;k} = Min\left\{\frac{(R_{t;m})_{mean}}{\xi_1}\ ;\ \frac{(R_{t;m})_{min}}{\xi_2}\right\} \quad (8)$$

According to Finnish piling instructions (RIL 254-2016, p. 81) in GL2 correlation factor can also be determined from the soil survey. When the tensile capacity is determined by the soil survey correlation factors ξ_3 and ξ_4 are chosen from the Table 5 by the number of soil surveys made. Thus the calculation for the characteristic tensile resistance is made by Equation 4 and 9 and the correlation factors are chosen from the Table 5.

$$R_{t;k} = Min\left\{\frac{(R_{t;m})_{mean}}{\xi_3}\ ;\ \frac{(R_{t;m})_{min}}{\xi_4}\right\} \quad (9)$$

Table 5. *Correlation factors based on the soil survey (RIL 254-20163, p. 84)*

ξ when n=	1	2	3	4	5	7	10
ξ_3	1.85	1.77	1.73	1.69	1.65	1.62	1.60
ξ_4	1.85	1.65	1.60	1.55	1.50	1.45	1.40

Piles should also be around in the similar depth than ground survey so that the calculation for the characteristic tensile strength $R_{t;k}$ is reliable. As an alternative method the modelling factor of 1.5 can be used to replace the factor of safety in the short term and the long-term situations (RIL 254-2016, p. 85).

3.2.5 The failure of the bedrock in the form of a cone

When the pile is drilled into the bedrock, the failure mechanism can also be the failures of the bedrock in a form of cone instead the failure of the rock socket. The necessary length for the pile shaft in the bedrock is derived from the unit weight of the rock and geometrical dimension of the cone. The required length is determined by Equation (RIL 254-2016, p. 85):

$$L_{min} = \sqrt[3]{\frac{3*F_{t;d}}{\gamma*\pi*tan\varphi^2}} \tag{10}$$

Where $F_{t;d}$ is design load for tension [N],

γ is unit weight of the rock [kg],

Φ is the angle of the cone which can be seen in Figure 7,

L_{min} is the minimum drilling depth [m].

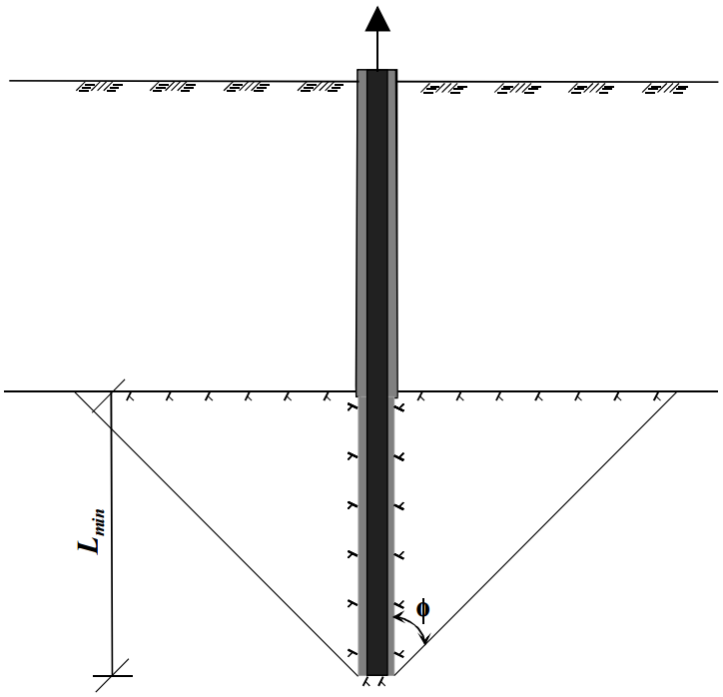

Figure 7. *Failure of the rock cone (RIL 254-2016)*

The form of cone is dependent on the quality of the bedrock. If the rock is fractured the cone angle φ is 30° and with the homogenous firm rock 45°. If the properties of the bedrock are not determined, anchoring length of the pile should be at least 3 meters. (RIL 254-2016, p. 86) According to RIL 263-2014 the buoyancy force should be also noticed in the design.

3.2.6 Tensile steel pipe pile design according to NCCI 7

NCCI 7 is an application directive of Finnish Transportation Agency for Eurocode standard SFS-EN 1997-1 geotechnical design and it is used for design of public roads, railroads, waterways and structures which is related to its infrastructure. This directive has series of instructions (SFS-EN 1997 2014, Appendix 8) for the design of tensile pile which are drilled and grouted to the bedrock. Many of the instructions are related to the piling work and are presented in chapter 2.

According to the directive in the design of drilled and grouted piles only the bond between bedrock and grout and the weight of the pile can be used in calculation (SFS-EN 1997 2014, p. 58). If the pile is installed according to NCCI7 Appendix 8, 100 kPa can be used as bond strength when the highest value for ultimate tensile force does not exceed values in Table 6 presented.

Table 6. *Highest value for tensile force according to NCCI 7 (Liikennevirasto 2017)*

Drilled and grouted steel pipe pile	
The diameter of the pile	Highest value for tensile force in ultimate limit state
[mm]	[kN]
170	50
320	100
508	150
≥813	250

Piles are not allowed to be used in design of bridges in serviceability limit state but tensile piles can be used in all other designs in all limit states. If so at least two or 20 % of the piles should be tested with dynamic or static load tests according to RIL 254-2016 (SFS-EN 1997 2014, p.58).

3.3 Structural resistance of the pile

Structural resistance of steel is designed according to Eurocode 3 (SFS-EN-1993-1; SFS-EN-1993-5). Structural tensile capacity of the pile can be calculated according to plasticity theory with Equation:

$$N_{Rd} = \frac{A_s * f_y}{\gamma_{M0}} \tag{11}$$

where f_y is yield strength of the steel material [N/mm^2],

N_{Rd} is tensile capacity [N],

A_s is cross-section area of the steel [mm^2],

γ_{M0} is material factor of safety (1.0).

According to Hoek`s law and elasticity theory steel will stretch when it is under the stress. The strain of the steel can be determined by Equation:

$$\varepsilon = \frac{\Delta L}{L} \tag{12}$$

Where ε is strain of the steel,

ΔL is change in length [m],

L is the original length [m].

According to theory the strain is related to stress and modulus of elasticity by Equation:

$$E = \frac{\sigma}{\varepsilon} \tag{13}$$

Where E is modulus of the steel [MPa],

σ is stress [MPa] on the cross-section area of the steel A_s [mm^2] which is induced by the pulling force F [N],

ε is strain of the steel.

With these equations the ultimate pulling force can be calculated for the study. The theory of elasticity is used to determine the strain of the steel pipe pile thus calculate net displacement of the pile. The strain is calculated on the free length of the pile thus it can be separated from the displacements which occur on the bond length.

3.3.1 Corrosion of the steel elements

In the design of steel pipe piles according to present instructions (RIL 254-2016, pp. 112–119) the protection against corrosion is to be considered. The main factors which affect the design is the aggressiveness of the environment, pile type, type of steel, type of load and required design working life. The protection against corrosion can be achieved by efficient cover of grout, a sacrificial thickness of steel for the corrosion, with use of sacrificial element or special coating or cover for the steel.

Environment of the pile affects the corrosion speed. The most important factors are the surrounding soil, changes of the ground water, the presence of oxygen and impurities on the pile surface. On the air corrosion speed is around 0.01 mm per year and in the conditions where the seawater is presence it is 0.02 mm per year. In normal conditions, a pile in the undisturbed natural soil as sand, till or clay the corrosion factor over 100 years is around 1.20 mm. In the fresh water the corrosion factor is 1.4 mm and in the ocean or polluted water around 3.5 – 7.5 mm. More accurate description refers to SFS-EN 1993-5 chapter 4 (Eurocode 3 2007).

In aggressive environment the water and corrosive elements may be in contact with the pile. Thus when choosing the diameter of the pile, the corrosion must be taken into account. The corrosion reduces the effective diameter of the pile and therefore the thickness of the pile pipe has to be larger. For design perspective this means that the pile diameter should increase at least the amount of the corrosion factor over the design lifetime.

Adding sacrificial steel is enough for the free length of the pile but if the pile is grouted and the shaft bond capacity is used in design, the thickness of the grout will determine the corrosion protection. Under the tensile load the grout may crack and the pile may be in contact with corrosive elements. Corrosion on this surface may break the bond on the

shaft surface and thus reduce the tensile capacity of the pile. Thus for tension piles it is important to have sufficient grout cover to protect from corrosion.

According to Finnish piling instructions the minimum layer over the pile surface for protective grouting is 30 mm on piles under tensile stress in normal soil conditions and corrosion category XC1−XC4. For more detailed description refers to RIL 254-1-2016, Table 4.25 (RIL 254-2016, p. 118). According to the NCCI7 (Liikennevirasto 2017, Appendix 8), the protective grouting layer should be at least 10 mm thick for ordinary corrosion conditions. Thus a ring bit diameter should be at least 20 mm larger than the pile diameter. If the corrosion conditions are more aggressive, diameter of the ring bit should be at least 30 mm wider than the pile which means 15 mm wide grout annulus.

4. FAILURE MECHANISMS OF THE TENSILE PILE

4.1 Introduction

According to Brown (2015), rock anchors have been widely used in various applications for last 80 years. Anchors are capable of restraining tensile forces example to stabilize sheet piles and retaining walls, anchor buildings and other structures. Rock anchors are also used to restrain the uplift forces when the depth of the soil overburden is not enough to provide the necessary shaft resistance.

When using an anchor, a pile or covering casing is drilled below the rock level to seal of the overburden soil. The drilling bit is left to the bottom to act as compression fitting. The casing is cleaned and the drilling is continued from the rock level with a centralizer to the required depth. The cutting is washed out of the hole with the reverse circulation or other method and the anchor cable or tube is lowered down to the drill hole in the bedrock. The hole is then grouted with injection cement and the annulus between the bedrock and the cable or tube is filled to designed level. The grout protects anchors from corrosion and creates a bond between the anchor and the rock. After installation, an anchor can be pre-stressed or leave unstressed. Unstressed anchors are called dead anchors and are usually made from steel tubes. Where the anchors are meant to with-stand higher loads a shear connector can be made over the dead anchors by welding a steel string over the tubular pile surface as seen in Figure 8 (Tomlinson *et al* 2008., p.315).

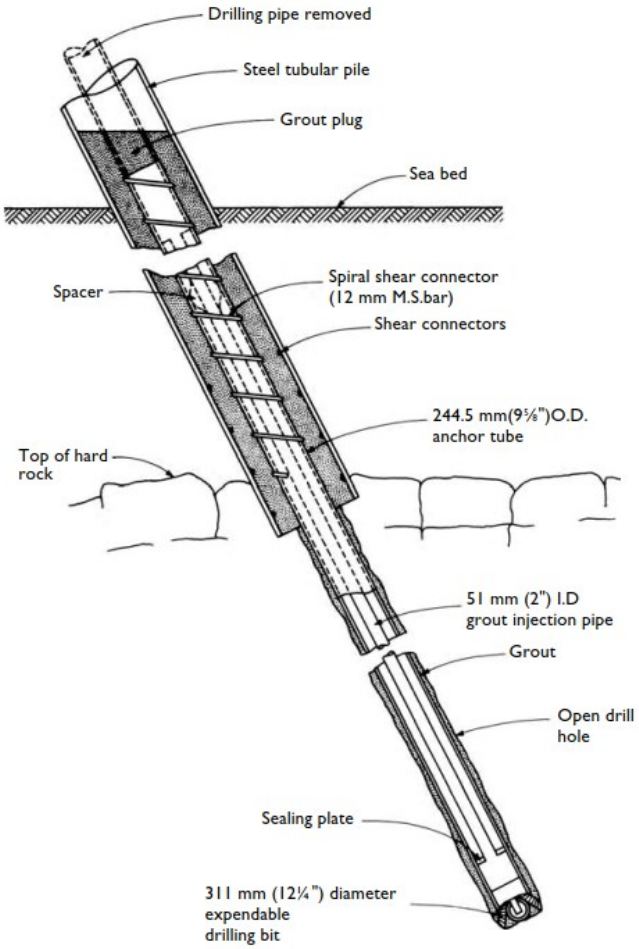

Figure 8. *A tubular dead anchor with shear connector (Tomlinson* et al. 2008*, p.317)*

According to Tomlinson et al. (Tomlinson *et al.*, p.317) the pull-out resistance of drilled and grouted anchor is known to dependent of five factors:

1. The steel structural and material properties
2. The bond stress (strength) between the anchor and the grout
3. The bond stress (strength) between the grout and the rock
4. The dead weight of the whole structure or soil which anchor can lift
5. The mass of lifted by the group of anchors.

These are also the components which Brown (2015) presented as principal modes for failure from (a) to (d) for the rock anchors as seen in Figure 9. Failure mode (a) is the failure of the steel bar or pile, failure mode (b) is the failure of the grout to steel surface, failure mode (c) is the failure of the grout to rock surface and failure mode (d) is the rock mass uplift.

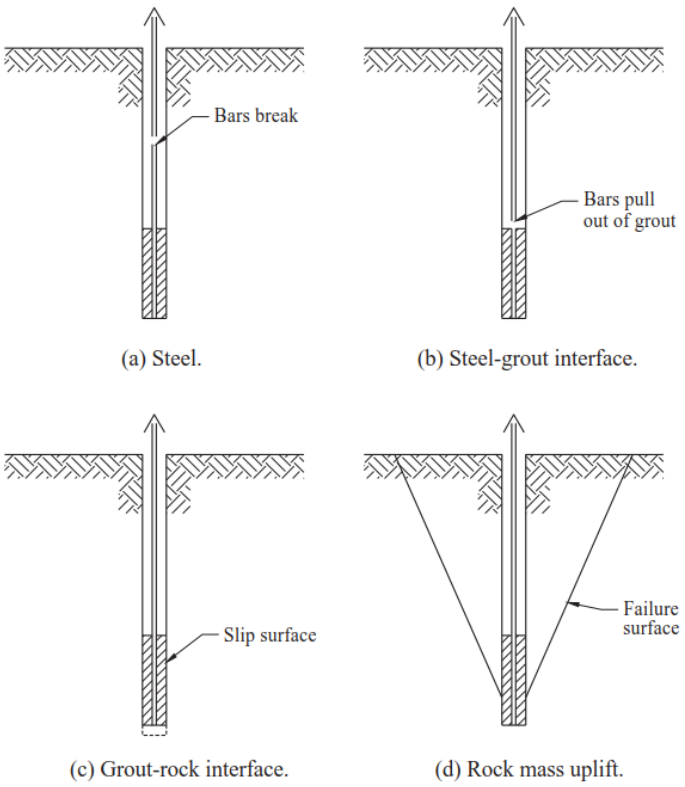

Figure 9. *Failure mode of the grouted anchors (Brown 2015, p.4)*

These are the elements which are studied by the literature review to understand the failure mechanisms of the anchor so that it could be implemented to the tensile pile design. Failure of the steel tube, bar or anchor is the failure mode (a) can be directly calculated from the structural properties of the steel which was presented in chapter 3.2 and thus bypassed here.

4.2 The bond strength between the anchoring element and the grout

The failure on steel to grout surface was indicated by Brown (2015, p.4) as failure mode (b). According to instructions in chapter 3.1.1 bond strength between a pile and grout is depended on the compressive strength of the grout and surface factor of the steel. Elements which were found to affect these factors are presented here.

One of the elements is caused due to elastic properties of the steel. According to Tomlinson *et al*. (2008, p.318) the reduction of diameter of the anchor, caused by the inward radial strain, which occur under the tensile load can lower the bond strength. Also, the shrinkage of the grout in relatively wide annulus can lower the bond strength. Thus, the transfer of the load from anchoring element can be affected wholly through shear keys which can be welded metal or steel strings on to surface of the anchor. Gomez *et al.* (2005) referred to similar effect as Poisson`s effect and dilation which cause compressive radial stresses to be smaller with larger annular width. This would mean that with

larger annulus would cause lower bond strength. According to Brown (2015, p.4) failure is resisted by adhesion and interlocking of the interfaces. After the displacement increases, pile shear strength fails, and the friction becomes the major factor for the resistance.

Brown discussed (Brown 2015, p.4) that the grout-tendon shear strength depends on the normal confining pressure, stiffness and roughness of the tendon, grout expansive properties and the bond length. He also presented that the shear stress along the bond length is not uniform. Recent study by Sirèn (2015) also indicates that radial stress decreases along the bond length. Thus, simplified Equation *(2)* presented may not be justified. Brown (2015) presented a Figure 10 by Coates and Yu (1970) to explain the stress distribution along the anchor. In Figure 10 E_a is referred as elastic modulus of the steel and E_g to elastic modulus of the grout. The Figure actually would indicate that the stress distribution will be more uniform with softer grouts.

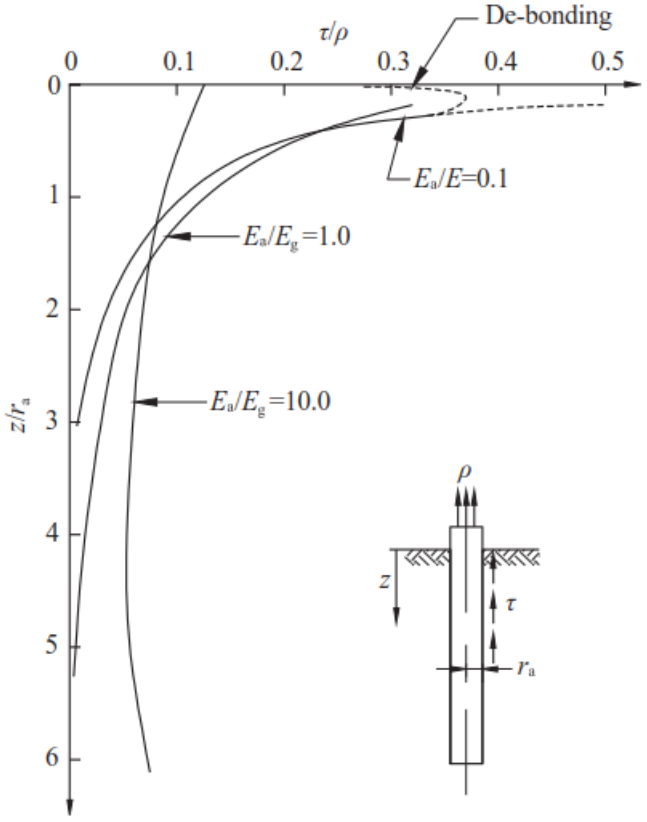

Figure 10. *Stress distribution along the bond length (Brown 2015)*

According to Brown (2015 p.4; originally Littlejohn et Bruce 1977) usually the grout to tendon failure is not necessary to calculate because rock-grout failure alone will produce adequate bond length.

When studying the bond between the pile and the grout, is noted that the pile acts as reinforcement and the grout prevents the pile from slipping under tensile force. When a

pile is under stress, the result is that steel and grout are deformed together to react to this stress. Barbosa et al. (2008) studied relative rib area of the reinforcing bars by various pull out test. Ribs on the surface of reinforcing bar provide mechanical interlocking between concrete and a steel bar. According to Barbosa *et al.* (2008, p.1) connection between a pile and the grout is mainly caused due to adhesion between the cement paste and the pile. When this connection is broken the pile is slipping along the concrete surface and after the bond strength appears in the form of skin friction between the pile and the grout. The intensity level of skin friction is based on the irregularities on the connection surface. Thus the force which can break this bond is proportional to the surface area between connections.

When the pile is grooved or in Barbosa *et.al* (2008) case the bar is ribbed, the strength is formed by mechanical connection between the grout and the pile, no slipping occurs before this connection is broken. Friction is affected only after the steel is displaced. The pile is affected mainly by the two main forces, compression and the tensile force. Grooves of the pile transfer this force to the grout and the grout is affected by these forces. Thus the strength of the connection is actually limited by the main stresses affecting to the grout. When either tensile or compression force exceeds the strength of the grout, mechanical bond between the pile grooves and the grout is broken.

Gomèz *et al*. (2005) discussed of the companion paper by Wilder *et al.* (2005) about the connection between the micropile and concrete footing. They did series of push out tests for micropiles grouted in concrete footing. The difference of their test to our research is that the pile was pushed through the footing not pulled and the footing dimensions were limited, thus the footing may not confine the stresses. They discussed that the bond strength of steel element in grout consists of adhesion, direct bearing on surface irregularities and friction. The bond resistance is subject to properties of the concrete, an confinement and volume of the concrete around the bar and the surface properties of a reinforcement.

Typically there were two types of failures in their tests, pullout failure or cracking failure. Pullout failure occurs when a reinforcement bar shear the concrete or grout between the top of the bar ribs. Splitting failure can occur when surroundings of the bar cannot hold the tensile radial stresses and cracks develops to the edge of the concrete resulting in loss of bond. After cracking the bar can retain major residual capacity due to frictional resistance. (Gomèz *et al. 2005)*

Gomèz *et al. (2005)* discussed also other factors controlling the strength. There were significant drop in bond strength after bond failure with the smooth casing insert and the larger diameter hole showed lower bond strength. With the textured casing the bond strength was higher and did not decrease after failure of the connection. During the test, mobilized bond stress also decreased along the insert length. They proposed theory to understand the frictional components of the bond strength. They interpreted that the

three major components induced friction to the surface; friction due flexural stresses, Poisson`s effect and dilation effect. (Gomèz *et al. 2005)*

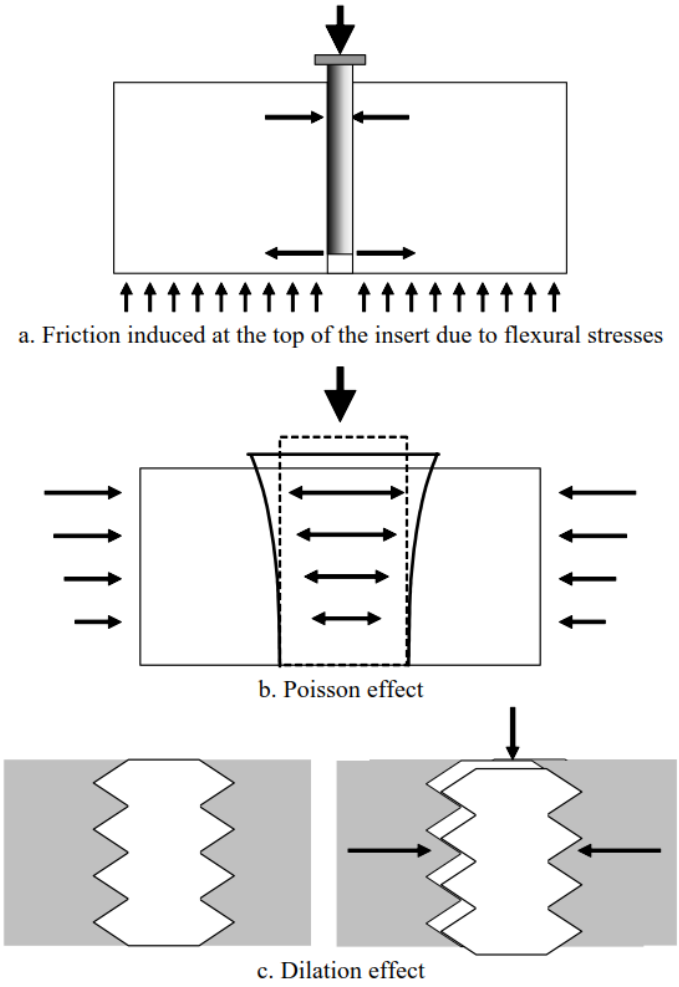

Figure 11. *Components which induce friction on pile surface (Gomèz* et al. 2005)

Figure 11 illustrates these effects. The first Figure show the friction effect due to bending of the casing which can lead the top part to generate more compressive stresses than the lower part. The second Figure illustrates the poison effect due to radial expansion when a pile is axially loaded. This also generates compressive stress to the top part of the pile as well as the tangent tensile stresses throughout the grouted annulus. Because of the neat cement has lower Young`s modulus than concrete it could be expected that radial compressive stresses between grout and the pile would be smaller for a larger annular width. Thus, increased diameter of the hole size can decrease the bond strength. The third Figure shows us the effect of the dilation where the irregularities of the micropile surface try to move over the grout surface. If the pile cannot do so the displacement can only occur due to failure of the grout between the pile ribs or grooves. (Gomèz *et al. 2005)*

It seems the connection between the pile and the grout is complicated but certain consistencies can be found out. In tests which have been made by compressing the results

can differ from the pullout test. In this research the micropile is under tensile force which means that the bending action cannot happen as the Figure 11 illustrates and also the Poisson`s effect is backwards. The pile stretches due to tensile force and it does not induce compressive strength to the grout but radial tensile stress as Tomlinson suggested. The stress distribution from the top to bottom of the pile is similar. The force is applied to the same point on the top part of the insert length, therefore radial tensile stresses maybe higher than the tip of the pile. The dilation effect is present as it is and plays major role with the bonding of grout and grooves on the pile surface.

4.3 The bond strength between the grout and the bedrock

According to Tomlinson (2008, p.320) The bond strength between the grout and the rock is depended on the compressive strength of the grout, compressive strength of the intact rock, cleanliness of the hole, roughening effect of the drill bit, diameter of the drill hole, annular space around the anchor and the quality of the rock. Also compression fitting in the bottom of the drill hole creates better bonding effect due to compression pressure to the grout column. In other words the bond is developed again by adhesion, friction and mechanical interlocking (Brown 2015, p.3).

Failure mode (c) can be noted as shear failure at the grout to rock surface. Thus the shear resistance on the surface of the rock is the main factor controlling the failure. The Equation *(2)* from the Eurocode can be used if the failure is assumed to distribute uniformly to the surface. According to Brown (2015) bond strength τ should be defined by the pullout test at the site but many times it is still derived by the rock type and by the values published by Littlejohn and Bruce (1997) where values for the rock ultimate bond strength range of 0.2 to 5.73 MPa. According to Brown (2015) rock to grout shear strength is assumed to be approximate 10% of uniaxial compressive strength of the rock up to maximum of 4.2MPa. Sometimes the values are determined by the compressive strength of the grout as it is in Eurocode. Therefore it may lead to too long bond lengths in design.

The compressive strength of Finnish rocks is around 150 to 300 MPa (Rantamäki *et al. 2009)* thus it is not limiting factor for the bond strength on rock to grout surface due lower compressive strength of the grout. Values for bond strength according to Table 2 are around 30% to 60% of the characteristic tensile strength of grout. This would indicate friction factor for rock surface should be 0.3 to 0.6. Between a smooth steel pile and the grout 0.7 is used. Therefore values in Table 2 seems to be quite low consider that the surface of the bedrock can be considered a lot rougher than the smooth steel.

It seems that in Table 2 the bond strength is calculated based Littlejohn and Bruce (1977, p.4) which is tenth of the compressive strength of grout divided by safety factor of 3. Calculation would get the value for bond strength of the grout to rock surface around 0.5 to 1.5.

Other elements of the grout to rock failure are similar to tendon to grout failure but it is acting on the rock to grout surface. The difference seems to be that only the quality of the rock and the compressive strength of the grout are taken into account on simplified equations. Other elements such frictional elements, fissures of the rock, cracking or distribution of the stress are not considered on the design according to Eurocode.

4.4 The failure of the bedrock or mass around the anchor

The last failure mechanism (d) (Brown 2015) is the failure of the mass around the anchor which it can lift without structural failure. Shape of the mass of rock is highly dependent of the jointing and fissuring of the bedrock. Various different failure planes were presented by Tomlinson (2008) which can be seen in Figure 13 and 14. Figure 13 presents examples of failure planes in several types of failure planes with different types of bedrock. The uplift of the rock mass is dependent on the form of the rock mass. Pile can either slide through fissures of the rock or lift parts of the bedrock. Brown (2015) discussed that the general idea is that the rock mass will lift as form of cone in angle of 60 or 90 degrees as seen in Figure 12.

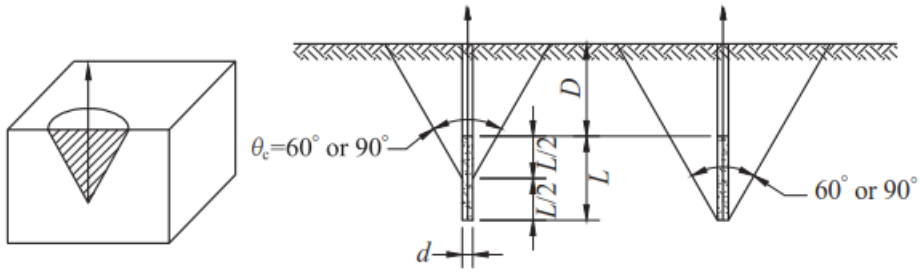

Figure 12. *Cone shaped failure of the bedrock (Brown 2015)*

The apex of the cone will start at the end, middle or the upper part of the bond length. The cone angle depends on the rock quality where smaller 60 degree cone is soft or fissured rock and the 90 degree cone is the firm rock. This method is conservative and approximate, due to absence of the effect of shear and tensile strength of the rock. The required bond length is usually calculated by equating the grout to rock bond resistance to the uplift force required to overcome the rock mass and applying factor of safety 2. (Brown 2015)

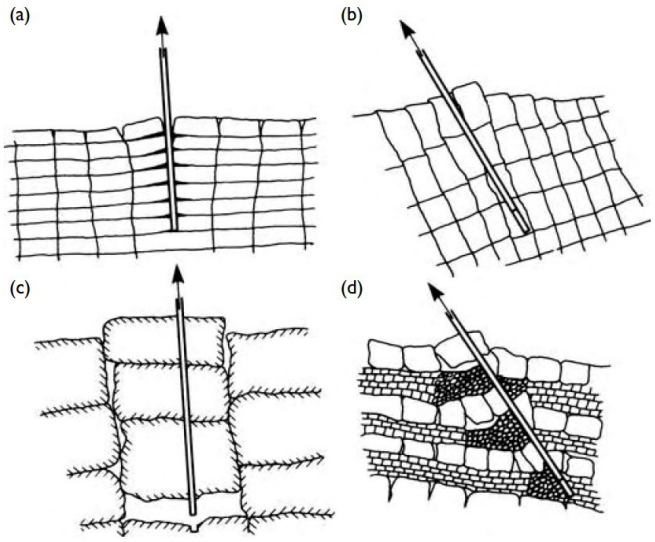

Figure 13. *Failure planes of the rock (Tomlinson 2008, p. 322)*

It has been discussed (Tomlinson 2008; Brown 2015) whether the cone starts from the bottom, middle or the upper part of the anchor. Due to multiple variables in bedrock properties it is hard to determine exact failure criterion for the failure of the rock. Therefore it may be justified to choose the conservative option for the failure criterion in most common cases.

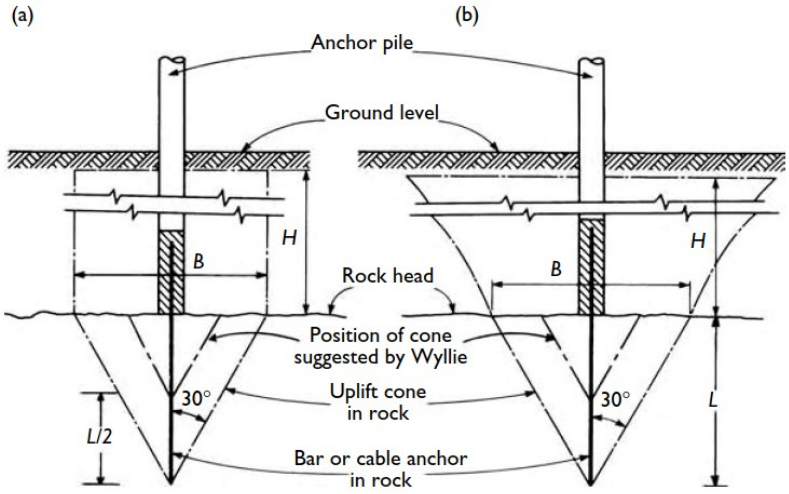

Figure 14. *Failure of the bedrock and the soil layer (Tomlinson 2008, p. 322)*

4.5 Rise of the soil due to failure of rock cone

Rise of the soil due to rock cone failure should acts as belled base due to fact that pile lifts a circular rock surface through a soil layer. Niroumand et al. (2012) reviewed previous works on uplift capacity of enlarged base piles in cohesion less soil. They found

summary from Dickin *et al.* (Niroumand *et al.* 2012*;* originally Dickin 1988*)* concerning of the failure mechanism of the soil over the belled pile base as seen in Figure 15. The most conservative approach from Majer (Niroumand *et al. 2012;* originally Majer 1955*)* for deep pile depths is the cylinder form for the soil failure while other presents the failure plane as formula of friction angle. Tomlinson *et al. (2008)* suggested that the resistance is traditionally calculated by the weight of the earth having sides that rise either vertically or 30° angles from the vertical line on top of the base. However these methods have not been proved to be reliable and the 30 degree cone method can give overestimate results with large depths and conservative values with shallow depths (Poulos *et al.* p.46; originally Turner 1962). In addition, Parr *et* Varner (Poulos *et al.* p.46; originally Parr *et* Varner 1962) showed that this may not apply to piles in clay.

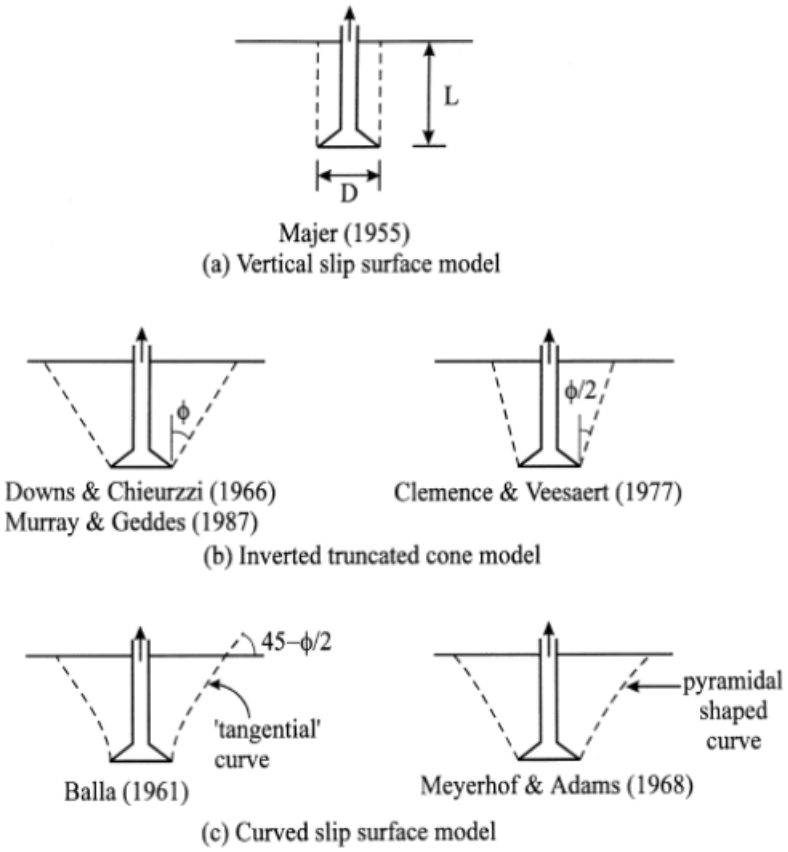

Figure 15. *Summary of failure mechanisms over belled pier* (Niroumand *et al.;* originally Dickin 1988)

If this knowledge is used in the case of rock cone failure where the rock cone acts as belled base and therefore tries to lift the soil over the rock. The most conservative approach is to use the cylinder form. If this weight is added to the weight of the rock cone, based on Eurocode, this failure mechanism is not critical in deep soil layers expect in case of fractured bedrock.

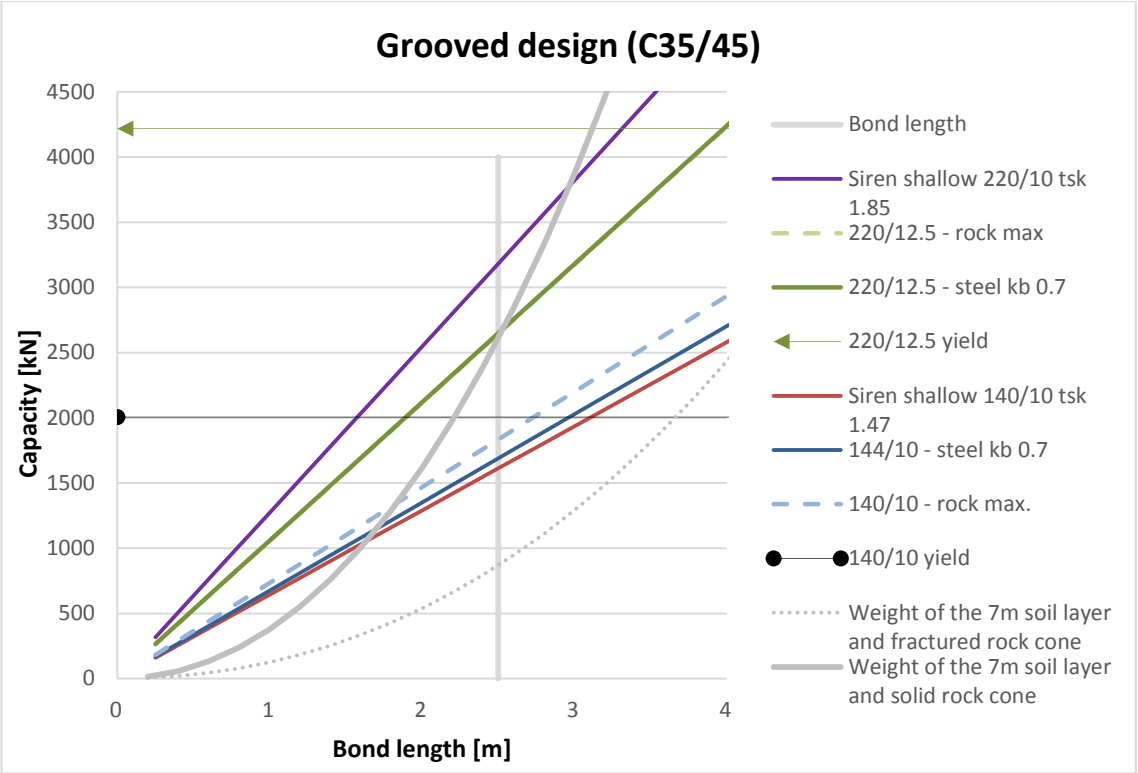

Figure 16. *Comparison of the capacity of each failure mechanism studied.*

Figure 16 represents the capacity of the pipe pile drilled and grouted into the bedrock with certain bond length and 7 m overburden clay soil layer. The calculations have been done according to tensile pile design presented in chapter 3. Also the average bond strength from the Siren`s (2015) research was used. The rock cone started from the bottom of the pile and the failure mechanism for soil layer was vertical slip surface as Majer (Niroumand *et al.* 2012; originally Majer 1955) suggested. From the Figure 16 can be seen that if the clay cone above the rock cone would be calculated it would not be the most critical failure mechanism in deep drilling depths.

Meyerhof *et* Adams (1968) suggested that the shear resistance of the clay could also be added to the ultimate uplift resistance in undrained conditions. (Poulos *et al.* p.46; originally Mayerhof *et* Adams). This would give even higher resistance to failure.

Hong *et al.* (2015) investigated the failure surface and uplift capacity of micropile embedded in sand by series of model tests. They observed sand particles plastic deformation near the micropile. From the observations they saw that in deformation there was a turning point which appeared to get closer to the micro pile when the depth increased. The point where it reached the pile was named as the critical embedded length L_{cr}. With this information they divided the pile by the embedded length of the pile to the short pile and long pile. If the pile is shorter than critical embedded length L_{cr}, failure surface will start at the bottom of the pile and the uplift capacity is depended on the shear resistance of the soil. Long micropile is deeper than the critical embedded length

and the uplift capacity is combination of soil shear resistance and skin frictional resistance on the pile as presented in Figure 17. (Hong *et al.* 2015)

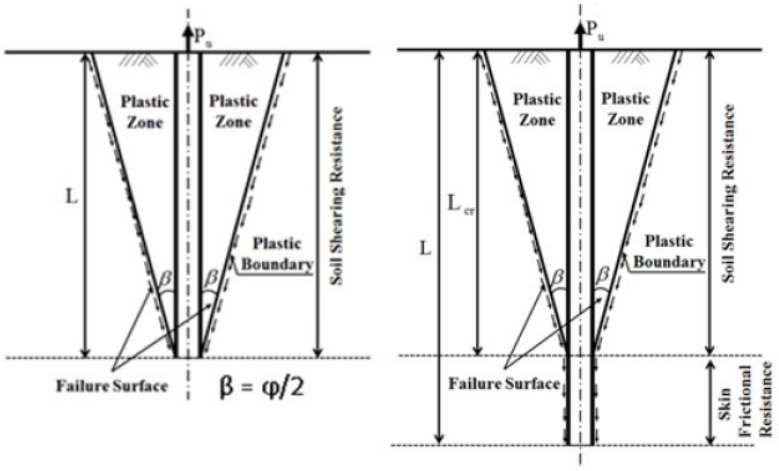

Figure 17. *The failure surface of the pile embedded in sand.* (Hong *et al. 2015)*

For skin friction and the failure surface to be developed, connection between the pile and the soil is needed. In this research the pile is drilled through soil layer and it should leave at least 10 mm gap between the pile and the soil. The pile is tested soon after drilling thus in theory there is no connection between the pile and the soil and the earth pressure or adhesion has no time to develop to form uplift resistance between a pile and a soil layer. But previous theory may explain the different approach from the literature where the rock cone failure surface starts.

Longer anchors which have reached the critical embedment length failure cone could start from the 1/3 or 2/3 of the bond length. Shorter piles may not reach critical embedment length and therefore failure surface of the cone is assumed to start from the bottom of the pile.

4.6 Effect of grout properties

Kilick *et al*. (2002) studied the grout properties of the rock bolt under the pull-out load. They confirmed many of the properties which affect the bond strength of the rock bolt. They conducted the pull-out test on rebars grouted into basalt block in laboratory. They measured the properties of the grout and monitored the pull out force in the test. They varied also the bond length of the bar and the water to cement w/c ratio and the curing time of the cement.

They observed that raising the bolt bond area raises also the maximum pull-out-load. Therefore, raising the diameter or bond length increased the maximum capacity. They also came to result that the bond strength depends highly on the strength of the grout.

Strength properties of the grout depend highly on the w/c ratio and the curing time. They get the best result with w/c ratio 0.34–0.4. Result with w/c ratio of 0.34 was marginally higher. Thus the w/c ratio needs to be controlled during the grouting to get higher bond strength. They got the highest bolt bond strength with the curing time of 28—35 days.

They also measured the Young`s modulus of the grout. The basalt block surrounding the rebar and the grout had Young`s modulus of 27.6 GPa and the grout young`s modulus varied around 0.1–9.2 GPa. The modulus for the steel was 210 GPa. They came to result that increasing the Young`s modulus of the grout also increases the bond strength. (Kilick *et al.* 2002)

4.7 Effect of the confinement around the pile

Veludo *et al.* (2009) studied the bond strength of reinforced concrete (RC) footings strengthened with micropiles. They did research including over hundred tests with grouted micropiles to study the parameters affecting the bond strength of the system interfaces. They did the test in three phases with different setups. In phase III thirty pull-out tests with textured micropiles was performed. The textured micropiles was reinforced with dywig bars and textured with steel rings (Veludo *et al.* 2009).

In Phase III all the piles which had been pulled out failed on the insert to grout interface. With smooth insert the bond strength obtained to be much smaller than in pushout test with textured insert. On the smooth piles bond strength slightly decreased with the hole diameter and embedment length did not have much effect to the bond strength. With textured micropiles in a pull-out test, the bond strength decreased linearly when the hole diameter increased and the bond strength increased with the embedment length. Bond strength also seemed to increase with the different confinement levels during the experiment.

The result of the test can be explained by the components which were presented in Figure 11 (Gomèz *et al.* 2005). When the pile is textured the frictional component of the pile is higher due to dilatation effect. It also result higher radial stress towards the confinement which create counter pressure delivering higher bond strength. If the size of the drilling hole is increased, this effect is smaller which may appear lower bond strength.

In this research the bedrock around the grouted pile acts as a confinement for the pile. When the pile is textured pulling force creates a radial stress to the grout and therefore to the confinement which is the bedrock around the pile. If the confinement has a high modulus it creates higher counter pressure delivering higher bond strength. Confinement resists the pull out force and this is why in tests which Veludo *et al. (2009)* performed, they obtained better results with textured micropiles with higher confinement.

Without confinement they also observed cracking of the concrete which lead the failure of the bond around the pile.

4.8 Summary of the findings

According to the findings it seems that the bond strength is caused due to grout properties as w/c ratio, strength of the grout, borehole or cement annulus diameter, thus thickness of the grout layer and by the frictional components as roughness of the rock on concrete or the steel surface. Also, the mechanical properties of the rock and the radial confinement on the outer layer of the annulus play a prominent role developing the bond capacity. Figure 19 from Littlejohn and Bruce (1977) is good representation of the major components which affects the bond.

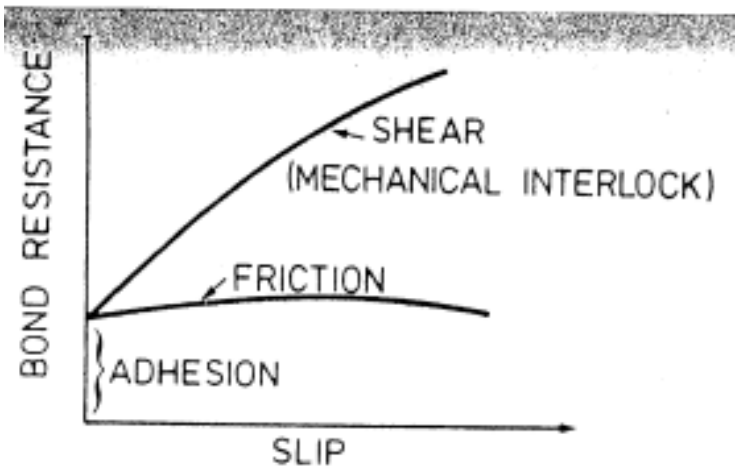

Figure 18. *Idealized representation of the major components acting on the bond. (Littlejohn et Bruce 1977)*

For the drilled and grouted steel pipe pile design, following observations from the other studies which will either lower or raise the bond strength should be noted:

1. The higher grout strength will raise the bond strength. In addition to the receipt of the cement mixture the water to cement ratio directly affects the strength of the grout and thus the bond strength,
2. The elastic modulus is a measure of stiffness of the material therefore it affects the material ability to resist permanent changes. Thus the higher modulus affect positively to the bond strength. The grout has lowest modulus between the rock, steel and grout. Thus, higher grout modulus raises the bond strength of the system. Elastic modulus of the grout has effect to the distribution of the stresses around the pile.
3. Annulus diameter affects thickness of the grout layer and through grout elastic properties to the stiffness of the grout. Wider annulus may decrease the bond strength between steel to grout surface.

4. The roughness of the rock surface improves the frictional components and thus increases the bond strength on that surface.
5. The roughness of the steel surface also increases the bond strength. Thus, it seems that it is easier to weld threads or turn grooves to the surface to improve the bond strength on grout to steel surface due to the mechanical locking and dilation.
6. The bedrock acts as a natural radial confinement and helps to create counter pressure on the pile surface due to expand of the grout.

According to findings, material properties of the grout, diameter of the annulus and friction factor of the pile are the factors controlling the bond strength in this research.

5. UNIAXIAL PULLOUT TEST

5.1 Previous field tests

5.1.1 Field test in Ylivieska 2014

The preliminary studies of SSAB drilled pipe piles under tensile forces were done by Ahomies 2014–2015 and Siren 2015 as their Master`s thesis. Both of these titles studied tensile resistance of the drilled and grouted steel pipe pile and the study was made by literature review and the pull out test. Literature reviews were made to study how to improve the pile tensile resistance and the pull out tests were made to measure the bond strength of the current design.

Ahomies (2015) studied the tensile resistance by investigating the theory of the tensile resistance from the literature review, interviews and from the implemented structures; many of these structures were combined pile and anchor structures. He also studied the grouted pipe pile bond strength by the experiment in Ylivieska. The main focus was to find out the possibility to use the grouted pipe pile to endure the tensile forces.

As the research suggests the anchored pipe piles are used in the structures like bridges, jetty structures and chimneys which are under influence of tensile forces due to lateral forces. Alternative choice for the structures to resist the tensile forces is the massive concrete slab or counterweight which usually also raise the compressive force to the pile. By the interviews Ahomies (2015) found out that the typical tensile forces in design are around 50 – 2000 kPa per pile and usually even the smallest tensile force will need anchoring.

In his study Ahomies (2015) also made a financial comparison between anchoring and the pipe which were grouted on the casing. Three pipe pile sizes (RD220, RD500 and RD800) with three different overburden layers (6m, 15m and 18) were compared. The result was that the grouted RD220 pile would be as average 25% cheaper and RD500 pile 10% cheaper than the anchoring. The RD800 was around the same price than anchored pipe pile.

The experimental study was made in Ylivieska where 15 piles were drilled and grouted 2m deep into the bedrock. In the study Ahomies (2015) used various ring bits and grouting methods for the pile installation. Preferred grouting methods were the 1 level manchette method and grouting through drilling shoe.

In the experimental test measured characteristic value for the bond strength varied between 130–414 kPA. The measured bond strength was around fourth of the design value form the Finnish piling instructions. The failure mechanism was between the pile and the grout surface. Ahomies (2014) noted that the bond strength could be higher if some modification or roughening would be made to the outer surface of the pile.

5.1.2 Field test in Masku 2015

Siren (2015) followed this path and continued to develop the tensile resistance of the SSAB`s steel pipe pile as her Master`s thesis. Literature study and field test were also made to investigate the bond capacity. Siren studied the basic failure mechanisms more closely and the factors which affect to pile designs. She discovered from literature review that the bond strength can develop by increasing the friction on the pile surface. The friction is dependent on normal force and it can be increased by shaping the pile surface.

The field test was arranged in Masku where 13 pipe piles were drilled and grouted into the bed rock that which one of the pile was instrumenting pile. There were two pile sizes from SSAB, RD140/10 and RD220/10 and two steel grades S550J2H and S440J2H. The real design for these piles was grooves at the end of the piles. The grooves had two different variations, the shallow groove and the deep groove. The grooves were designed to give higher friction between grout and the steel and thus higher bond strength. This was meant to be tested in the field test. The Figure shows the pile design. The letter "s" in the pile markings indicates the higher steel grade in the Table 6. More detailed description refers to Sirèn (2015).

The bedrock quality was investigated, and the piles were drilled into the bedrock 2.5 m depth. When drilling, the piles were flushed with pressure air and afterwards with the water, to ensure the cleanliness of the drill holes. Then the piles were grouted with Nonset 50 cement. Both the flushing and the grouting was made with the single stage tube-à`-manchette. The quality of grouting was ensured by test samples. (Sirèn 2015)

After installing the piles were pulled out by jacking. The combined maximum force of the jacks was 3.7 MN. The purpose was to have enough power to produce the pile failure. The maximum force to be used was limited by the steel grade and the grooves of the pile. In the test, mistakes also were made. At the construction site, different steel grades were mixed and thus could not be sure which pile was made from which steel grade. This limited also the jacking force. During the test, pile and the bedrock displacement, the strains and the jacking force was monitored. The strains were monitored from three stages from the instrumented pile. (Sirèn 2015)

In the test only four of the installed piles could be loaded into failure. The maximum applied load was too low for the failure for all other piles. The bond strengths can be seen in Table 7 and it is calculated from the maximum tensile loads.

Table 7. *Bond strengths of the grooved pipe piles (Sirèn 2015)*

Pile type	Groove type	Maximum tensile load (MN)	Bond strength (MPa)
RD140/10	shallow	1.6	1.47
RD140/10	deep	1.3	1.20

Pile number and type	Groove type	Bond failure load (MN)	Maximum tensile load (MN)	Bond strength (MPa)
7 RDs220/10	shallow	2.01	3.07	1.79
8 RDs220/10	shallow	2.48	3.07	1.89
9 RDs220/10	shallow	2.85	3.07	1.86
10 RD220/10	deep	no failure	2.07	1.20
11 RD220/10	deep	no failure	2.07	1.19
12 RD220/10	deep	1.93	2.10	1.30

As described before, Sirèn (2015) also noticed that the stress does not distribute evenly along the pile. The most of the stress were at the free length of the pile and the upper part of the pile. Sirèn designed the grooves to the pile tip thus it seems that it could have been more effective to design the grooves to the upper part of the pile. Now the grooves limit the yield strength of the pile even it is not affected by the maximum stress. Thus they have lower load capacity. The stress distribution which was described can be seen following Figure 19.

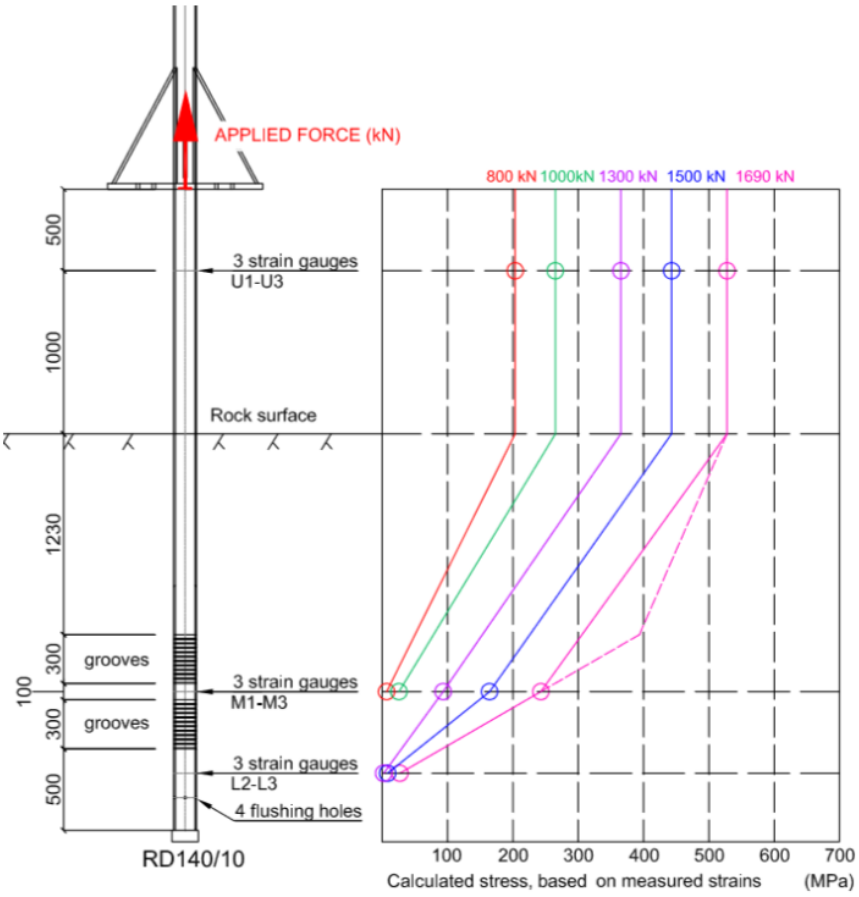

Figure 19. *Stress distribution of the grooved pipe piles (Sirèn 2015).*

It is worth to notice that Siren (2015) also calculated the bond strength according to Eurocode where can be seen that the lowest bond strength should have been between rock and the grout but from the field test results and calculation from the Table it clearly was not. Thus the design should be based on the field test results.

Table 8. *Bond strengths calculated according to Eurocode (Sirèn 2015)*

Pile number	Designed bond strength between grouting and … (MPa)			Measured average bond strength from the test (MPa)	
	Smooth steel	Threaded steel	Rock	Grooved	Note:
1, 2, 3	1.54	2.68	1.13	1.47	no failure
4, 5, 6	1.54	2.68	1.13	1.20	no failure
7, 8, 9	1.26	2.20	0.91	1.85	all failed
10, 11, 12	1.40	2.44	0.99	1.23	one failed

As for the continuing study she left clear expectations where to focus on further studies. She pointed out that the flushing and grouting process may be the key for success and the effects of the overburden soil layer to the installation should be studied. Otherwise the design of the grooves was successful according to results of her study.

The installation process was made on the top of the bedrock so they could see the installation, flushing and grouting process through the whole process. In this study piles are installed through a soil layer and therefore it may be hard to investigate if these preliminary steps are succeeded properly. It could be possible to excavate the piles afterwards but due to circumstances failure behavior was studied and analyzed by the results of the test.

5.2 Field test in Rusko 2017

This chapter describes the experimental part of the research. The field test studies tensile capacity of the steel pipe pile which is drilled and grouted to the bedrock through a soil layer and tested by a uniaxial pullout test. The test focuses to implement theory to the construction like situation which can be used in similar cases at the real construction site. Therefore, the site was chosen with similar ground conditions were piling would be necessary in usual Nordic coastal ground conditions where bedrock is under 7–10 m clay layer and a small moraine layer. The difference from the test to the real situation is that normally is not necessary to load the piles to the failure. In this case it is done for the research purposes and to study the bond strength of the system. There were also waiting time of couple weeks between drilling and grouting which may not be the case at the busy construction site.

The test was carried out in summer of 2017 between May and June at Turun Siirtomurske Oy`s yard. The test site was measured and marked according to design layout before drilling so that piles could be drilled to the right spot as planned. The test site was marked and can be seen in Figure 22. The drilling and grouting was done by Suomen Teräspaalutus Oy and Tampere University of Technology was responsible for the loading and monitoring during the pull out test. Turun Siirtomurske prepared the load structure for the load test. They cut the support piles all to the same level around 10cm over the ground level and made the pile consoles for the loading test. The loading structure can be seen in Figure 23.

Figure 20. *Marked test site in Rusko*

For the loading test, 16 support piles labelled as T1 to T16 were drilled in to the bedrock and 9 test piles labelled as P1 to P9 were drilled and grouted into the bedrock. The test piles were drilled into the depth of 2.5m and support piles minimum of 0.5m. The test piles were delivered by SSAB. Three of the piles were RDs 140/10 and six of the test piles were RDs 220/12.5. All the support piles were RDs 140/10. Steel grade of the piles were S550J2H.

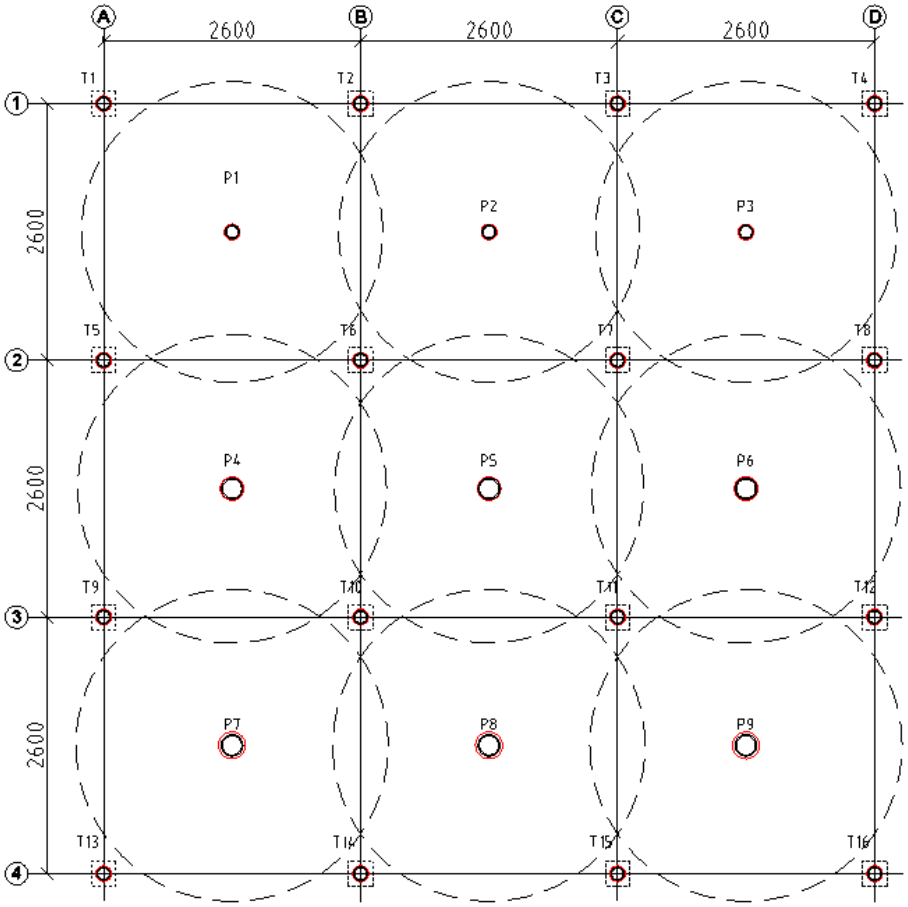

Figure 21. *Layout of the site*

Testing procedure and the site layout was designed according to guidelines from the failure criterion of the rock cone (RIL 254-2016) and available loading structure. The design layout can be seen in Figure 21. In this research it may be difficult to see the failure of the rock cone due to a deep soil layer. The layout was designed so that displacements may be seen happening with 30 degree rock cone angle if the bedrock is fractured. Otherwise the failure probably will not occur in the bedrock. That led the design layout to be a grid of 2.6 m times 2.6 m support piles where the test pile is situated in the middle. The dashed line represents a failure line of the rock cone and the dimensions are millimeters. The support piles are marked as T1–T16 which all are RDs 140/10 piles and test piles are marked as P1–P9 where P1–P3 are RDs 140/10 with ring bit size of 161 mm and P4–P6 are RDs 220/12.5 with ring bit size of 241 mm and P7–P9 are RDs 220/12.5 with ring bit size of 273 mm.

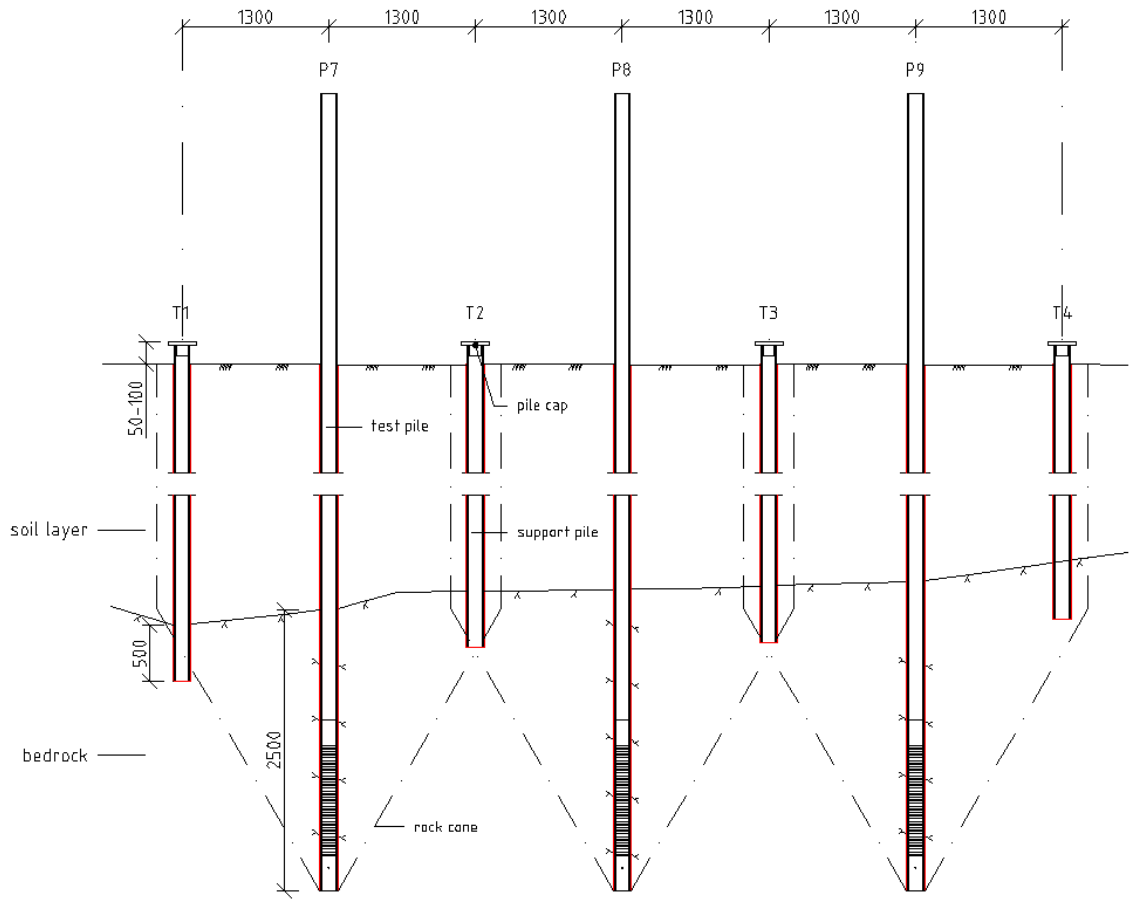

Figure 22. *Section P7 - P9 of the site design*

According to our design and by the previous experience from the study by Ahomies and Sirèn, 2.5 m drilling depth into the bedrock was chosen. From the Figure 22 can be seen a section of the site design. The bedrock level was that time for the demonstrative purposes but it actually seemed to be quite accurate. The dash dot line from the pile bottom represents the failure line of the rock cone and clay layer. The clay layer is expected to break in a form of cylinder over the bedrock.

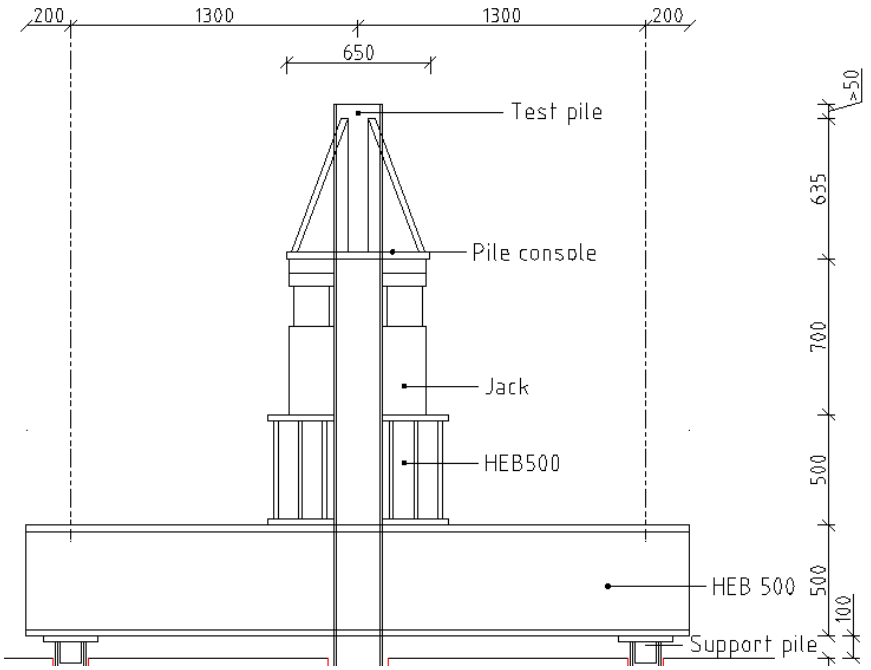

Figure 23. *The loading structure*

The loading structure around a test pile consist of four 3m long reinforced HEB500 beams, four pile caps over the support piles, four 1 MN hydraulic jacks and the pile console to transfer the pulling force from the jacks to the test pile. The loading structure can be seen from Figure 23 and 39. The main idea was to test the pile first and then move the structure to the next test pile. Pile consoles were already welded to all test piles.

5.2.1 Ground conditions

The construction site was located in Rusko. The ground conditions consist of around 0.5–1.0 m deep filling layer, 5–7 m deep clay layer and the granite bedrock. The conditions were known from the experience of the landlord and were estimated with the test drills. From the database of the Geological Survey of Finland (2017) can be seen that the soil at the site is clay and the bedrock is plutonic granite rock. It is worth to notice that the site is situated next to transition zone of the bedrock where the rock changed from biotite paragneiss to granite. By the drill chipping and the rock samples, which could get during drilling, the bedrock was estimated to be granite with some gneiss particles as seen in Figure 24. Granite was estimated include lots of quartz.

Figure 24. *Gneiss and granite particles from the site*

During drilling the driller estimated bedrock to be a firm rock. The way of the fracture for the rock is brittle and the compressive strength of the Finnish granite is estimated to be around 200 – 250 MN/m^2 and gneiss 140 – 300 MN/m^2. The tensile strength of the rock is around 10% of the compressive strength. (Rantamäki *et al.* 2009). According to previous information the bedrock should be firm.

5.2.2 Pile types

All the pile elements which were used can be seen in Figure 25 and was delivered and manufactured by the SSAB. All the piles were either RDs 140/10 with outer dimension 139.7 mm and wall thickness 10 mm or RDs 220/12.5 with outer dimension 219.1 mm and wall thickness 12.5 mm. All the piles were made from high yield strength steel S550J2H. According to inspection certificate the piles and the parts meet the demands of European standards by European technical assessment ETA-12/0526 and are CE marked. The welds are tested with NDT-test by SSAB and the yield strength from tensile test clearly exceeds the declared strength. By the chosen steel grade S550J2H and the chosen groove type, better yield strength and bond strength should be acquired based on the previous research. Also 12.5mm wall thickness chose to be used to avoid any limits to the yield strength during the loading. For RDs 140 piles only 10 mm wall thickness was possible.

Figure 25. *RDs pile elements*

All the 9 test piles were made from 12m elements. Three of these piles were RDs 140/10, and six of the piles were RDs 220/12.5. Test piles were cut into two parts before delivery, 1.5 m part and 10.5 m part. The smaller bottom part of the elements were grooved with the similar profile to Siren`s (2015) shallow profile. Also four holes with diameter of 11.75 mm were made to the bottom of the piles for the flushing and grouting. The lower profile of the piles can be seen in Figure 26.

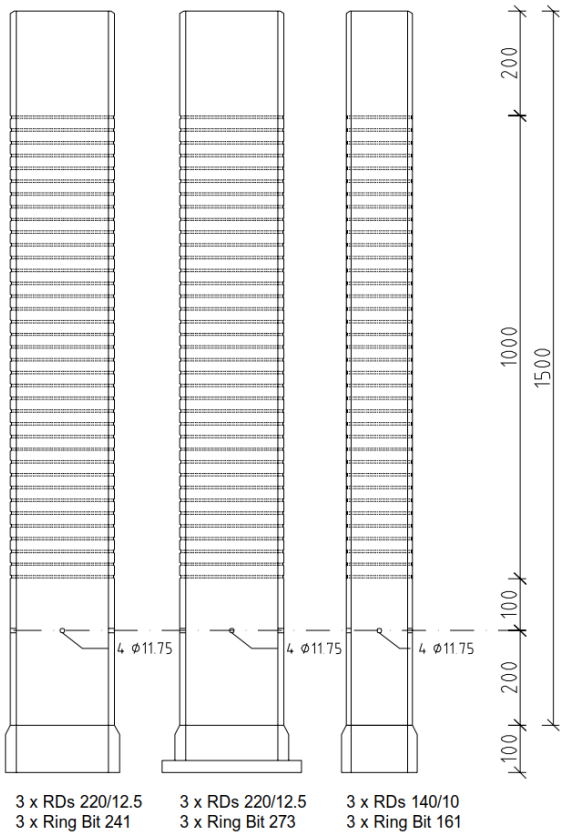

Figure 26. *Grooved pipe pile design*

At the test site the lower part of the pile and upper part was joined together by manual metal arc welding. Ring bits were also added to the piles by welding to complete the test pile profile. The complete pile structure can be seen in Figure 27.

Figure 27. *Grooved part of the test pile and final RDs 140/10 piles*

The support piles were 12 meters long RDs 140/10 elements which ring bits were added at the site before drilling. To the test it was chosen to use 12 m elements due to ground conditions at the site. Thus pile splices may not needed during the drilling phase. All the 16 support piles were without grouting holes or grooves. These piles were used to support the compressive load from the loading and conduct it to the bedrock. The carrying capacity of the clay layer would have not been enough to support the pressure from the loading and weight of the load structure. This is also how the load structure would not interfere with the results of the loading process.

5.3 Drilling

5.3.1 Drilling equipment

Suomen Teräspaalutus used excavator with separate SPD drilling rig and separate compressor for the drilling which was proven to be very flexible combination. The drilling rig which can be seen in Figure 28 used compressed air for the down the hole hammer and for the flushing the soil from inside. Water was used to bind the dust and the drill cuttings while drilling. Water could also be used to flush the pile from inside after drilling.

Figure 28. *Drilling rig and compressor*

The pilot bit for the support piles was one from Atlas Copco with separate reamer and casing shoe. The pilot and the reamer from Atlas Copco can be seen in Figure 29. Robit`s and Atlas Copco`s solutions for the reamer and casing shoe was a bit different. Atlas Copco`s model had a separate casing shoe which was welded to the pile before reamer installation. The reamer was attached to the pilot bit just before drilling after the drilling rod, hammer and pilot was installed through the pile case.

Robit`s model had a reamer integrated into the casing shoe which was welded to the pile. Thus when the reamer was not separate, the piles could be lifted from the hole to ensure that the grouting valves was on place after drilling process and the reamer would not fall off. The integrated ring bits were also chosen for the test because it makes the failure more plastic due to its oversize comparing to the steel pipe pile. Robit also offered better solutions for the ring bits due to its reamer size options. Reamer was chosen to be 10–30 mm oversized so that the test could be done with different sizes of annulus which was needed for corrosion protection.

Figure 29. *The pilot bit and the reamer from Atlas Copco*

The method for the drilling was down the hole concentric drilling which was described in chapter 2.3. The pilots for the drilling were DTH-Prime and DTH-RoX DS. Ring bits for the test piles was DTH-Prime 139.7/10 with reamer diameter of 161 mm , DTH-Prime 219.1/12.7 with reamer diameter of 241 mm and DTH-RoX DS XL2 with the oversized reamer diameter of 273 mm which can be seen in Figure 31. Pilots and ring bits can be seen in Figure 29 and Figure 30. Four inch down-the-hole hammers were used for the RDs 140 piles and six inch hammers were used for the RDs 220 piles.

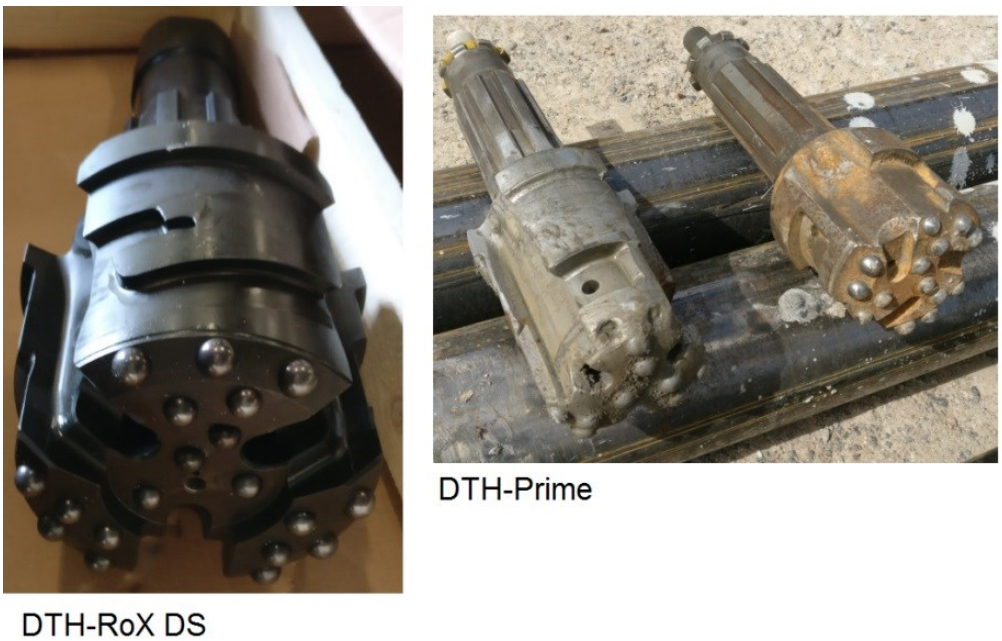

Figure 30. *Pilot bits which was used for drilling*

Figure 31. *Robit DTH-Prime (left) and DTH-RoX DS XL2 (right) ring bits*

The grouting valves were installed into the grouting holes just before drilling. Grouting valves which can be seen in Figure 32 were used to prevent grout to flow back to the pile after grouting. Valves were installed into the holes with a hammer. The tolerances were designed so that the valve would fit tightly into the hole. According to manufacturer valves opens with the 2/3 bar pressure and can ensure 50 l/min grout flow. Thus at least 2/3 bar over pressure is needed for the grouting.

Figure 32. *Grouting valves before and after drilling*

For the test purposes valves were also checked from the piles P4 and P1 if they still are intact after drilling process. One of the 8 valves got sucked halfway into the pile; otherwise they seemed to be intact.

5.3.2 Drilling process

The drilling was done in two phases. At the first phase support piles T1 to T16 were drilled into the bedrock at least to the depth of 0.5m. In the second phase test piles P1 to P9 were drilled exactly 2.5 m to the bedrock. Due to limitations of the machinery it was better to drill some of the support piles deeper to the bedrock so the drilling rig could move more flexibly at the site. Drilling started from the support piles and while support piles were installed the test piles could be prepared for the drilling. This way the pilot bit needed to be changed only after first 16 piles. The preparation included welding pile parts together and a ring bit and a valve installation.

While drilling piles some machinery problems were encountered but the drilling itself was successful. At first the driller noticed that the bedrock may be fractured due to drilling speed but after first pile T1 he changed his mind due to slow drilling speed. From the drilling speed and drill cutting it was clear that there were around 0.5 to 1.0 m filling layer and 6 to 7 m clay layer over the bedrock. The pile could be pushed through clay layer and while flushed with the pressured air. Pressured air clearly conducted into the soil while drilling the piles. This was observed due to ground movement while drilling. This was noted only few of the piles.

During drilling, drill cutting samples were taken and observed. The moraine layer was not noticed by the drilling. The end blows to the top of the piles were done with the drill hammer to all support piles to ensure the contact with the bedrock. This was not necessary with the test pile due to grouting and tensile load.

The exact drilling and the soil depths for the test piles can be seen from the Table 9 below. The pile P6 was risen 10 cm during grouting phase and therefore the depth varies a bit.

Table 9. *Drilling depth of the test piles*

[m]	**P1**	**P2**	**P3**	**P4**	**P5**	**P6**	**P7**	**P8**	**P9**
Soil	7	7,15	7,7	6,1	7,05	7	6,2	6,45	6,65
Bedrock	2,5	2,5	2,5	2,5	2,5	2,4	2,5	2,5	2,5

The final test site after the drilling can be seen in Figure 32. At this point it was clear that some of the test piles were too short for the load structure assembly and thus they needed to be continued by welding extra lengthening pieces.

Figure 33. *The test site after drilling*

5.4 Flushing and grouting

5.4.1 Flushing of the annulus between pile and the bedrock

Flushing of the piles before grouting was designed by the present instructions and by the previous studies. Finnish guideline for the geotechnical design according to Eurocode (Liikennevirasto 2017) guides that the grout annulus should be flushed with water volume at least 5 times the size of the annulus volume or at least with 300 liter. In previous research 1000 liter of water was used for flushing. Due to different annulus sizes and to ensure proper flushing, water was used 500 liter for piles P1 – P3, 750 liter for piles P4 – P6 and 1000 liter for piles P7 – P9. For exact information refer to Appendix 1.

Flushing was done with the same single stage tube-a-manchete method than grouting. At first the manchette was laid down to the pile bottom and then lifted 400 mm to ensure that manchette is just over the grouting valves. The manchete was tighten either with the pneumatic jack in RDs 220 piles and with hydraulic pressure in RDs 140 piles due to different type of tube-a-manchette setup. Both tube-a-manchettes can be seen in Figure 34.

Figure 34. *Tube-à-manchettes*

The water valve was then opened and flushing started. The water gauge was used to ensure the right water volume for flushing and the pressure of the water was followed with the pressure gauge. At first the flushing was made with grout mixer which had 8 bar pump. The pressure of 3 bar water flow was obtained with the grout mixer. After the first pile the water tube was connected directly to the main water line. The water flow was around 50−70 liter per minute according to water meter. After the designed volume had reached, the grouting was done immediately after flushing. Thus it was easier to use main water line for flushing so that the grout could be prepared with the cement mixer at the same time.

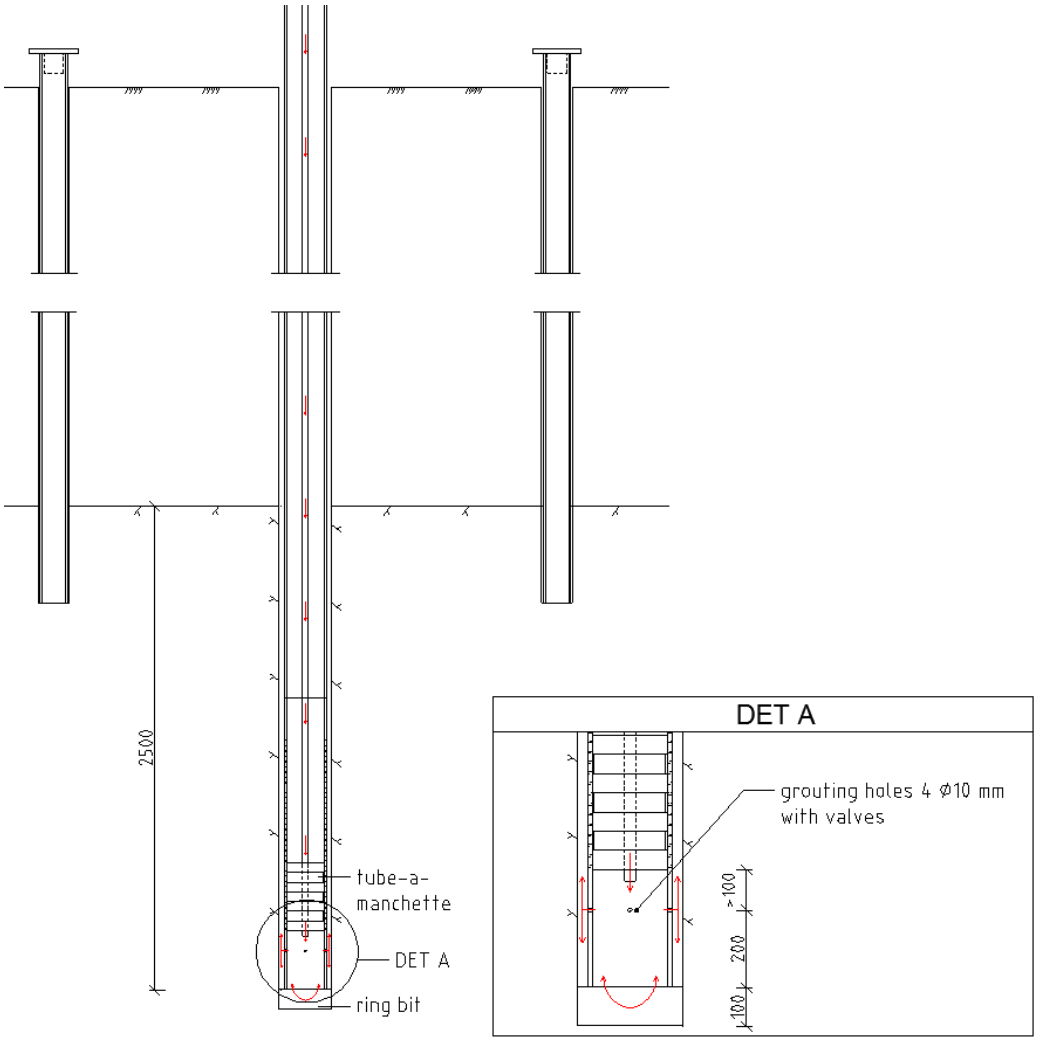

Figure 35. *The design of the flushing and grouting process*

Flushing pressure varied between 2 – 4 bars. It seemed that the water started flowing after 4 bar pressure was reached and after that the pressure dropped around 2 bars. The route of water flow could not be confirmed if it went through the valves or through the pile bottom. Some of the flushing water from the larger piles did find its way to the annulus of other piles and rose to the surface. Also a water stream could be found from the ground level around 10 meters away from the test pile P9. This should be normal phenomena and it should not affect the test. After flushing was done with a pile then the line was connected to the cement mixer and grouting was started.

While the flushing and grouting process was started there ended up having problems with the first manchette which could not endure the pressure and got broken. The manchette was replaced next day. There were some problems with the piles also. Pile number P2 was clearly clogged and the water could not flow into the pile. The manchette was moved upper position to the 50-60 cm from bottom and the pressure was lifted up until 100 bars but still the holes did not open. The pile was tried to lift up with the excavator but it did not move at all. The pile was decided to test afterwards without the

grouting because it could not be flushed and grouted or even lift from the ground. It is possible that the drill cutting or clay was fallen down to the annulus and clogged it.

Challenges continued with flushing process on pile number P5. The pressure was raised until 18 bar when our water tube got broken. At the same time the pile opened and water started flowing when the water tube was changed. The pile managed to be flushed with 1.5 bar pressure straight from the main water line.

Pile number P6 also got stuck but it managed to get open with flushing pressure of 12 bars. At the same time pile rose upwards 10 cm from the drill hole which can be seen in Figure 33. At this point flushing and grouting was continued because the studied bond strength does not actually depend on the bond length thus the results from the test will still be comparable. Later same problem occurred with pile P4 while grouting and it started rose continuously. The pile was first anchored to the support pile and after grouting pushed back with the HIAB crane which was used to lay down the tube-a-manchette into the piles.

Figure 36. *P6 RDs 220 pile which rose from the ground*

During the flushing and grouting process piles number P4 to P6 was also welded a small joint where the tube-a-manchette could be anchored so that the tube would not rise from the pile. Although the pressure was so high that when it could not move the manchette, two of the piles mentioned rose from the drilling hole instead. The pile P4 was already lifted from ground after drilling when the valves were checked, so the movement of pile could be expected.

5.4.2 Grouting

Grouting was designed so that the pile would have a grout layer to make a connection between the bedrock and the pile to withstand the tensile load and have at least 10 mm thick grout cover to protect from corrosion. Thus for the research ring bits with oversized reamers was used. With thicker grouting layer, horizontal cracks which may occur during the loading cannot reach the grout surface and therefore impurities cannot conduct to the pile surface. If this could happen and corrosion would occur on the pile surface it may break the bond between the pile and the grout and therefore lower the bond strength and tensile capacity of the pile. Although literature review indicates that thick grout layer can also decrease the bond strength of the pile due to lower stiffness of the grout material compering to the bedrock or the pile.

By the ring bits available from the supplier, grout layer thicknesses 10.5 mm and 26.5 mm were chosen. According to instruction and by the previous research, annulus between the pile and the bedrock should be grouted at least three times of the volume of the annulus to ensure proper grouting quality.

Grouting was done after flushing process as described in Chapter 5.3.1. The tube-a-manchette was laid down to the pile with the HIAB crane and tightened to the pile 40 cm from the pile bottom as shown in Figure 32. The pile was flushed and after the tube was connected to the cement mixer the grouting process was started. Grouting pressure with grout mixer was assumed to be 3 bars as measured with water flow meter before. Grout mixer can be seen in Figure 37. The maximum pressure of the pump in the mixer was 8 bars. The volume of the mixer was for total 200 liters which means that 100 liters of grout could be ready in the lower chamber and 100 liters could be at the mixing chamber at the same time. The designed mass for the grouting varied between 60 to 200 liters. With the equipment available, grout mass was not easy to measure accurately so these two chambers actually helped to divide a grout batch in to two parts for proper amount.

The grouting was done in two phases. The first phase was to grout a pile three times the volume of annulus plus volume of the pile tip. Second phase was to release the tube-a-manchette and continue grouting with the second part of the batch and lift slowly the tube-a-manchette up from the pile. The second phase was made to provide counter pressure and may prevent grout backflow from the annulus. The piles had also grouting valves installed to prevent the backflow but grout could flow back to pile from the bottom of the pile. Thus the grouting quality wanted to be ensure. When the designed volume of the grout was used the manchette was completely lifted up and moved to next pile.

Figure 37. *The grout mixer*

Nonset 50 cement was used to make the grout. Nonset 50 is cement based grout which is used for anchoring reinforcing steel bars and it was also used in previous research. It is 1—3% expandable grout with maximum grain size of 0.2 mm. It can be used if the temperature is at least +5 degrees Celsius. Nonset 50`s compressive strength after 28 days is 45 MPa and tensile strength is 6 MPa. 1 kg of grout mass consumes 1,3kg of Nonset 50 which means that 25 kg with 10 liters of water can make around 20 liters of grout mass which water to cement (w/c) ratio is 0.4. Bleeding of the grout is under 0.5%. Elastic modulus of the grout was unknown due to lack of response by the supplier.

The grouting process took for total two and a half day. On the first day the weather at the site was rainy and temperature was around 10–11 degrees Celsius. On the second and third day the weather was sunny and the temperature rose to the 18–20 degrees Celsius. Thus the condition for the grouting was good. Grouting continued to the third day mainly because pile number P2 was clogged and stuck in the ground. The pile was not managed to get it open or lift from the ground. The detailed specification for the flushing and grouting process is shown in Appendix 1.

On the first day P1 to P3 (RDs 140) piles were flushed and grouted. The tube-a-manchette for the smaller piles did work very well. The manchette for the RDs 220 piles got broken on the first try and was replaced on the next day. Thus the process started from the smaller piles P1–P3. 60 liter of grout mass was used for the grouting; 40 liter for the first phase and 20 liters for the second phase. 60 liter grout mass was made from 75kg of cement and with 30 liters of water. Thus the w/c ratio was 0.4. The volume of the grout mass was divided to two batches approximately from the cement mixer. The grouting process did go as planned for the piles P1 and P3. The pile number P2 was

clogged and it tried to get open on the third day without result. It decided to be loaded without grouting.

On the second day flushing and grouting was done for the piles P4 to P9 with the new tube-a-manchete. Grouting started from the pile number P7. The manchete was laid down to pile as deep as it did go and the flushing and grouting process started. The grout was used 200 liters for the piles P7 to P9 due to larger reamer size 273 mm. In this process the grout mass was divided 150 liter for the phase one and 50 liter for the second phase. When the grouting was in progress problems was not encountered with pile number P7. Although it could be pointed out that the tube-a-manchette rod was covered with grout up to the 6 m from the bottom. The grout seemed to go up to the pile in the second phase of grouting.

After the pile P7 manchette was moved to pile P8. When the manchette was laid down to the pile, it was noticed that mistake was made with the pile P7 because the tube-a-manchette went deeper than with the previous pile. There were also noted some problems when the manchette was laid down to the pile. The manchette got stuck around 1.5 m from the bottom. It was immediately noticed that it was probably the weld in the pile joint where manchette got stuck. The manchette was lifted up from the pile and measured on the ground surface. The length of the manchette was 12.1 m so exactly the same than our test piles. Therefore, with the P7 the manchette were somewhere just over the joint 1.6 m from the bottom. Refer the Figure 38. From the technical point of view the grouting process with the pile P7 did not go as planned. The annulus was grouted only two times its volume at first phase and there is a risk that the grout has been mixed with the water. If the grout have displaced the water from the annulus and mixed with the water inside the pile it would make the w/c ratio approximately around 0.6.

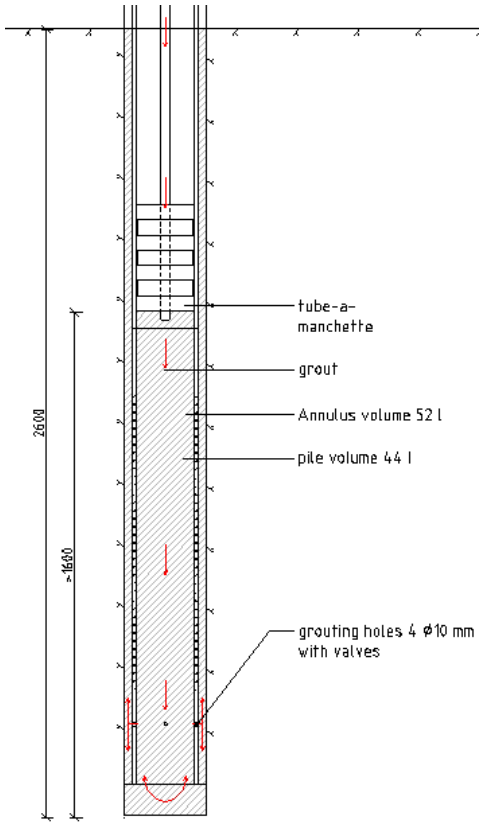

Figure 38. *Grouting process of the pile P7*

After the manchette was measured and could be verified that it is at right level inside the pile the flushing and grouting process continued. On the pile P8 200 liters of grout was used in two phases. Some problems were encountered when installing the tube-à-manchette but otherwise grouting process did go as planned. The rubbers in the manchette needed to be repaired after the grouting because it got stuck inside the pile. This was not major issue but slowed the work in progress. After pile P8 the P9 was grouted without any issues.

After larger reamer sizes pile numbers P6–P4 on the next row was grouted. For the piles P4 to P6 the grout mass was 135 liters which meant 175 kg of cement. Thus the first batch was 100 kg and the second 75 kg which meant around 75 liters of grout in faze one and 60 liters of grout mass in phase two. With this method the pile annulus could be grouted 3 times the volume. After the issues in flushing process, the grouting went according to plan expect one break down. While grouting pile P5 the grouting tube got broken and around 10–20 liter of grout got lost. The tube got changed and 20 liters of grout was added to mass recover the loss. After these piles the grouting was completed and the grout was let to settle for 29 days.

5.5 Loading

Design for the loading structure was mostly same which was used in previous (Sirèn 2015) study. Difference for her research was the length and size of the upper steel beams. These beams were longer thus it gave more space to examine the movement of the soil. The loading structure for the test which can be seen in Figure 39 composed of four steel beams, four hydraulic jacks and the loading console which was welded to the test pile. Idea was to use the jacks to lift the console structure which was welded to the pile. Thus the tensile force was induced to the pile. The force and displacement of the pile was measured and recorded electronically.

Figure 39. *The loading structure and the test site*

The steel beams was laid over the support piles which will conduct the compressing force to the bedrock and thus it do not disturb the soil around the pile and interfere with the test results. The steel beams used for the loading were 3 meters long reinforced HEB 500 beams. These were calculated to endure the maximum force from the hydraulic jacks. The hydraulic jacks which can be seen in Figure 40 were RRI-10010 jacks from Enerpac which were driven by Enerpac ZE4440MW compressor unit. The maximum capacity for the hydraulic jacks was 931 kN per jack and the maximum pressure induced by the compressor was 700 bars. For total the jacks could therefore lift up to 3.7 MN. The force could be controlled by the pressure screw from the compressor unit. The controller screw was not quite accurate method for controlling the uplifting force due to pressure changes in the system.

The force was measured with the load cells which were installed between the console structure and the jacks. There were also two calottes with spherical surface on both sides of the load cell to ensure that the load cell is at balance and measures only vertical force component. The load cell type was BL-100TE from Kyowa which could monitor a maximum load of 1 MN. Force was recorded on every second.

Figure 40. *Hydraulic jacks and load cells*

Displacement of the pile and the soil were also monitored during loading. Under the steel beams next to the pile a steel rack was installed for the displacement gauges. Two displacement gauges were installed on both side of the pile to monitor the displacement of the pile. As seen in Figure 41, steel bands with two metallic corner pieces were installed to pile surface and two displacement gauges to the rack next to pile. The displacement sensors were installed so that the sensor touched the metallic corner piece on the pile. In the gauge was spring which try to push the sensor upwards. The corner piece was made to prevent the movement. Thus when the pile moves upwards due to uplifting force the corner piece and the sensor also moves upwards and measures the displacement. The sensors displayed an average displacement from these two sensors. Model of the sensors was Novotechnik TRS 100. Accuracy of the sensors was 0.002 mm and the maximum displacement of 100 mm. Measuring interval for the test was 1 second. Results for the test could be seen live from the computer as force – displacement graph.

Figure 41. *Displacement sensors*

There were also two laser displacement sensors installed to the rack. These sensors were installed away from the pile at the distance of 50 cm and 110 cm. Idea for the sensors was to observe the ground movement around the pile on the soil surface. The laser was pointed on to the soil surface thus it could measure variance of the distance to the rack. This position was calibrated as zero thus the difference could be seen if the displacement occurred. After installation there was some fluctuation on the results of the sensor so accuracy of the laser was estimated to be around 1 mm probably due to disturbance from the sunny weather conditions.

The steel rack which was used for the displacement gauges was placed so that the foot of the rack would be as far they would not interfere with the results. In other words the rack would not move or rise with the soil. The leg of the rack was nearest at 1,8m from the pile surface. This was further than the theoretic rock cone failure and thus would be far enough.

5.5.1 Estimated tensile capacities

Tensile capacities for the different failure modes were calculated according to Finnish piling instruction (RIL 254-2016) so that it would be easier to estimate how the loading should be done and which point the failure should occur. Figure 42 was made from the calculations. The maximum force from the loading jacks was 3.7 MN. From the Figure 43 can be seen that the yield strength of the piles with diameter of 220 mm was higher than the highest loading force so it could not be the issue. Only piles with diameter 140 mm the yield strength could have been the liming factor although both of the rock and the pile surface have lower tensile capacity and thus should fail before the structural failure of the pile. The yield strength was calculated based on the manufacturer material certificate and by the shallow grooved design.

Based on the previous research by Sirèn (2015) and Ahomies (2015) the tensile capacity on the rock surface should not be the issue even it should have lower tensile capacity by the calculations. Therefore tensile capacity on the pile surface is studied in this research.

Based on the average bond strength from the Sirèn`s research the average tensile capacity for the piles could be calculated by Equation *(2)*.

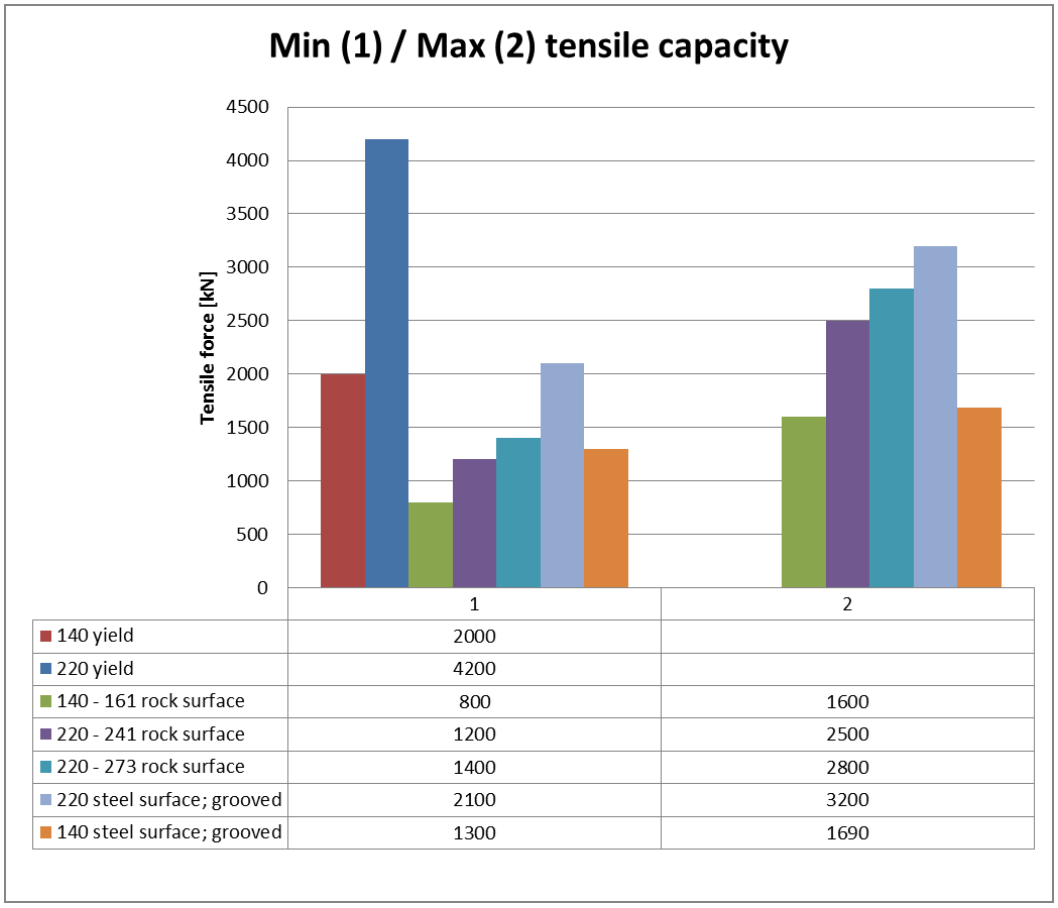

Figure 42. *Minimum and maximum tensile capacity for the estimated failure modes before loading [kN]*

5.5.2 Loading steps

The test was decided to make as a static loading test with 10 loading steps. On every step the waiting time was at least 5 minutes or the time when displacement did not occur anymore. Every test had more than 10 loading steps if the displacement did not reach the maximum of 100 mm. The loading steps were decided to be after every 200 kN for the piles with diameter of 220 mm and 150 kN for the piles with diameter 140 mm. The loading speed was around 50 kN per minute.

After the first test on pile P7, the loading steps were changed to be 250 kN for the piles P8 and P9 and 300 kN for the piles P4–P6. The loading was not quite accurate due to inaccurate pressure operating system. It took some time for the system to stabilize when the loading stopped or in other words the raising of pressure stopped. Thus the variety for the loading steps were around 10–30 kN. Actual loading steps and total loading times can be seen in Table 11.

Table 10. *Loading steps of the test*

Time	32 min	78 min	122 min	47 min	78 min	94 min	101 min	132 min	130 min
Loading steps	P1 (140/161)	P2 (140/161)	P3 (140/161)	P4 (220/241)	P5 (220/241)	P6 (220/241)	P7 (220/273)	P8 (220/273)	P9 (220/273)
Step 1	175	155	215	160	200	145	175	245	160
Step 2	300	300	300	300	300	302	1050	505	250
Step 3	495	535	455	655	635	615	1220	745	515
Step 4	649	675	605	885	905	912	1440	1005	750
Step 5		775	755	1190	1225	1245	1630	1225	1035
Step 6		930	905	1228	1525	1545	1840	1535	1270
Step 7		1150	1050		1795	1865	2045	1785	1520
Step 8		1370	1205		2135	2145	2240	2045	1770
Step 9		1525	1370		2415	2420	2460	2285	2015
Step 10		1608	1505		2596	2690	2680	2560	2270
Step 11			1670			3496	2868	2785	2520
Step 12			1790				2944	3074	2785
Step 13			1991					3310	3020
Step 14								3489	3285
Step 15									3580

The loading was started from the pile number P7 and continued to piles P8 and P9 which were piles with reamer size 273 mm. The continued afterwards with the piles P6–P4 with reamer size 241 mm and finally with the smallest reamer size 161 mm P1–P3. Loading was monitored with the load cell and displacement gauge and recorded to computer log every second. From this raw data could be drawn force, displacement graph which helped to monitor the behavior of the pile during loading. The force – displacement graphs for the piles can be found from the appendices 2–13.

Some technical difficulties were encountered on the first loading cycle and only 1 MN maximum force could be obtained. The pile number P7 was tested and loaded two times to the load of 1 MN and the force was dropped to zero. The problem was solved after pressure regulation valve was found from the compressor and the test could be continued as originally planned.

6. RESULTS AND DISCUSSION

6.1 Results

Summary of the results from the uniaxial pull out test is presented as force displacement graph in Figure 43. Development of bond strength is shown as graph in Appendix 15 and is calculated in Table 11 and 12. Individual graphs for the test piles and raw data on every loading step is presented in Appendices 2–16. In displacement graphs the net displacement of the pile refers to displacement where elastic strain is reduced from the measured total displacement. In literature three failure criterions were presented for ultimate settlement failure. These are net displacement which corresponds to 0.5%–1%, 5% (SPO-95) or 10% (RIL 254-2016) displacement of the pile diameter. Net displacement which corresponds to 5% and 10% of diameter of the pile is calculated as capacity failure criterion. The bond failure criterion is determined from the point where the net displacement reaches 1% of the pile diameter. At first piles are assumed to fail from the steel to grout surface and afterwards as combination of the failure modes. All the piles were loaded until failure.

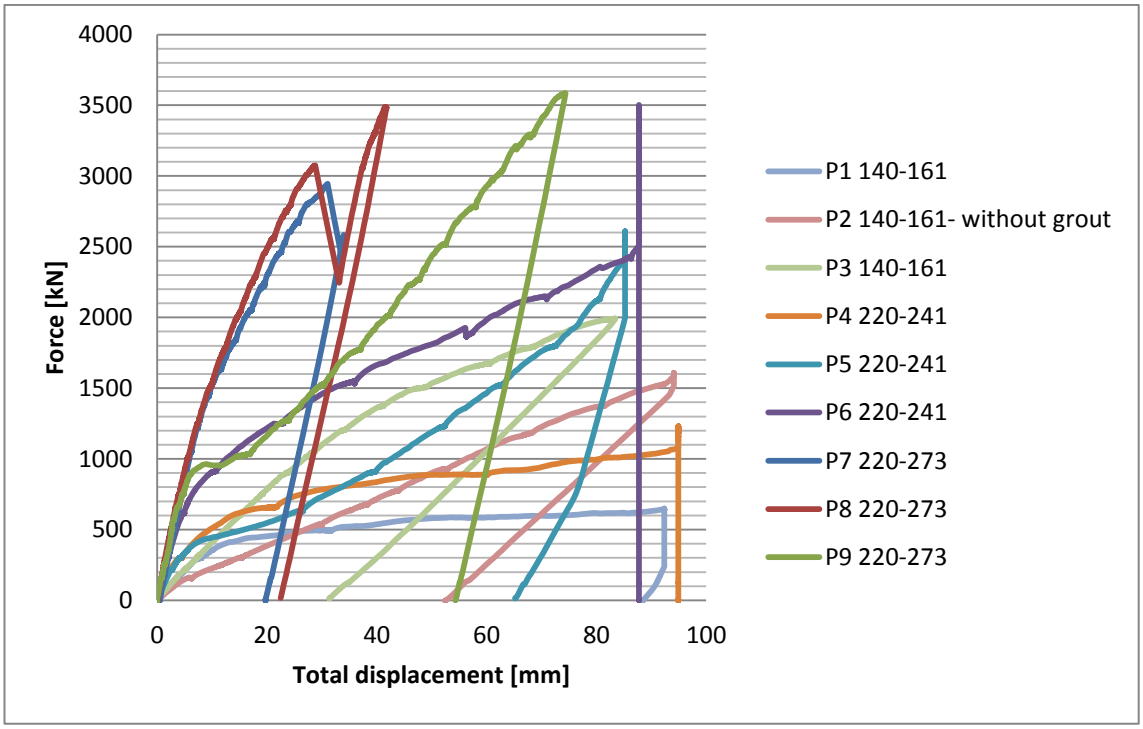

Figure 43. *Force - displacement graph of tested piles*

All the piles expect the pile P7 were loaded until the maximum displacement which could be measured or until around 90% yield strength of the pile was reached. On piles

P3, P8, P7 and P9 yield strength was limiting factor during loading. All other piles reached the maximum measurable displacement before yield strength. The highest load peaks of 2944 kN, 3485 kN and 3585 kN could be measured with piles P7–P9 with the reamer size of 273 mm and resistance of 1979 kN could be measured with pile P3 with reamer size of 161 mm.

In Table 11 three individual events from the loading process are presented. The first point is the bond failure where the net displacement grew over 1% of the pile diameter. It is the point where the bond failure is assumed to happen. The 5% and 10% are indicated as capacity failure criterion. These are the points where plastic failure occurs and the rate of the displacement starts to grow rapidly. The bond strength is calculated from the capacity at the bond failure. Higher capacity gives information about the capacity due to friction and interlocking effect of the pile. Displacements at the these points are also presented in the Table 11.

Table 11. *Tensile capacities net displacements analyzed by the literature*

	P1	P2	P3	P4	P5	P6	P7	P8	P9
Tensile capacity at 5% [kN]	**380**	**216**	**543**	**602**	**476**	**1147**	**2530**	**2866**	**1130**
Displacement at 5% [mm]	7	7	7	11	11	11	11	11	11
Tensile capacity at 10% [kN]	**448**	**340**	**959**	**741**	**627**	**1457**	**2938**[1]	**3068**[1]	**1509**
Displacement at 10% [mm]	14	14	14	22	22	22	16,9	13,7	22
Bond failure at 1% [kN]	**129**	**73**	**138**	**278**	**277**	**750**	**1440**	**1497**	**921**
Displacement at 1% [mm]	1,4	1,4	1,4	2,2	2,2	2,2	2,2	2,2	2,2
Bond strength at 1% [MPa]	**0,12**	**0,07**	**0,13**	**0,16**	**0,16**	**0,44**	**0,84**	**0,88**	**0,54**

([1]). Piles were loaded until failure which occurred around 6% displacement mark

Previous method to analyze the result is mechanic way to approach the result. It is used in compressive load for settlement and thus may not fully relate to tensile load. Therefore, following results for the failure in Table 12 are visually extrapolated from the loading graphs and the raw data. These are the points where the rate of displacements started to grow. These results are at the conservative side and are considered better conclusion than capacities presented in Table 11 by the estimate from the literature.

Table 12. *Estimated bond capacity from the displacement curve*

	P1 (140/161)	P2 (without grout)	P3 (140/161)	P4 (220/241)	P5 (220/241)	P6 (220/241)	P7 (220/273)	P8 (220/273)	P9 (220/273)
Estimated bond failure at [kN]	**380**	**217**	**543**	**440**	**417**	**913**	**1440**	**1497**	**921**
Displacement... [mm]	7	7	7	5,5	5,5	5,5	2,2	2,2	2,2
...of the pile d	5,0 %	5,0 %	5,0 %	2,5 %	2,5 %	2,5 %	1,0 %	1,0 %	1,0 %
Bond strength [Mpa]	**0,35**	**0,20**	**0,50**	**0,26**	**0,24**	**0,54**	**0,84**	**0,88**	**0,54**

6.2 Discussion of the results

6.2.1 Introduction

Loading and monitoring of the data was successful process and finished without major difficulties. During the loading it seemed that most of the piles rose steadily from the ground and any major breaking point did not occur. At first the piles seemed to give more resistance for the movement until it reached a point where rate of displacement started to grow. This can also be seen from the results that the displacement were rather high in this test.

Often displacement started to grow before failure. The clearest breakage could only be seen on piles with 273 mm reamer. On pile P9 in Figure 44 can be seen the actual breakage when the force drops and displacement grow rapidly after failure.

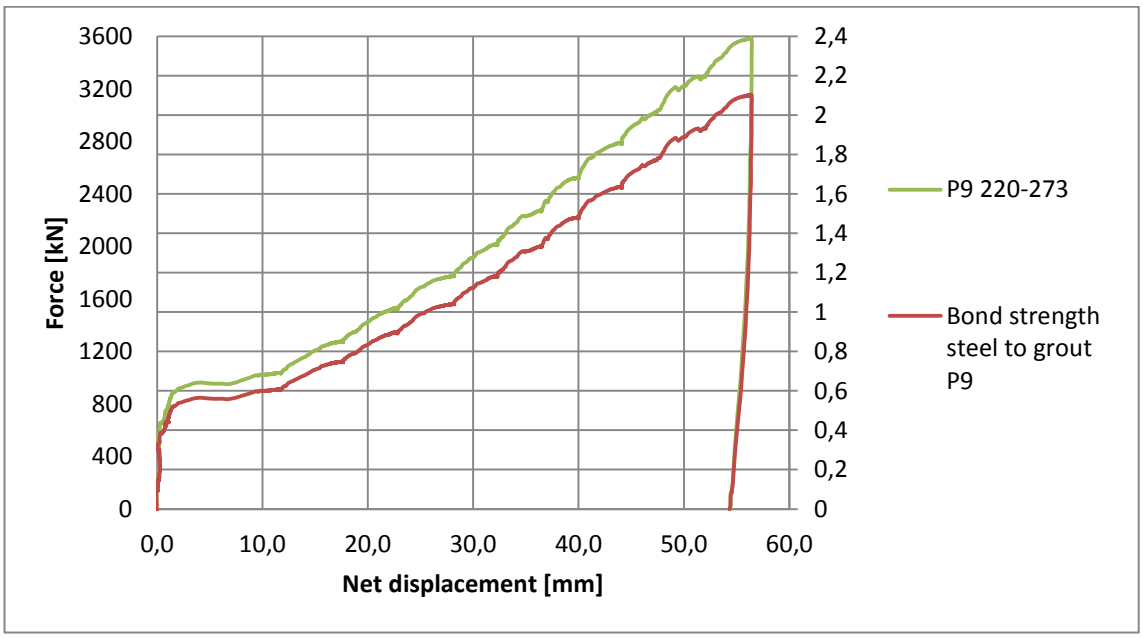

Figure 44. *Displacement curve of the pile P9*

Also while loading piles P7 and P8 the force dropped suddenly and loud noise could be heard at the breaking point (Figure 45). This may occurred due to the reattachment of the pile after the bond failure. Thus, could be said that the maximum bond capacity of the piles P7 and P8 would have been around 3000 kN mark with displacement of 6% rather than 1400–1500 kN as presented in Table 12. In this case displacements started to progressively grow after 1500 kN mark. It is the end of the elastic zone and the start of partly plastic zone starts as Heinonen (1998) presented as failure criterions. This could also be described as failure zone which lasts until the ultimate failure occurred at 3000 kN mark.

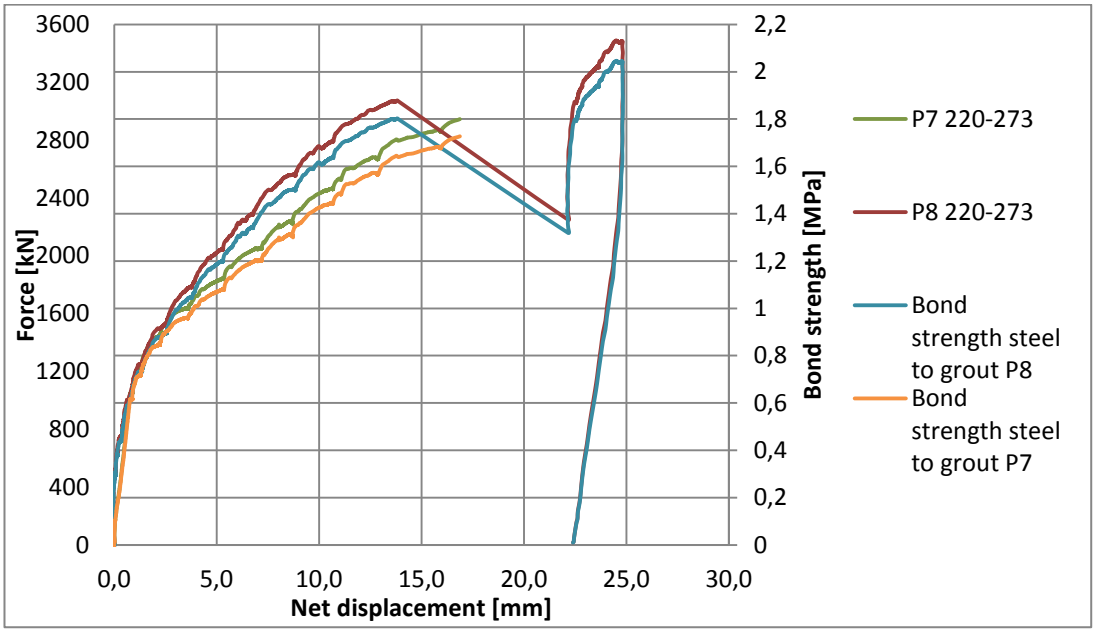

Figure 45. *Displacement curve of piles P7 and P8*

On all other piles there was not clear breakage during the loading but there were point where the rate of displacement started to grow. Displacements on pile P2 (Figure 46) grew linearly throughout the loading process due to lack of grouting.

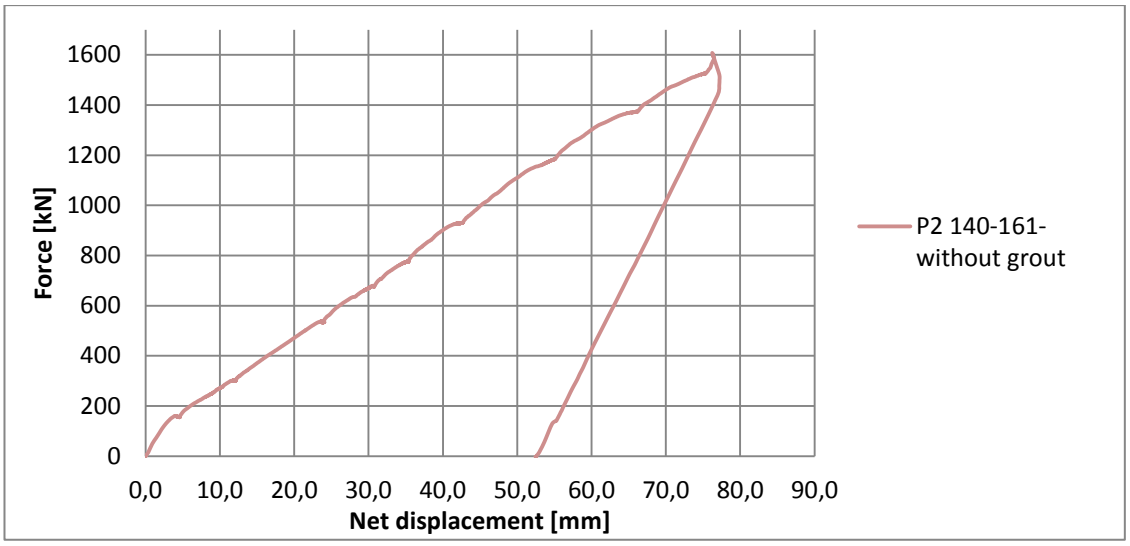

Figure 46. *Displacement curve of the pile P2 (RDs140/161)*

6.2.2 Displacements and elastic strain

Displacements of the piles and the ground were monitored during the loading. Any special problems were not encountered during the pile displacement monitoring. Displacement of the ground was monitored with lasers sensors. Sensors did not pick up any major movement of the ground on the measuring points which were 50 cm and 110 cm away from the test pile. Sensors picked up 1 mm movement even when piles were not loaded. It was probably due to changes in weather conditions at the site and therefore these results are ignored. Displacements on the ground could only be seen just next to the pile where the pile rose from the ground during loading as can be seen in Figure 47. This is normal phenomena and it seems that only small part of the filling on the upper part of the soil which was collapsed to the drilling hole rose with the pile. Therefore could be said that a larger failure of the rock cone did not occur due to lack of the larger ground movements on the testing area.

Figure 47. *Displacements next to test piles after loading*

During the loading process displacements of the test piles were measured and the force-displacement graphs were drawn from the results. By equations *(11, 12 and 13)* presented in Chapter 3.2 the steel elastic strain could be calculated for the free length of the pile when the loading force was measured. Thus the elastic strain graph was also added to the force-displacement graph to identify the point where the displacements grow larger than the elastic strain. These graphs for the individual piles are presented in Appendices 2–14.

Displacements of the piles in this research were larger comparing to the previous studies by Ahomies (2015) and Sirèn (2015). In Siren`s study displacements of the piles were caused mainly due to elastic strain of the steel and displacements grew rapidly only after the bond failure. Displacements on RD140/10 piles were 4–6 mm and on RD220/10 piles around 4–8 mm before failure. Strains were small due to short free length of the pile. In research of Ahomies (2015) displacements before the bond failure were rather small around 0.5 – 1.0 mm and after the failure displacements started to grow rapidly. In both of these studies point of the bond failure could be clearly seen from the force - displacement graph and the behavior of the curves on all piles were similar.

In this research the point where the displacements separate from the elastic strain graph are hard to recognize due to fact that in most cases the displacements start to grow faster

than the elastic strain. This would indicate that either the elastic strain graph is misplaced or due to lack of adhesion between the pile and grout. Only with piles P6, P7, P8, P9 the displacement seems to follow the strain graph to the point where the expected failure of the bond occur. This can clearly be seen from the force – displacement graphs (Figure 48) and raw data in Appendix 16. From the displacement graphs can be seen that the failures occurred after around 5–15 mm of total displacement. Elastic behavior of the piles could be observed when the force was released.

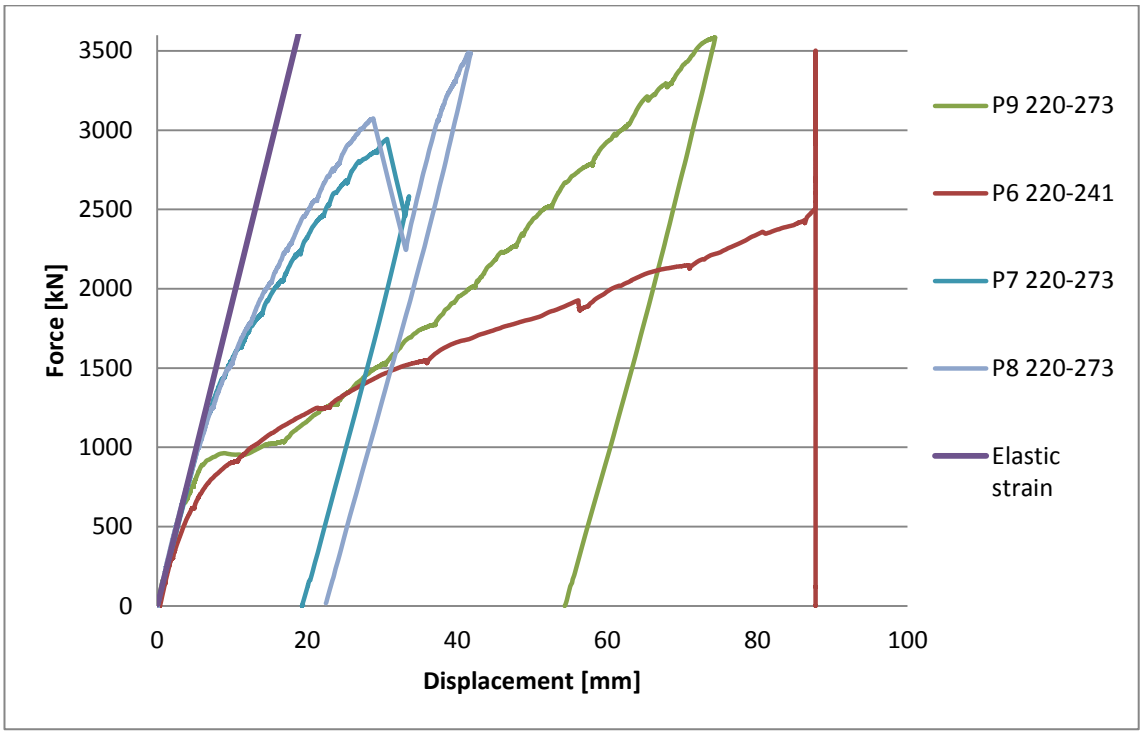

Figure 48. *Displacement curves of the piles P6, P7, P8 and P9*

The rate of the displacement curve shows that certain piles follow the same failure mode with each other. The behavior of the displacement curve with piles P5 and P9 indicates that the tensile capacity of the piles were mostly formed due to interlocking effect of ring bit and the friction between the pile and the grout. The interlocking effect makes the failure more resilient and causes the ring bit to reattach to grout column. This effect is seen with the piles P5 and P9 in Figure 49. After the failure of the bond around 5–6 mm mark, these piles seems to slide before the ring bit reattaches. On pile P9 the ring bit is wider therefore it can resist higher tensile force than pile P5.

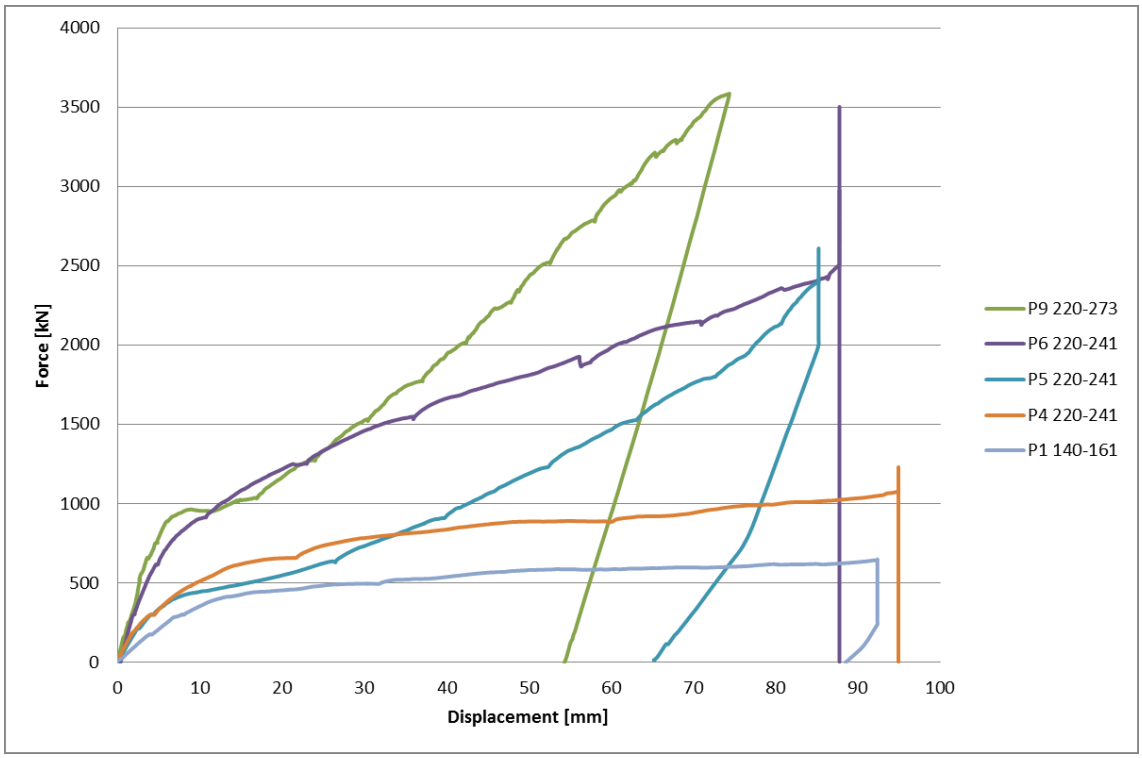

Figure 49. *Pile P5 and P9*

From Figure 49 can be seen that behavior with the piles P1 and P4 seem to be different than with previously mentioned. The displacement starts to grow rapidly after the failure and reaches its maximum with lower force. This indicates lower friction between the pile and grout surfaces. Displacement curve of the pile P6 seems to be somewhere in the middle of these previously mentioned failure modes. It indicates more of shear failure but has better bond capacity than piles P4 and P5 in the same design group.

Displacement behavior of the piles P2–P3 and P7–P8 which are presented in Figure 50 are in their own class. The pile P2 represents pure friction curve due to fact that it was not grouted into the bedrock. The pile P3 has similar behavior and represents more the friction curve than the previous failure modes. Rate of curves are almost standard until they reach the maximum displacement or the yield strength. The difference with pile P2 and P3 that pile P3 have more resistance due to shear failure.

Piles P7 and P8 had the best result in terms of displacement - force relation. Displacements grew really slow through the whole loading process. After 20 mm mark a loud bang noise could be heard and after displacement grew rapidly. This can indicate that the ring bit reached the compression strength of the grout and crushed some of the grout column and reattached afterwards.

This is how the P9 also should have behaved. On pile P9 an unusual behavior occurred during flushing and grouting process. When the pile was flushed the water flow did find its way away from the test site. A hole in the lawn was found where the water came out.

So it is possible that the flushing water and the grout found a crack which led the grout and water away from the drilling hole. It could indicate that grouting process would have not succeeded.

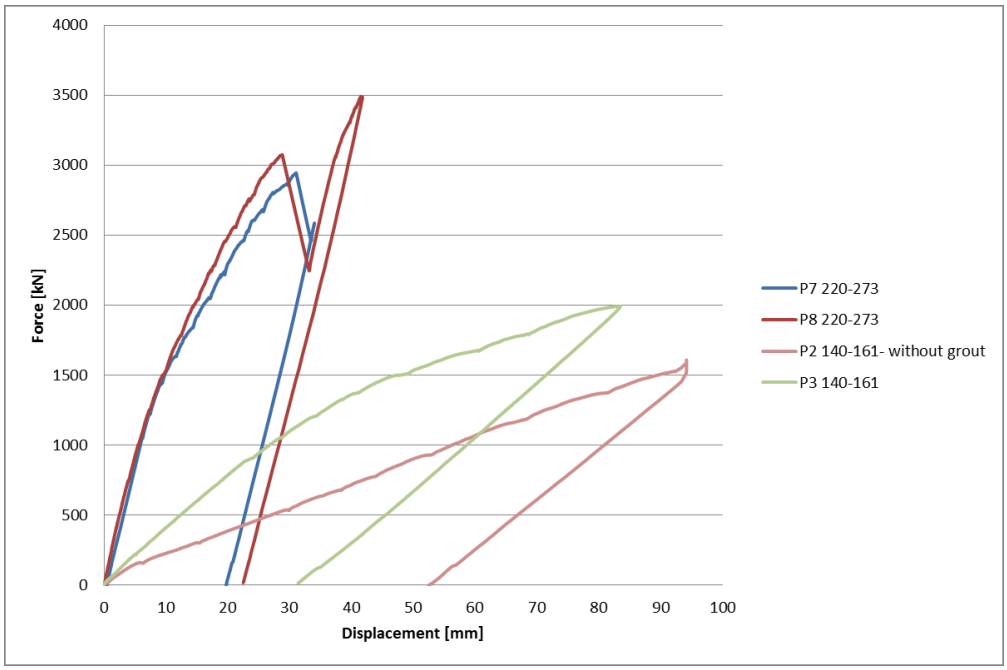

Figure 50. *Piles P2, P3, P7 and P8*

6.2.3 Failure mode of the piles

Due to deep soil layer and other activity near by at the testing site, the nature of the failure method cannot be determined directly from the breaking point by excavating the site. Method of the failure is needed to be estimated from the observations at the site and from the test results. Possible failure modes for the piles are discussed here. Calculated capacities for the failure modes are presented in Appendix 14.

According to analysis of the failure which occurred during the 5% displacement of the pile diameter, the bond strength was on pile P1 380 kN, P2 217 kN and P3 543 kN. If this is compared directly to the calculated capacities this would indicate failure of the bedrock as 45 degree cone. Due to lack of grouting it is known that pile P2 represents pure friction resistance and the failure of the rock cone did not observed at the site.

Failure of the pile P3 could also be the failure of rock to grout surface if it would be analyzed by approximate tensile capacity. If the failure is analyzed based on the displacement curve it also may refer to shear failure until the failure around 40 mm total displacement mark which after it follows almost exactly the friction curve of the pile P2. The displacement curve has wide partly plastic zone and thus clear breaking point is hard to determine. This may also indicate that the grouting was not successful and therefore exact failure or breaking point is hard to recognize.

If the pile P1 is analyzed based on the displacement curve (Figure 51) it clearly indicates that the failure occurred between the 5% (380 kN) to 10% (448 kN) displacement. After this plastic failure zone of the curve represents failure of the steel to grout surface due to lower friction curve. As conclusion on piles P1—P3 three different failure methods could be occurred, pure friction failure, steel to grout and rock to grout shear failures.

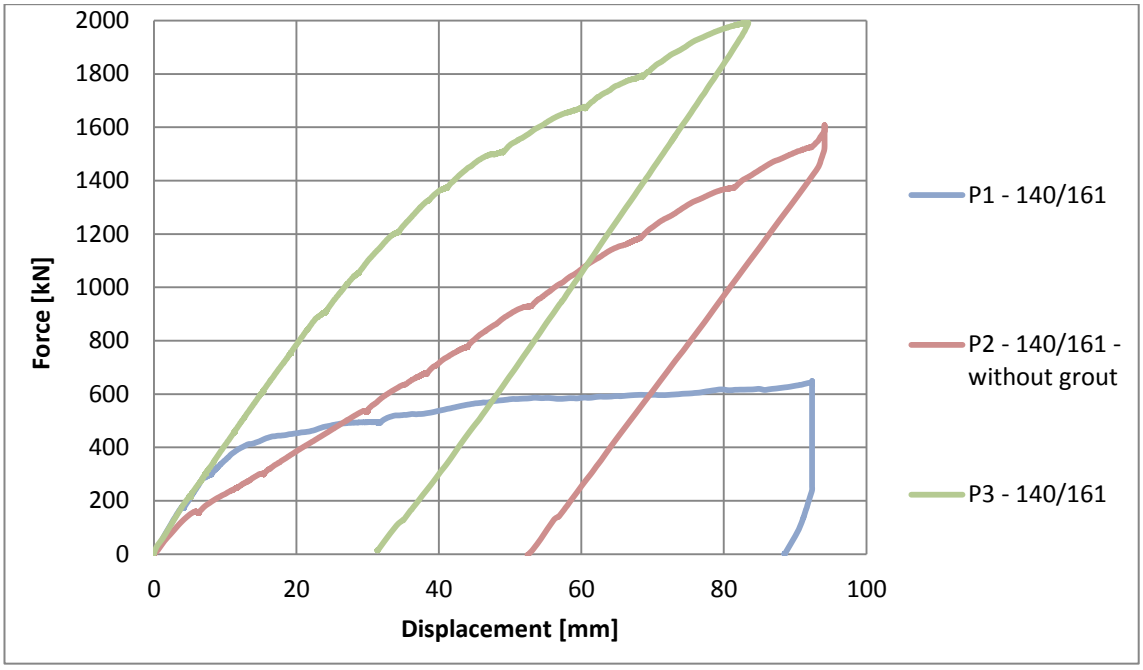

Figure 51. *Displacement curves of the piles P1, P2, and P3*

Piles P4 and P5 could represent rock cone failure if it compared directly from the calculation. Pile P6 had at least double capacity comparing to rock cone failure but did not quite reach the rock to grout mark. If the displacement from the Figure 52 are analyzed the failure of the P4 and P6 are similar although P6 has more resilient failure and better bond capacity. Pile P6 could represent the failure of the steel to grout surface which after it indicates shear failure. Pile P4 could indicate the failure of the steel to grout surface but afterwards it indicates more of friction failure due to lower angle of the curve. Pile P5 has clear failure point which is actually around the same area with the pile P4 but the failure behavior afterwards is different. The pile slips around 10 to 15mm with very low force but after that the curve continuously rises and it seems that the pile is reattached. As conclusion P4 and P6 represents steel to grout failure and P5 represents probably the combination of the failure modes. On piles P4–P6 the bond failure seemed to be around 2.5% of displacement mark.

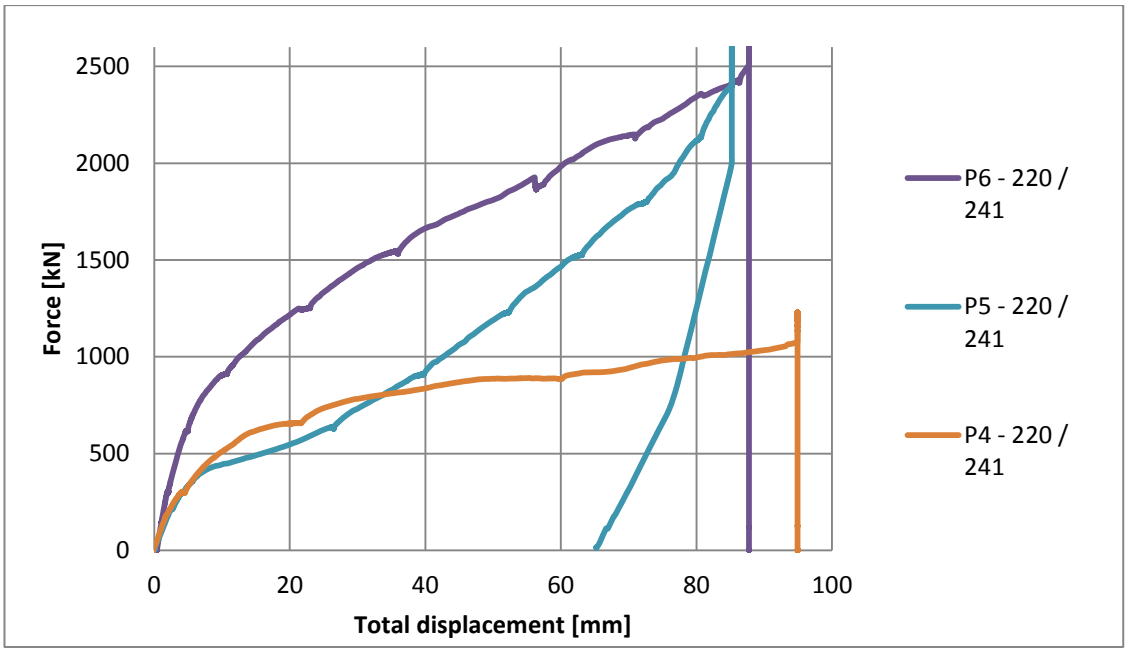

Figure 52. *Displacement curves of the piles P4, P5 and P6*

Piles P7–P9 clearly represents the most resilient bond strength. On piles P7 and P8 the failure was almost identical with each other which could also be noticed during the loading. Piles reached full capacity around 3000 kN and failed suddenly. Due to sudden compressive failure, noise could be heard and a clear drop in a force graph can be seen in Figure 53. Also reattachment of the ring bit can be seen on the pile P8. This indicates that the failure is on the steel to grout surface.

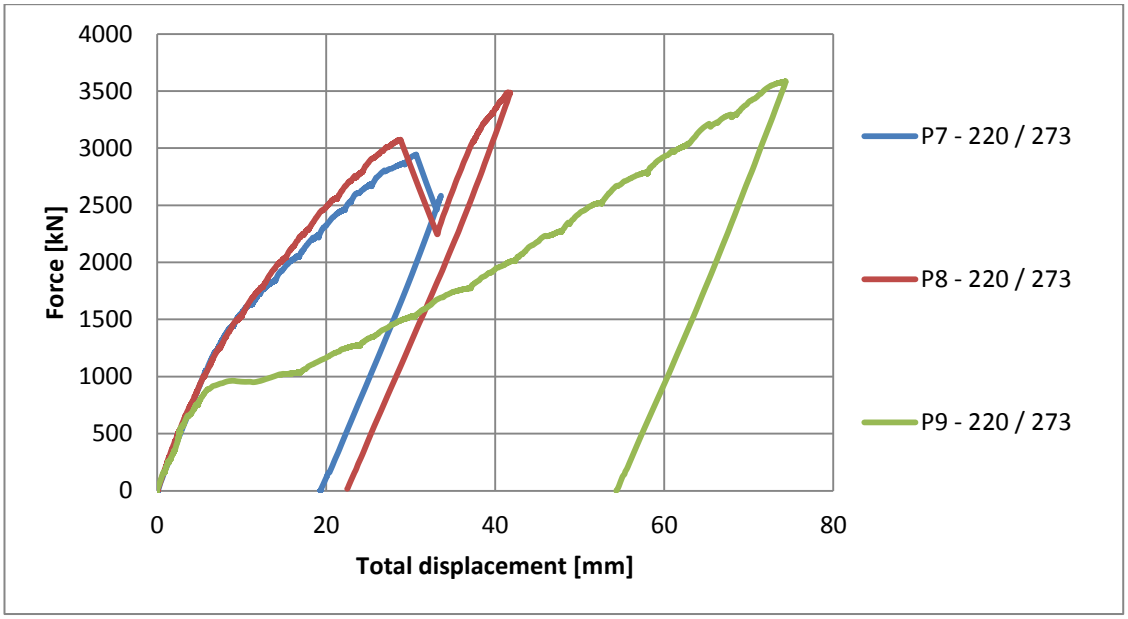

Figure 53. *Displacement curves of the piles P7, P8 and P9*

On piles P7 and P8 the bond capacity was around 3000 kN which was the same area as it was in Sirèn`s research. The point where the displacements started to grow was at 1%

mark. On pile P7 this point was at 1440 kN mark and on pile P8 at 1497 kN mark. This could indicate rock cone failure with the overburden soil layer. Force which is needed to the failure of the rock cone with 7 meters thick cylindrical soil layer, which starts from the bottom on top the pile, is around 1500 kN. The force that is needed for the failure of the rock cone without overburden soil layer is 150 kN to 400 kN. Due to fact that capacities of the piles were much higher than the failure of the firm or shattered rock failure of the overburden was not observed at the site, could be said the failure of the rock cone did not occur in this case.

On pile P9 is it clear that the failure occurred at 1% mark. The failure of the pile P9 probably did occur on the steel to grout surface which led reattachment of the ring bit afterwards. At this point the capacity of the pile was around 921 kN. As noted before the water flow did find its way away from the site during the flushing process. It could indicate that the grouting was not successful and therefore the test resulted in lower bond capacity.

Major failure of the rock cone did not seem to happen in any case of the tested piles. If the failure occurred as a failure of the rock cone, it occurred during loading the piles P7 and P8 around 3000 kN mark which is ten times more than calculated with present standards. This was only time when any major event occurred. If the failure of the bedrock would have occurred it should have be seen also as movement of the support piles which was not observed. Therefore can be said that the major failure of the bedrock did not occur in this test.

In conclusion the failure mode is hard to estimate just from the displacement graphs due to fact that the event is a combination of events which occur below the ground surface. When the displacement graphs are analyzed it seems that most of the tested piles seemed to fail from the grout to steel surface.

6.2.4 The estimated bond strength

The bond strength of the piles can be determined from force – displacement graphs and raw data. In Appendix 16 column named *difference [mm]* represents difference between the displacement and elastic strain curve. From this data can be found the point where displacement curve separates from elastic strain. This difference gives a good reference for the bond strength analysis due to the fact that in most of the tests clear breaking point did not occur. Thus the point where the rates of the displacements grow is the failure point. From this difference can be seen where the rate of the displacements start to grow and where the failure occurred. The result for this analysis is presented in Table 13.

Table 13. *Tensile capacities of the piles*

	P1 (140/161)	P2 (without grout)	P3 (140/161)	P4 (220/241)	P5 (220/241)	P6 (220/241)	P7 (220/273)	P8 (220/273)	P9 (220/273)
Estimated bond failure at [kN]	**380**	**217**	**543**	**440**	**417**	**913**	**1440**	**1497**	**921**
Displacement... [mm]	7	7	7	5,5	5,5	5,5	2,2	2,2	2,2
...of the pile d	5,0 %	5,0 %	5,0 %	2,5 %	2,5 %	2,5 %	1,0 %	1,0 %	1,0 %
Bond strength [Mpa]	**0,35**	**0,20**	**0,50**	**0,26**	**0,24**	**0,54**	**0,84**	**0,88**	**0,54**

From the results can be seen that the bond strength is higher on the piles with larger diameter and clearly the highest on piles with the oversized ring bit. It is clear from results that the bond between grout and the pile was broken somewhere around the "bond failure" point. Due to reattachment of the oversized ring bit and the friction between the pile and grout surface, piles could resist the tensile force also after the ultimate failure. Piles P7 and P8 had highest tensile capacity. On pile P7 tensile capacity was between 1440 – 2938 kN and on pile P8 between 1497 – 3068 kN. This is in the same area which Sirèn (2015) had in her research.

Bond strength in Table 13 is calculated based on analysis and it should be quite accurate estimate for the piles P1–P6. For the piles P7–P9 could also be thought other approach. Piles P7–P9 had much wider ring bit than all other piles. For the displacement to occur it needed to either reach compression strength of the grout or fail from the joint of the ring bit after the bond failure. Bond strength on the piles P4–P9 should be same on steel to grout surface due to fact that the surface area of the pile is identical. But after the bond failure, the reamer push through the grout column. It needs to reach the compressive strength of the grout to be displaced. In both designs, on piles P4–P6 and P7– P9 have same grout formula, thus the compressive strength of the grout is standard but the reamer size is different. Therefore the area where the force is affected is different. When the area increases, the force needs to be higher to achieve the ultimate limit strength. On piles P7–P9 the reamer area is 28% larger than on piles P4–P6, thus tensile capacity was higher and displacements were smaller. This effect is seen when plastic failure of the pile occurs. Plastic failures of the piles P7 and P8 were around 1% to 5% mark which after at the 6% mark, breakage of the grout column occurs. The capacity of the piles was doubled but increments to displacements were small comparing to other pile types. Thus tensile capacity and also could be calculated from the point where the major failure occurred. In this case capacity could also be calculated from the 5% mark which is nearly double than presented in Table 13.

Due to nature of the bond failure it is better to estimate right at the point where the displacements start to grow. Then the bond strength is comparable and it is more conserva-

tive estimate for the failure. In Figure 15 is shown summary of the bond strength displacement graphs of all piles.

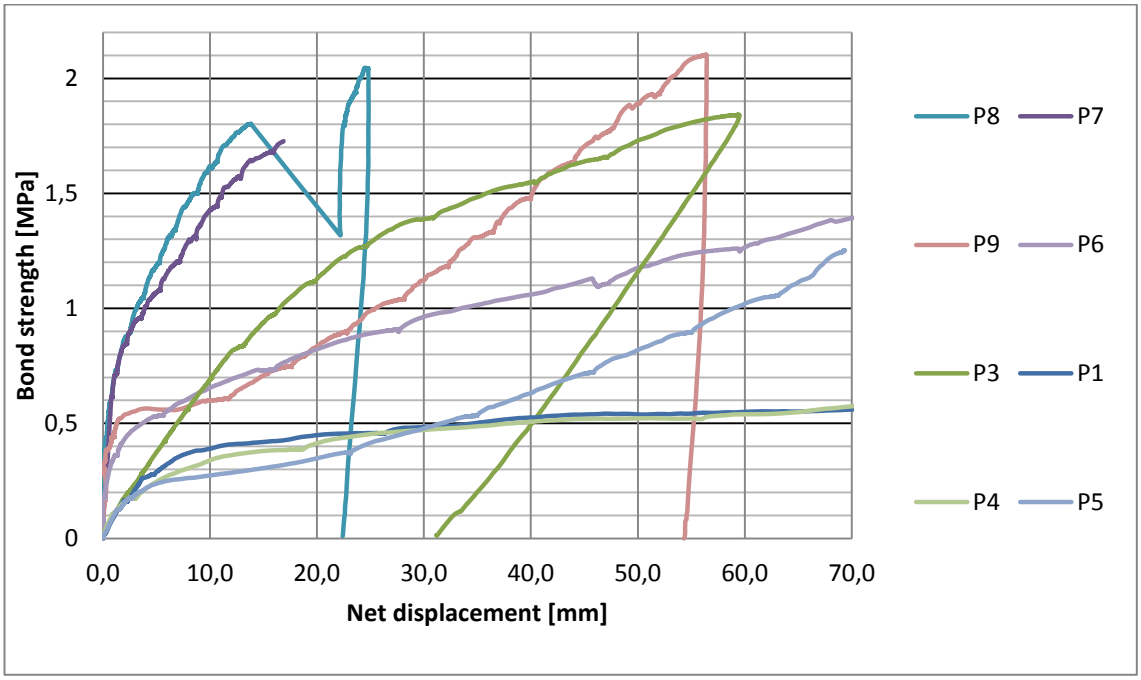

Figure 54. *Summary of the bond strength graphs*

6.2.5 Bond strength comparison to other studies

Test results are compared to the previous research with similar pile design in Figure 55. From the chart can be seen that in this test bond strength was significantly lower than in Siren`s research which is shown as red columns. In Ahomies`s (2015) research average bond strength was 0.26 MPa with smooth pile surface which is displayed as green column.

In theory the bonds strength should have been at least the same as Siren`s research on piles P4—P6 due to similar design. Only difference in this research was the soil layer on the bedrock which led to the fact that flushing, grouting and bedrock quality could not be verified in situation. In this research less grouting mass was used than in Siren`s test and less flushing water with smaller piles.

In other studies much higher values for bond strength have been obtained. Myers (Siren 2015) measured 4.0 MPa and Gomès (Siren 2015; originally Gomez 2005) over 3 MPa value for bond strength in laboratory conditions on piles with ribs. Although these results are not entirely comparable due to laboratory conditions and different design models but it gives good idea what can be achieved. Due to fact that results in laboratory conditions and at the construction site are not comparable, piles should be tested by the load tests before it is used in foundations.

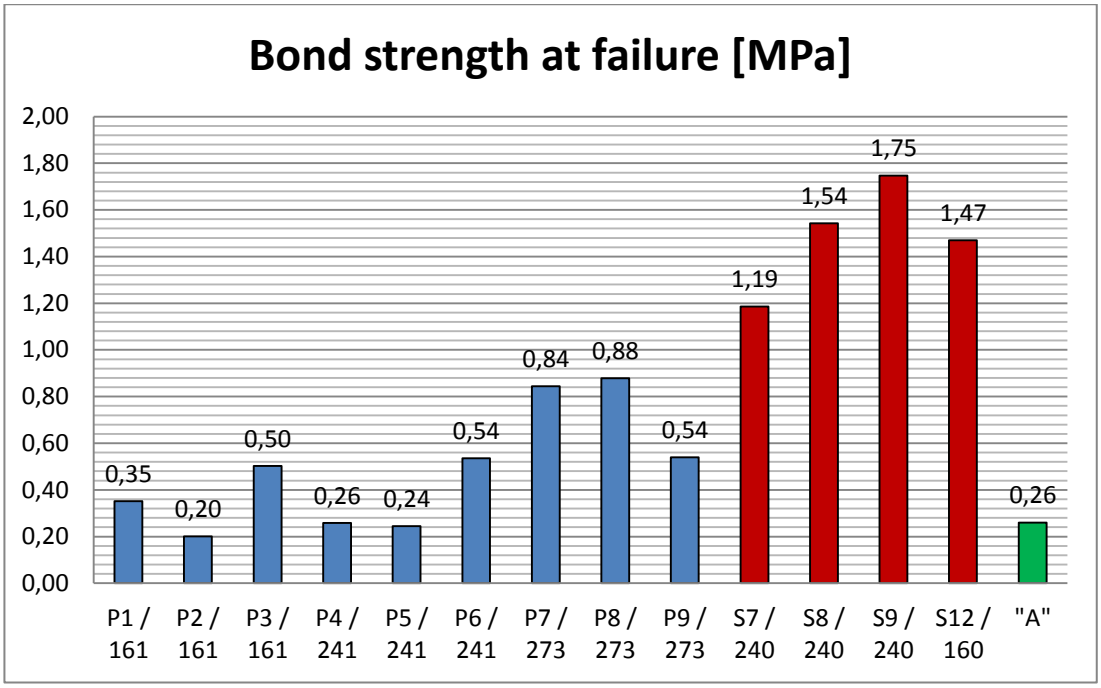

Figure 55. *Bond strength comparison to Siren`s (2015) similar design*

6.2.6 Quality of the work

During the research any major problems was not encountered which would have led to the failure of the work. Some minor issues were acknowledged during the process. During field test weather and site conditions were great to work on. Preparations and welding process could be made inside the hall and therefore proper welds could be ensured when preparing the piles for the installation. The preparations and drilling phase went according to the plans excluding couple minor machinery problems which probably did not affect the results.

In this research grouting valves were used to reduce disturbance of the soil during drilling process. During drilling, waving movement of the filling layer could be seen from the ground level and thus it seems that the grouting valves did not have much effect.

During the flushing and grouting process weather conditions were rainy and around 10 - 11 degrees Celsius on the first day. The second day was sunny and around 16 to 18 degrees. Grouting was done immediately after flushing and lasted maximum of 30 minutes per pile even with the pipeline failures which was fixed rather quickly. The action time before the grout started to settle was 40 minutes by the manufacturer. Grout recipe was measured by mixing 25 kg cement bag and a 10 liter bucket of water and by the experience of the workers. An even value for the grout recipe was selected to ensure proper quantity of water and the cement. Water temperature was around 10 degrees which is around the area as temperature in the bedrock. The grout should reach the same compressive strength after 28 days in 20 degrees than in 5 degrees Celsius. Therefore could be said that the grout quality should be as good as and could be in a construction like situation.

In this test most issues were in grouting phase with the larger tube-a-manchette which got stuck to the welds inside the piles. For this reason the grouting with the pile P7 did not go as planned and the w/c ratio was estimated to be at the worst around 0.6. Although this pile did gave one of the best results in the loading phase and therefore the grouting can be count as successful. Problems with the manchette occurred usually when the manchette was lowered down to the pile and when it was lifted up. It got stuck to the welds and the packing had to be repaired afterwards. Therefore the operational reliability was lower than expected. When the problem was acknowledged it should not have had effect to the end quality of the grouting.

During the flushing and grouting process minor issues were encountered when flushing and grouting of piles P4–P6. Piles needed pressure over 12 bars for the grouting. Due to high pressure piles P4 and P6 begun to rise from the soil and needed to be anchored to the support piles when the pressure was over 4 bars. Pile P5 opened only after 18 bar pressure which led to breakage of the grouting tube. When the manchette was lifted up from the piles it was covered with clay in some cases. High flushing pressure and the clay over the manchette`s packer could indicate that piles P4—P6 were also plugged and flushing process may not have been sufficient enough. This may have lowered quality of the grouting. For tensile pile to work, proper flushing and grouting are the most important phases due to fact that these processes ensure proper bond between the surfaces. Therefore these minor issues can lead to major issue and should be thought carefully. Also one major problem was encountered which led to inability to proper installation of pile P2. The pile was clogged, and it did not open either with 100 bar water pressure or by lifting with an excavator. The pile was decided to load without grouting.

It also seemed that the annulus of the piles P1–P6 could have been clogged by soil which affected the quality of the grouting process. Clogging of the piles can be due to the fact that there was waiting time of 2.5 weeks between drilling and grouting process. Between this time periods the soil on top of the bedrock could have fallen down to the drilling hole and filled the annulus between the pile and the bedrock. It also could be the case that grouting valves did not have enough space to open and therefore significantly lowered the grouting quality.

This may be why the piles with wider ring bit achieved better results. Due to two and a half times wider annulus the soil may not be clogged the annulus so tightly and most likely there were more space to flush it out. Also, reamer size 273 had grooves at the bottom of the reamer. These could have ensured cleaner annulus and better grouting quality thus better results.

During flushing, water will find its easiest way out of the drilling hole and if some of the valves are stuck it could be the case that the water did not flush that side of the annulus properly. Actually the water could not even reach the soil next to grouting hole due to fact that the valve has rubber blocking its way and the soil is blocking the rubber part. Without the valve the water would have reached clogging material and maybe could have found its way to open the plug. This effect on one side of a pile could have led to incomplete grouting of that side of the annulus and also failure of the grouting process. The pile should be flushed and grouted soon after the drilling to avoid the problems.

The loading phase was successful and any issues which could have been affecting the results of the test were not encountered. Loading of the piles did go as planned. Laser sensors which were used to measure the displacement around the pile seemed to be accurate enough even with the minor variance. Mechanical device is recommended to be used due to changing weather conditions. The loading jacks were operated by the change in hydraulic pressure and therefore adjusting the force was inaccurate. Pressure needed to be leveled before the loading stopped completely and therefore there were minor variance in loading steps. The force could be still measured accurately. These are really minor issues but for further notice can raise the quality of following studies.

The major issue which affected the quality was that the piles were clogged and could not be flushed properly. Also again more effective flushing methods should be considered to ensure the cleanliness of the annulus. This will greatly improve the quality of the system.

It seems that quality is mostly affected by the working methods at the site. Usually minor issues like machinery problems or grouting tube breakdowns will normally be handled in situation and therefore should not be calculated as deteriorating factor for the quality in this research.

However, flushing and grouting methods have major impact on the quality of the work and thus should be priority issue. The problem was that proper flushing and grouting could not be verified and therefore the failure of the process could have lowered the bond quality tremendously.

6.2.7 Limitations for the design

Finnish Transportation Agency instructions for the geotechnical design limit the design for tensile piles. The highest value which can be used for the ultimate tensile force in ultimate state would be 50 kN for drilled and grouted steel pipe piles with diameter of 170 mm and 100 kN for pile diameter of 320 mm. This is low value for the design due to fact that the tensile force in this research exceeds this value multiple times. Also the bond strength of the piles tested exceeded the limits. The values in Appendix 8 of NCCI7 are derived directly from the research of Ahomies where smooth pipe piles were used.

Table 14 was made to compare this and previous study to the regulations which limits the usage of the drilled and grouted steel pipe pile as tension pile. In Table 14 different designs from this research were presented as *design 1* which is for annulus size 10 mm and *design 2* which is oversized reamer with 26.5 mm annulus. In Table 14 bond strength is the lowest values which were achieved in the tests. Value for the tensile force could be then derived by diameter of the pile and by the values from the NCCI7.

Table 14. *Design by instructions compared to the results (min. bond strength)*

Drilled and grouted steel pipe pile				
	NCCI7	Siren	Design 1	Design 2
Bond strength $\tau_{s;k}$ [kPa]	100	1200	240	540
diameter of the pile > …	Highest value for tensile force in ultimate limit state			
[mm]	[kN]	[kN]	[kN]	[kN]
170	50	600	120	270
320	100	1200	240	540
508	150	1800	360	810
≥813	250	3000	600	1350

As it can be seen from Table 14 and 15 tensile capacity of the drilled and grouted steel pipe pile can be higher than is instructed even with the most conservative bond strength values achieved from the studies. The average bond strength of the drilled and grouted steel pipe pile in table 14 is around 3 times higher than smooth pipe pile when grooved design and wider ring bit is used. If capacity of the grooved *design 2* is compared to the

limitations from the NCCI 7 it is over 5 times higher than it is instructed. If the results of the test are compared to the instructions by the individual pile it is clear that the piles P7 – P9 clearly exceeds these limitations as can be seen in table 14.

Table 15. *Individual piles compared to the design limitations*

	P1 (140/161)	P2 (140/161)	P3 (140/161)	P4 (220/241)	P5 (220/241)	P6 (220/241)	P7 (220/273)	P8 (220/273)	P9 (220/273)
NCCI7	50	50	50	50	50	50	50	50	50
Result from the test	**380**	**217**	**543**	**440**	**417**	**913**	**1440**	**1497**	**921**
Difference	330	167	493	390	367	863	1390	1447	871

6.2.8 Suggestions for further studies

The first main problem was the clogging issue which could have been caused due to several reasons. One was the time between the drilling and grouting process. This left a question if the time between drilling and grouting have effect to the clogging issue or was it just a coincident.

The second question was if the flushing process was succeeded. In this research flushing method was chosen to be the one which was successfully used in previous research. It may not be the best way to flush the piles in the case of clogged pile thus innovative flushing and grouting methods should be tested to ensure the flushing quality. Larger flushing holes, higher pressure and more grout could help to success in this process.

Grouting valves were chosen to help with the grout backflow and to decrease the air flow to the soil. Although grouting valves may have a part in clogging issue. It could be useful to grouting valves functionality before it is used in field test. Also larger grouting valves could ensure better functionality.

Design with wider reamers gave the best results in this test. It seems that the wider reamer has positive effects to flushing and grouting process and the tensile capacity of the steel pipe piles. Thus the design should be retested.

In this research, grooves on the pile surface were low at the pile tip although stress distribution theory indicates that the higher stresses are at the top of the bond length. Design should be tested so that the grooves would be on the top part of the pile bond length thus lower drilling depth could be used and this could get better results according to theory of stress distribution. Thus it gives some consideration that if the grooves should be on the whole bond length of the pile.

These issues which may have affected the quality of the test should be investigated. This way could be ensured that one individual element does not create more issues. Following studies should not have too much variance between designs to achieve reliable and comparable results.

7. CONCLUSIONS

In this research the main focus was to develop the design of grooved tensile steel pipe pile, implement theory on the field test and compare the results to previous studies. Also, effect of the soil layer to the installation methods and bond strength was one of the big questions.

As found out, the results on the field gives lower results than the theory and the results in laboratory or laboratory like situations. As presented the bond strength of 3.0 MPa have been achieved in laboratory but on the field results have been much lower around 0.3 to 1.0 MPa. Sirèn achieved on the field around 1.85 MPa without overburden soil layer. In this research the piles were tested from the ground level with 6 to 7 meter soil layer and 2.5 meter drilling depth in construction like situation with similar design. The bond strength stayed between 0.24 to 0.88 MPa with larger displacements. The highest tensile capacity before sudden failure was 3068 kN. Failure mode of the piles could not be verified, but from the results piles assumed to be failed from the steel to grout surface.

Due to nature of the research actual comparison to theory presented in literature review is hard to make. In this case it seems that better bond strength was achieved with wider annulus and thicker grout layer. It may have been the case that the wider reamer acts as a compression fitting at the pile tip which creates pressure to the grout column thus increases effect of mechanical interlocking on the pile surface. Also the bedrock around the pile acts as a natural confinement and strengthens this effect.

The best results were achieved on piles P7—P9 with wider ring bits and thus wider annulus between the bedrock and steel pipe pile. Wider annulus was assumed to help to succeed in flushing and grouting process and thus end up to have better results. Wider ring bit also had resilient failure although the absolute failure was sudden. The annulus size in the design was 26.5 mm which would also be good thickness for corrosion protection and would meet the standards. Therefore RDs220/12.5 pile with grooves and 273 oversized ring bit would be recommended design for the tensile pile according to this research.

Quality of the research was mostly affected by the working methods during the flushing and grouting process. Increase on flushing or grouting pressure indicates that the annulus was clogged and therefore the cleanliness of the annulus should be ensured. In this research displacements of the piles were rather large before estimated failure which indicates unsuccessful bond between the pile and the grout. Thus, volume of the flushing

water and grouting mass on piles P1—P6 may not have been sufficient enough or due to clogging effect the grouting valves did not work as they were designed to. The effect of flushing can be increased by raising the pressure and total volume of flushing agent. Also the volume of the grout mass used and the grouting pressure will affect the grouting quality. Success in the grouting process is the priority issue thus the procedure should be thought through. Grouting process is recommended to do as soon as possible after the drilling of the piles to avoid the clogging issues caused by the overburden soil layer and drill cuttings.

Results of this test were compared to the design according to present instructions and it seems that design according to failure of the rock cone is too conservative. In this research the failure of the rock cone was not observed on the ground surface with the 3000 kN load and 2.5 m drilling depth. By the instruction the drilling depth should have been 7 meters with shattered bedrock and 4.9 meters with firm bedrock to counter the rise of bedrock. The bedrock should have failed with the load of 400 kN in this research. From the observations at the site could be determined that it did not occur.

Present instructions limit the design for tensile piles to the highest value for the ultimate tensile force which is much smaller than achieved in this and previous study. Capacity of the grooved tensile pipe piles can be over five times higher than is instructed. Average bond strength of the drilled and grouted steel pipe pile was at least three times higher than with the smooth steel pipe pile when the grooved design and wider reamer was used.

Research left some questions about the effect of the overburden, effect of the time between drilling and grouting process, flushing and grouting method and effect of grouting valves for further studies. Overall the research process and the field test were successful. Any major problems with the testing method were not encountered and valuable information was adapted for tensile steel pipe pile design.

REFERENCES

Ahomies, M.,(2014), The grouted and anchored drilled pile in the bedrock, Master of Science Thesis, Tampere, Tampere University of Technology, Civil Engineering Tampere, 135 p.

Barbosa, M.T.G., Filho, E.S.S., Oliveira, T.M., Santos, W.J., (2008), Analysis of the Relative Rib Area of Reinforcing Bars Pull Out Tests, Materials Research, Vol. 11, No. 4, pp. 453-457.

Brown, E. T., (2015), Rock engineering design of post-tensioned anchors for damns – A review, Journal of Rock Mechanics and Geotechnical Engineering, Vol. 7, 2015, pp. 1-13.

Coates, D.F. Yu, Y.S. (1970), Three-dimensional stress distribution around a cylindrical hole and anchor. In: Proceedings of the 2nd congress, International Society for Rock Mechanics, Belgrade, 3; p.175—82.

Concrete. Specification, performance, production and conformity, SFS-EN 206:2014 + A1:2016, (2016), Finnish standard association, Helsinki, 92 p.

Dickin, E. A., Leung, C.F.,(1990), Performance of Pile With Enlarge Base Subject to Uplift Force, Canadian Geotechnical Journal, Vol. 27, pp. 546—556.

Eurocode. Basis of structural design, SFS-EN 1990 + A1 + AC, (2006) Finnish standards association, Helsinki, 184 p.

Eurocode 2: Design of concrete structures, Part 1-1: General rules and rules for buildings, SFS-EN 1992-1-1 + A1 + AC, (2014), 218 p.

Eurocode 3: Design of steel structures, Part 1-1: General rules and rules for buildings, SFS-EN 1993-1-1 + A1 + AC, (2014) 99 p.

Eurocode 3, Design of steel structures, Part 5: Piling, SFS-EN 1993-5 + AC, (2007), Finnish standards association, Helsinki, 88 p.

Eurocode 7. Geotechnical design, Part 1: General rules, SFS- EN 1997-1 + A1 + AC, 2014, Finnish standards association, Helsinki, 161 p.

Eurokoodin soveltamisohje - Geotekninen Suunnittelu - NCCI 7, Siltojen ja pohjarakenteiden suunnitteluohjeet 21.4.2017, (2017), Liikenneviraston ohjeita 13/2017, Liikennevirasto, Helsinki. ISBN 978-952-317-387-3

Execution of special geotechnical works, Grouting, SFS-EN 12715, (2001) Finnish standards association, Helsinki, 53 p.

Execution of special geotechnical works, Micropiles, SFS-EN 14199, (2015), Finnish Standards Association, Helsinki, 62p.

Finnish Road Administration, Instructions for drilled piling, Design and execution guide, Guidelines for design and implementation,(2003), Edita Prima Oy, Helsinki, ISBN 951-803-027-8 Available: http://alk.tiehallinto.fi/sillat/julkaisut/drilledpiles_03.pdf

Geological Survey of Finland, Map Services, Maankamara service, web page. [Accessed 9 August 2017] Available: http://gtkdata.gtk.fi/Maankamara/index.html

Gòmez, J., Cadden, A.W., Traylor, R.P., Bruce, D.A., (2005), Connection Capacity between Micropiles and Concrete Footings: Interpretation of Test Result and Design Recommendations. [Accessed 9 August 2017], Available at: http://www.geosystemsbruce.com/v20/biblio/215%20Connection%20Capacity%20between%20Micropiles%20and%20Concrete%20Foot.pdf

Gòmez, J.E. Veludo, J., Julio, E., Robinson, H.D., (2013), New Findings on the Capacity of Connections between Micropiles and Existing Footings, [Accessed 9 August 2017] Available at: https://www.researchgate.net/publication/268802828_New_Findings_on_the_Capacity_of_Connections_Between_Micropiles_and_Existing_Footings

Heinonen, J. (1998). Suurpaalujen geotekninen kantavuus. Julkaisu 44. Tampereen teknillinen korkeakoulu. Geotekninen laboratorio. Lisensiaatintutkimus. 99 p. ISBN:951-722-961-5

Hong, W.P., Chim N., Prediction of Uplift Capacity of a Micropile embedded in Soil, (2015), KSCE Journal of Civil Engineering, Vol 1, pp. 116-126

Kilic, A., Yasar, E., Celik, A.G., (2002), Effect of grout properties on the pull-out load capacity of fully grouted rock bolt, Tunnelling and Underground Space Technology, Vol. 17, 355 — 362

Leppänen, M., (1992), Teräspaalujen korroosio, Master of Science Thesis, Tampere University of Technology, Civil Engineering, Tampere, 1992, 203 p.

Littlejohn, G. S., Bruce, D. A., (1977), Rock anchors state of the art, Foundation publications LTD.

Littlejohn, G.S., (1980), Design estimation of the ultimate load-holding capacity of ground anchors, [Accessed 9 August 2017] Available at: https://www.geplus.co.uk/download?ac=1423718

Meyerhof, G. G. Adams, J.I. (1968). The ultimate uplift capacity of foundations. Can. Geot. Jnl. vol. 5, no. 4: 225-244

Niroumand, H., Kassim, K. A., Ghafooripuour, A., Nazir, R., (2012), Uplift Capacity of Enlarged Base Piles in Sand, Electronic Journal of Geotechnical Engineering, Vol. 17, pp. 2721-2737

Parr, R.G. & Varner, M.J, (1962), Strength Tests on Overhead Line Tower Foundations. British Electrical and Allied Industries Research Association.

Perälä, A, (2017), personal conversation.

Poulos, H.G., Davis, E.H., Pile Foundation Analysis and Design, Wiley, (1980), 397 p. ISBN 9780471099567

Rajapakse, R., (2008), Pile Design and Construction Rules of Thumb, Buttwerworth-Heinemann 2008, 464 p, ISBN: 978-008-055-916-2

Rantamäki, M., Jääskeläinen, R., Tammirinne, M., (2009), Geotekniikka, 22. painos, Hakapaino Oy, Helsinki, 307 p.

RIL 254–2016, Paalutusohje 2016, PO-2016,(2016), Grano Oy, Suomen Rakennusinsinöörien Liitto RIL ry, 296 p, ISBN 978-951-758-615-3

RIL 263–2014, Kaivanto-ohje, (2014), 2. painos Tammerprint Oy Suomen Rakennusinsinöörien liitto RIL ry, ISBN 978-951-758-590-3

RIL 207-2017, Geotekninen suunnittelu, Eurokoodin EN 1997-1 suunnitteluohje (2016), Grano Oy, Suomen Rakennusinsinöörien Liitto RIL ry, ISBN 978-951-758-619-1

Siren, R., (2015), The tensile capacity of steel pipe piles drilled into the bedrock, Master`s thesis, Helsinki, Aalto University, School of Engineering, Structural Engineering and Building Technology, 107 p.

SSAB, (2016), RR and RD piles, Design and installation manual, [Online], [Accessed 8 August 2017], Available at: https://ssabwebsitecdn.azureedge.net/-/media/files/en/infra/rr-and-rd-piles---design-and-installation-manual.pdf

Tomlinson, M., Woodward, J., (2008), Pile design and construction practice, Fifth edition, Taylor & Francis e-library, 2007. ISBN 0-203-96429-2

Turner, E.A., (1962) Uplift resistance of Transmission Tower Footings, Journal of the Power Division, Vol. 88, pp. 17-34

Veludo, J., Dias-da-Costa, D., Jùlio, E.N.B.S., Pinto, P.L., (2011), Bond strength of textured micropiles grouted to concrete footings, Engineering Structures, Vol. 35, pp. 288-295.

Veludo, J., Dias-da-Costa, D., Jùlio, E.N.B.S., (2012), Compressive strength of micro-pile-to-grout connections. Construction and Building Materials, Vol. 26, pp.172-179, 2012.

Veludo, J., Jùlio, E., Pinto, P.L., (2009), Bond strength of Micropile/Grout/Concrete Interfaces in RC Footings Strengthened with Micropiles, [Accessed 9 August 2017], Available at: https://www.researchgate.net/profile/Eduardo_Julio/publication/268817614_The_Influence_of_Different_Parameters_on_the_Structural_Behaviour_of_the_Connection_Between_Existing_RC_Footings_and_Strengthening_Micropiles/links/5478ab240cf2a961e4877ca8/The-Influence-of-Different-Parameters-on-the-Structural-Behaviour-of-the-Connection-Between-Existing-RC-Footings-and-Strengthening-Micropiles.pdf

Wilder, D., Gomèz, J., Cadden, A.W., Traylor, R.P., (2005), Pilkington, M., Compressive Load Transfer in Micropiles through Concrete Footings: A Full Scale Test Program, Companion paper in Geo3 Conference Proceedings.

Ympäristöministeriö, (2016), 13/16 Ympäristöministeriön asetus geoteknisen suunnittelun yleisiä sääntöjä koskevista kansallisista valinnoista sovellettaessa standardia SFS-EN 1997-1, [Acessed: 21.10.2017] Available: http://www.finlex.fi/fi/viranomaiset/normi/700001/42818

APPENDIX 1: MINUTEBOOK OF THE GROUTING PROCESS

Table for grouting / flushing - Nonset 50

Pile									Grouting - designed					Flushing		Grouting					
Date	Pile type RDs	Reamer Ø [mm]	Pile number	Pile length [m]	Bond length [m]	Soil layer [m]	Annulus volume 2.5 m [l]	Pile volume 2.5m [l]	Water [l]	Grout [kg]	w / c [goal 0.4]	Grout mass [l] kg / 1.3	Pressure [MPa]	Volume [l] min.300 l.	Pressure [bar] 5-10	Water [l]	Grout [kg]	w / c [goal 0.4]	Grout mass [l] kg x 1.3	Pressure [bar]	Nonset 50 - action time 40 minutes. Mix with water temp 25. Notes
5.6.17	140/10	161	**P1**	12	2,5	7,0	12,6	28,0	22-35	55 86	0,4	42 **or** 66	0,5 - 1,0	500	3	30	75	0.4	60	3	Temp. 10-11 °C. Grout was divided by 40 l / 20l
5-6.6.17	140/10	161	**P2**	12	2,5	7,2	12,6	28,0	22-35	55-86	0,4	42 **or** 66	0,5-1,0								Could not be flushed or grouted
5.6.17	140/10	161	**P3**	12	2,5	7,7	12,6	28,0	22-35	55-86	0,4	42 **or** 66	0,5-1,0	500	3	30	75	0.4	60	3	Temp. 10-11 °C. Grout was divided by 40 l / 20l
6.6.17	220/12.5	241	**P4**	12	2,5	6,1	19,8	74,0	37-69	92-173	0,4	71 **or** 133	0,5-1,0	750	2 open 4	70	175	0.4	135	3	Temp. 16-18 °C. Grout was divided by 75 l / 60l. Other refer under.
6.6.17	220/12.5	241	**P5**	12	2,5	7,1	19,8	74,0	37-69	92-173	0,4	71 **or** 133	0,5-1,0	705	3,5-4,0 open 18 bar	70	200	0.4	155	3	Temp. 16-18 °C. Grout was divided by 75 l / 60l. Other refer under.
6.6.17	220/12.5	241	**P6**	12	2,5	7,0	19,8	74,0	37-69	92-173	0,4	71 **or** 133	0,5-1,0	750	4 open 8 bar	70	175	0.4	135	3	Temp. 16-18 °C. Grout was divided by 75 l / 60l. Other refer under.
6.6.17	220/12.5	273	**P7**	12	2,5	6,2	52,0	74,0	87-120	218-299	0,4	168 **or** 230	0,5-1,0	1000	2 open 4	100	250	0.4-0.7	200	3	Temp. 16-18 °C. Grout was divided by 150 l / 50l. Other refer under.
6.6.17	220/12.5	273	**P8**	12	2,5	6,5	52,0	74,0	87-120	218-299	0,4	168 **or** 230	0,5-1,0	1000	2 open 4	100	250	0.4	200	3	Temp. 16-18 °C. Grout was divided by 150 l / 50l. Other refer under.
6.6.17	220/12.5	273	**P9**	12	2,5	6,2	52,0	74,0	87-120	218-299	0,4	168 **or** 230	0,5-1,0	1000	2 open 4	100	250	0.4	200	3	Temp. 16-18 °C. Grout was divided by 150 l / 50l. Other refer under.
Total														6205		570	1450		1145		Water temperature was cold. Around 10°C
Total																					

Other notes: From the previous research: Water and cement consumption was 15% larger. They estimated about same amount but did use more than than planned. RD140 -161 (water 40-50 l & cement 100-125 kg), RD 220-241 (water 80-100 l & cement 200 - 250 kg) --> RD 220-273 (w: 140 l & c: 340 kg)

P4: The manchette got stuck into the pile and the pile rose with the manchette. Manchette was released and the pile was pushed back to the ground.

P5: Water could not flow into the pile. The pile opened with 18 bar pressure when the tube got also broken. The flushing continued with 1.0 (1.5) bar pressure. The pressure was now measured on the top of the pile while other times on the ground level. While grouting the grouting tube got also broken and 20 liter of grout mass was added to recover the loss

P6: Water did not flow at first. The pile got open with 12 bar pressure when the pile also rose around 10cm. Flushing and grouting process was continued normally.

The piles usually got open with 4 bar pressure and the flushing continued with 2 bar pressure from the main water line. Usually the manchette was covered with clay in the piles which was glogged. This may mean that the period between drilling and grouting was too long and soil collapsed into the annulus.

APPENDIX 2: FORCE — DISPLACEMENT GRAPH P1

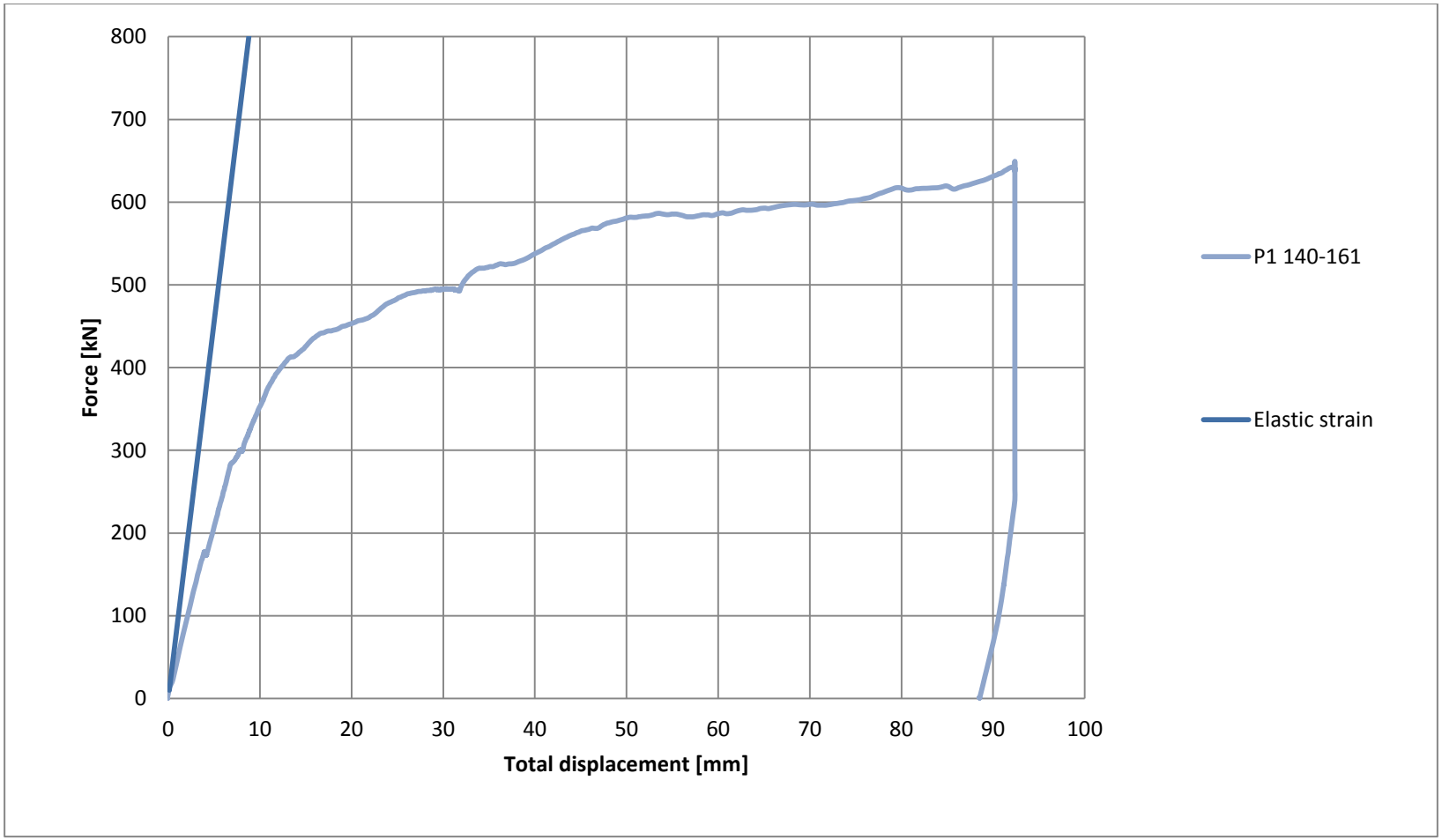

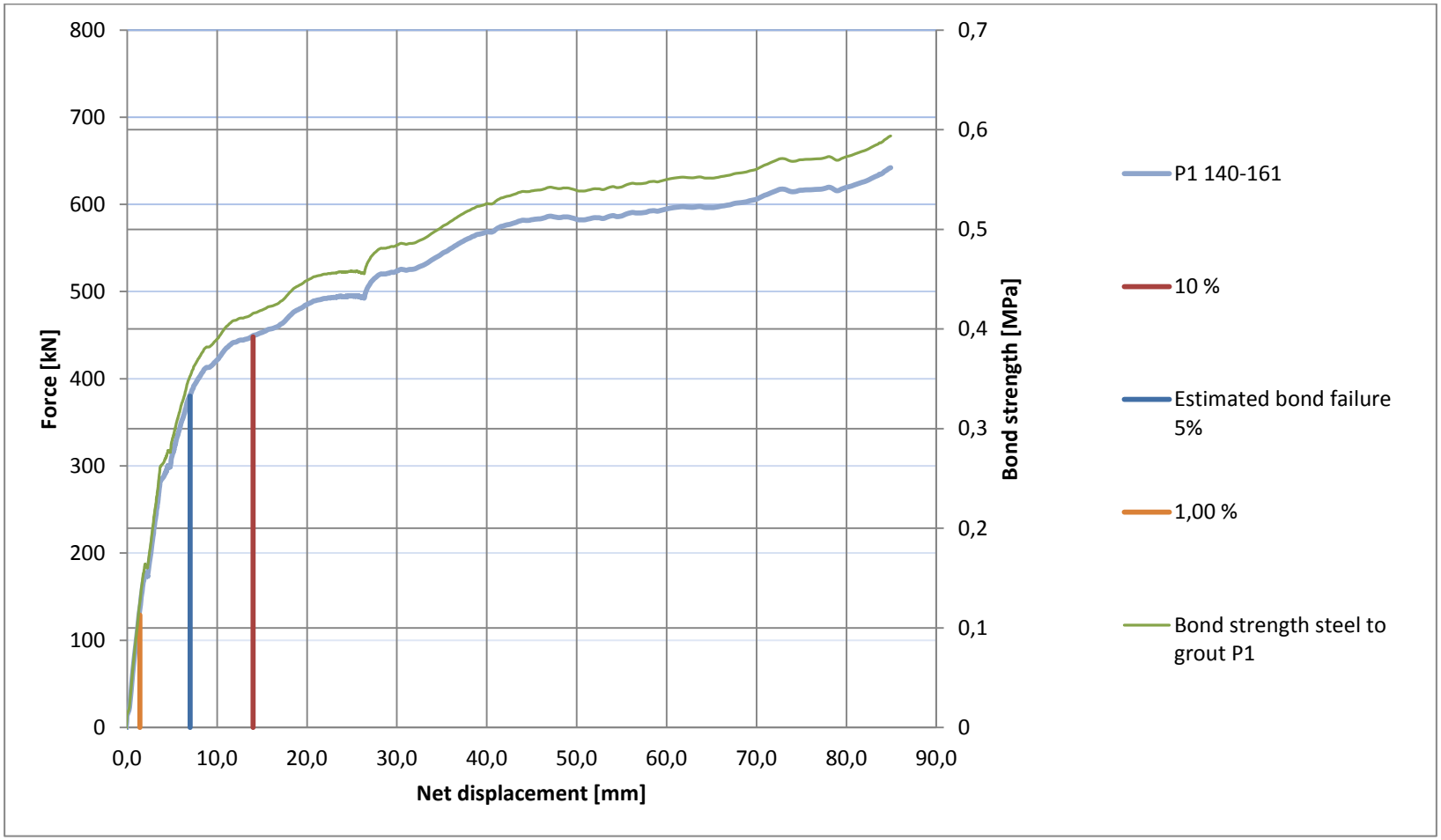
800
700
600
500
400
300
200
100
0
0,7
0,6
0,5
0,4
0,3
0,2
0,1
0
0,0
10,0
20,0
30,0
40,0
50,0
60,0
70,0
80,0
90,0
Force [kN]
Bond strength [MPa]
Net displacement [mm]
P1 140-161
10 %
Estimated bond failure 5%
1,00 %
Bond strength steel to grout P1

APPENDIX 3: FORCE — DISPLACEMENT GRAPH P2 WITHOUHT GROUT

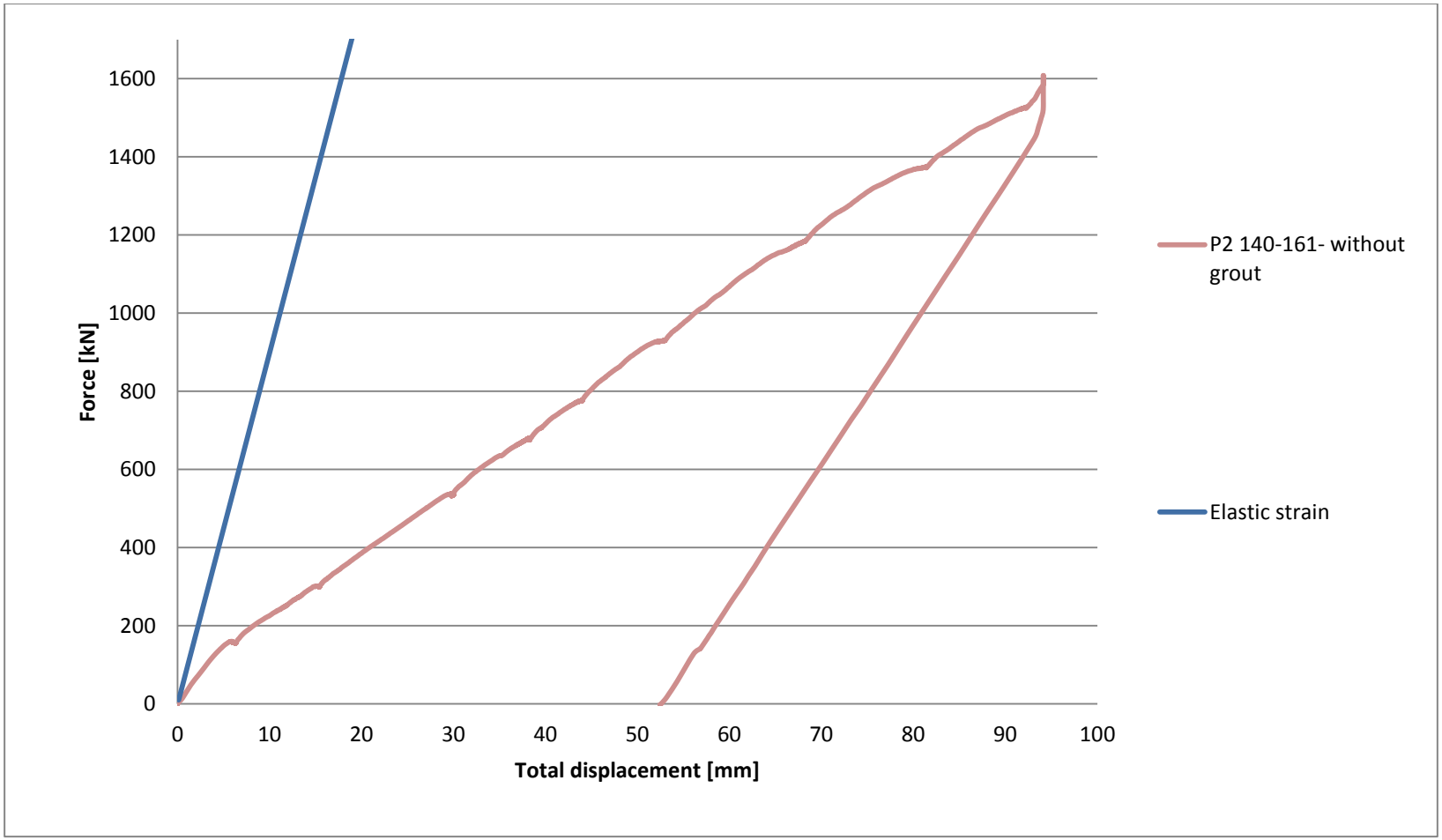

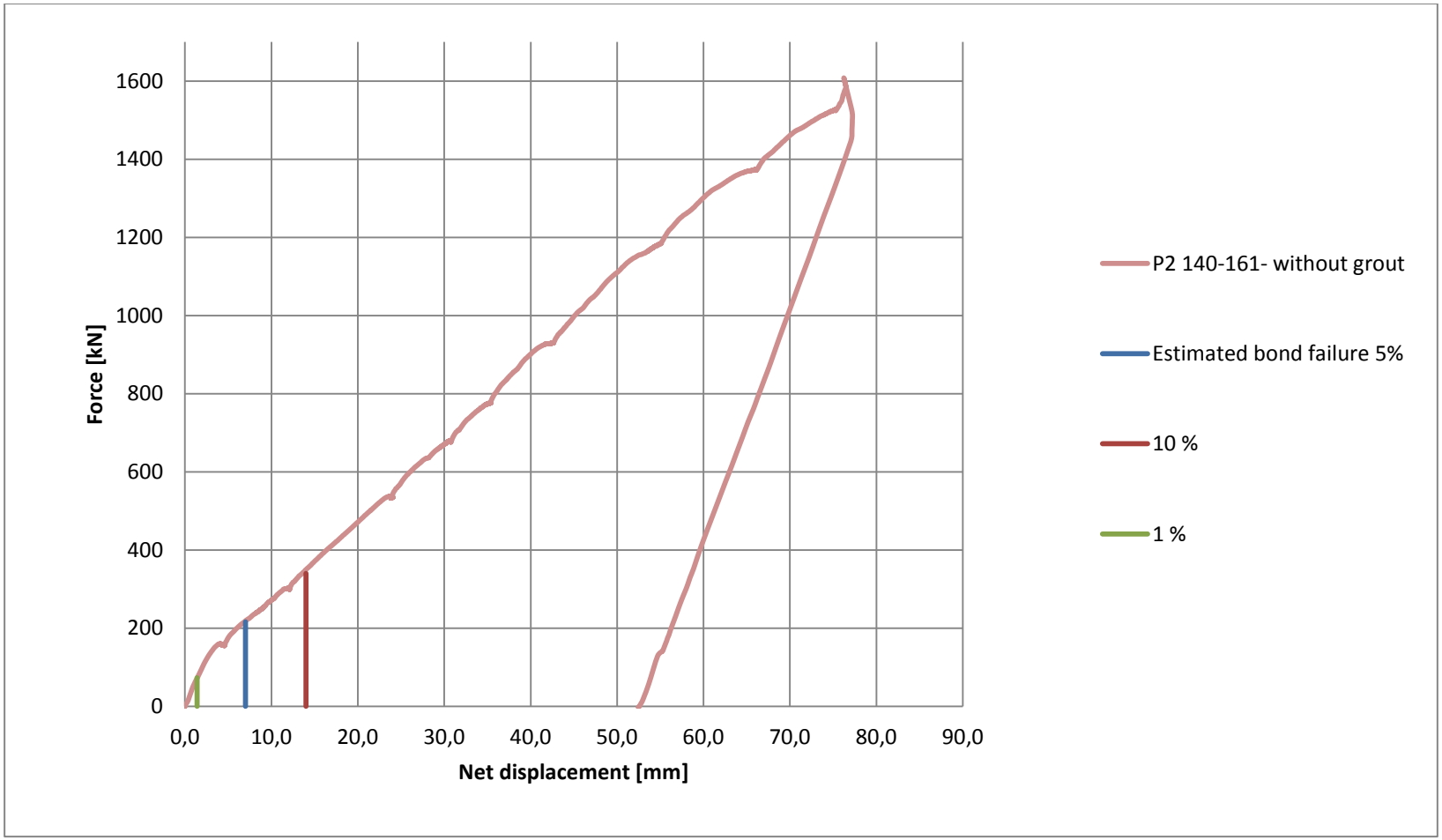
1600
1400
1200
1000
800
600
400
200
0
Force [kN]
0,0
10,0
20,0
30,0
40,0
50,0
60,0
70,0
80,0
90,0
Net displacement [mm]
P2 140-161- without grout
Estimated bond failure 5%
10 %
1 %

APPENDIX 4: FORCE — DISPLACEMENT GRAPH P3

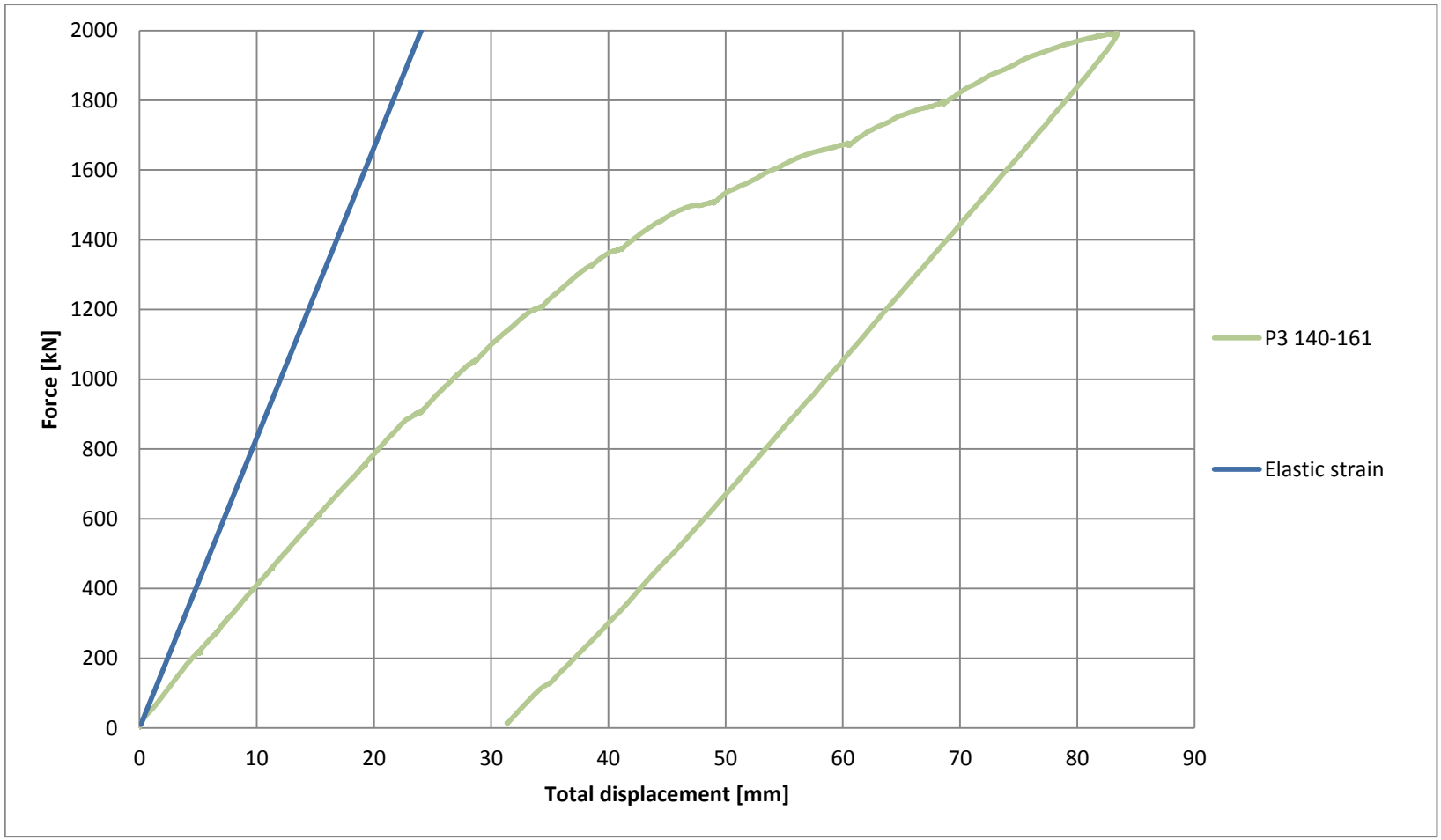

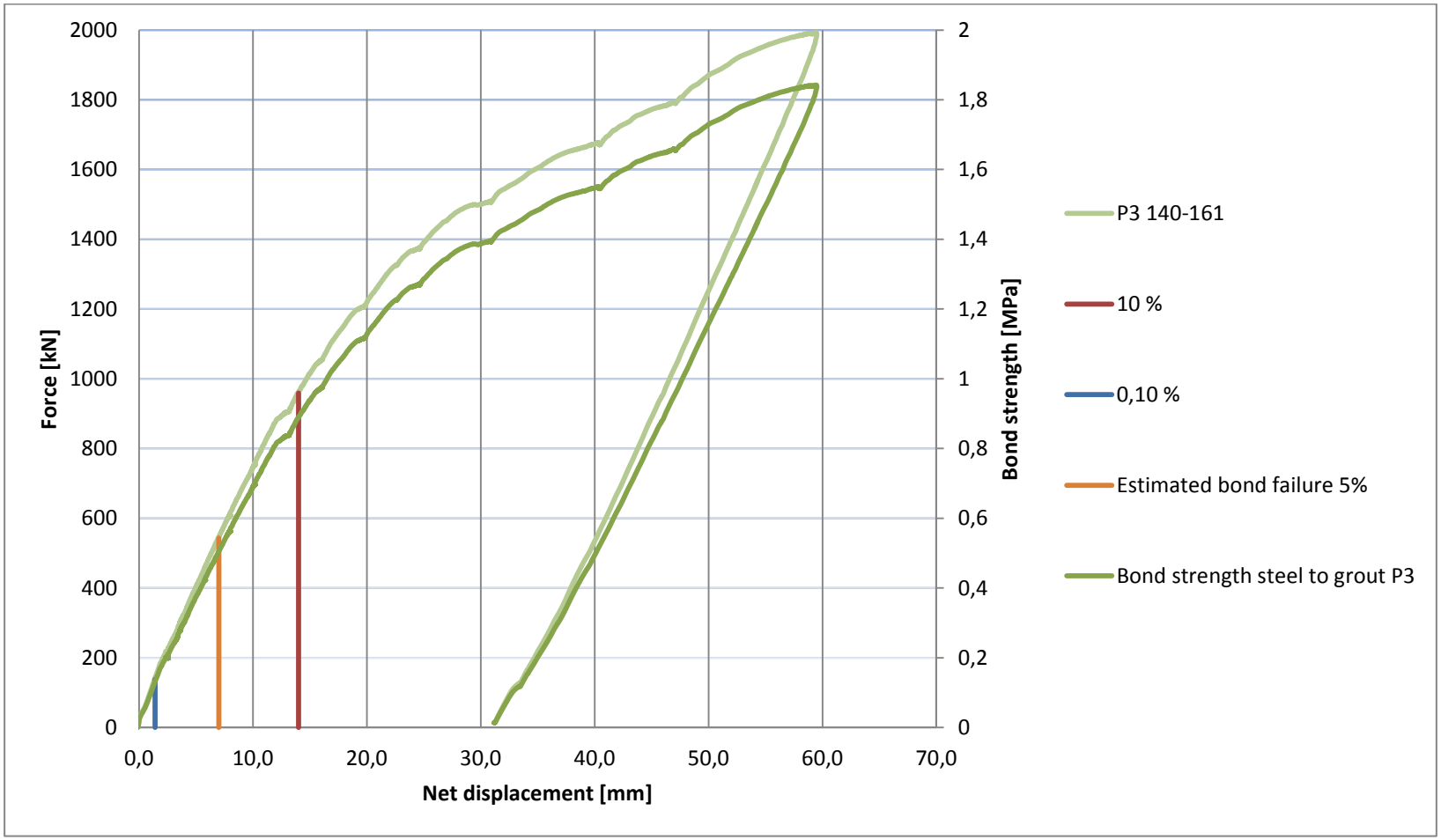
2000
1800
1600
1400
1200
1000
800
600
400
200
0
Force [kN]
2
1,8
1,6
1,4
1,2
1
0,8
0,6
0,4
0,2
0
Bond strength [MPa]
0,0
10,0
20,0
30,0
40,0
50,0
60,0
70,0
Net displacement [mm]
P3 140-161
10 %
0,10 %
Estimated bond failure 5%
Bond strength steel to grout P3

APPENDIX 5: FORCE — DISPLACEMENT GRAPH P4

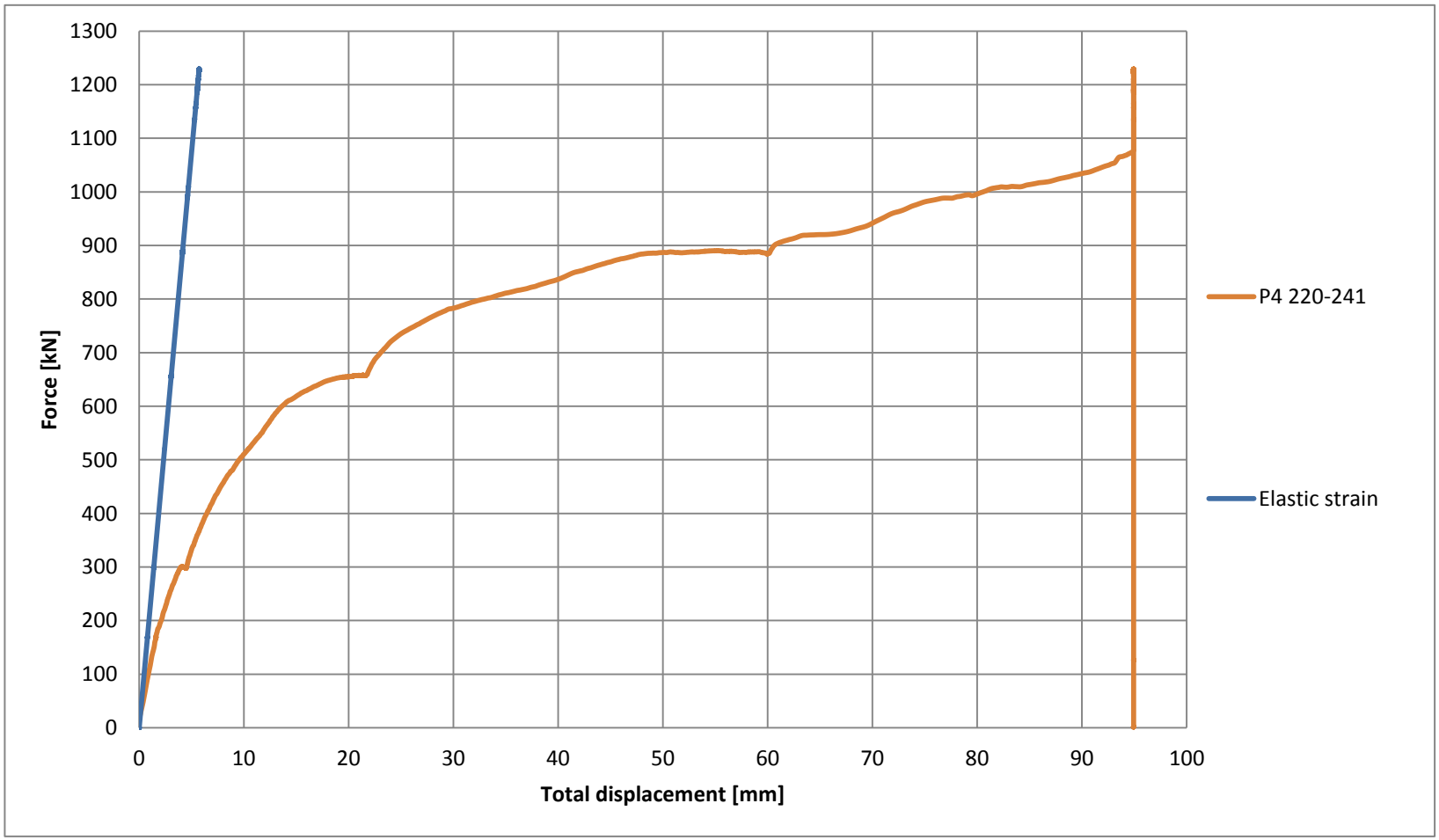

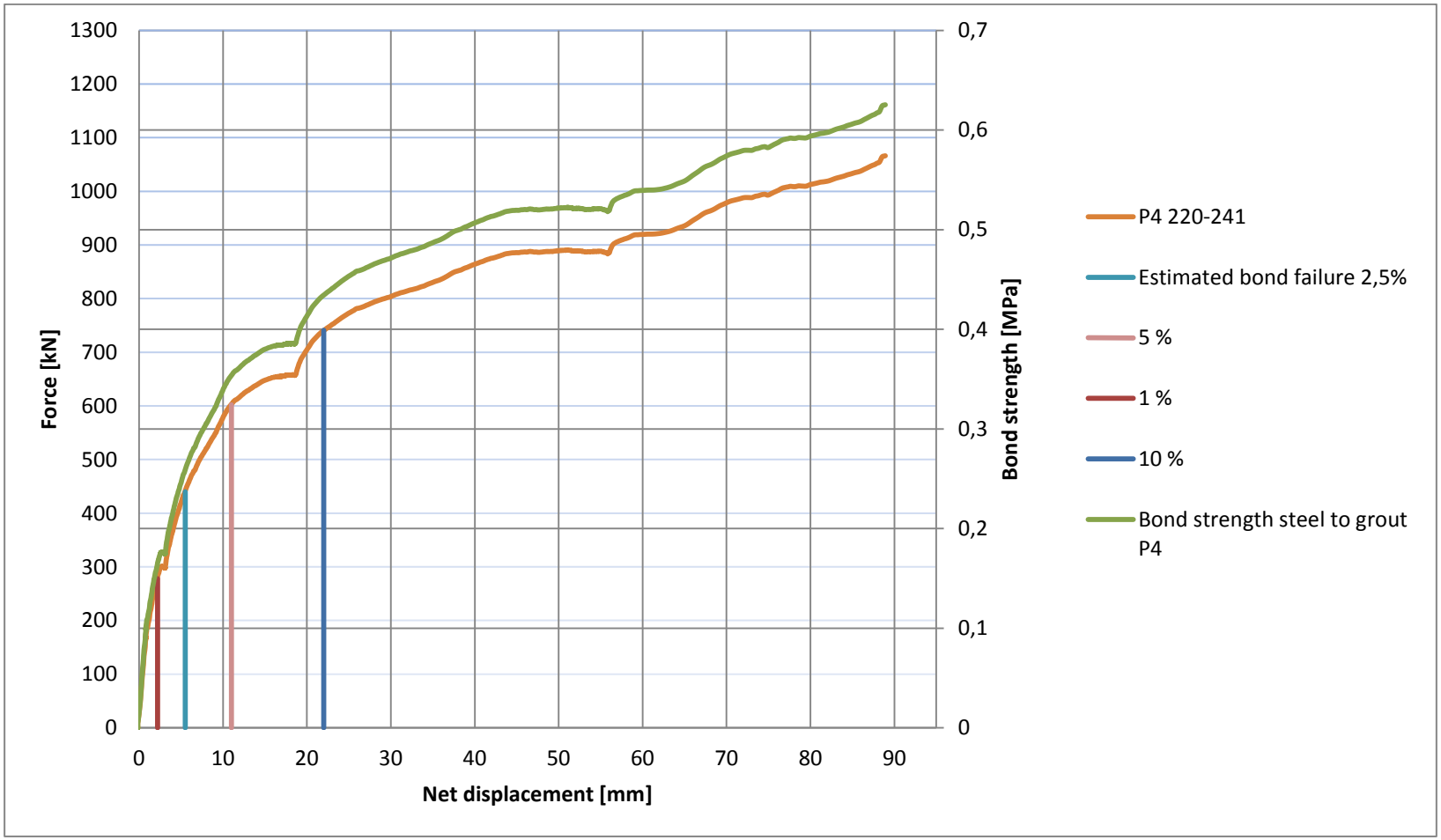
1300
1200
1100
1000
900
800
700
600
500
400
300
200
100
0
Force [kN]
0,7
0,6
0,5
0,4
0,3
0,2
0,1
0
Bond strength [MPa]
0
10
20
30
40
50
60
70
80
90
Net displacement [mm]
P4 220-241
Estimated bond failure 2,5%
5 %
1 %
10 %
Bond strength steel to grout P4

APPENDIX 6: FORCE — DISPLACEMENT GRAPH P5

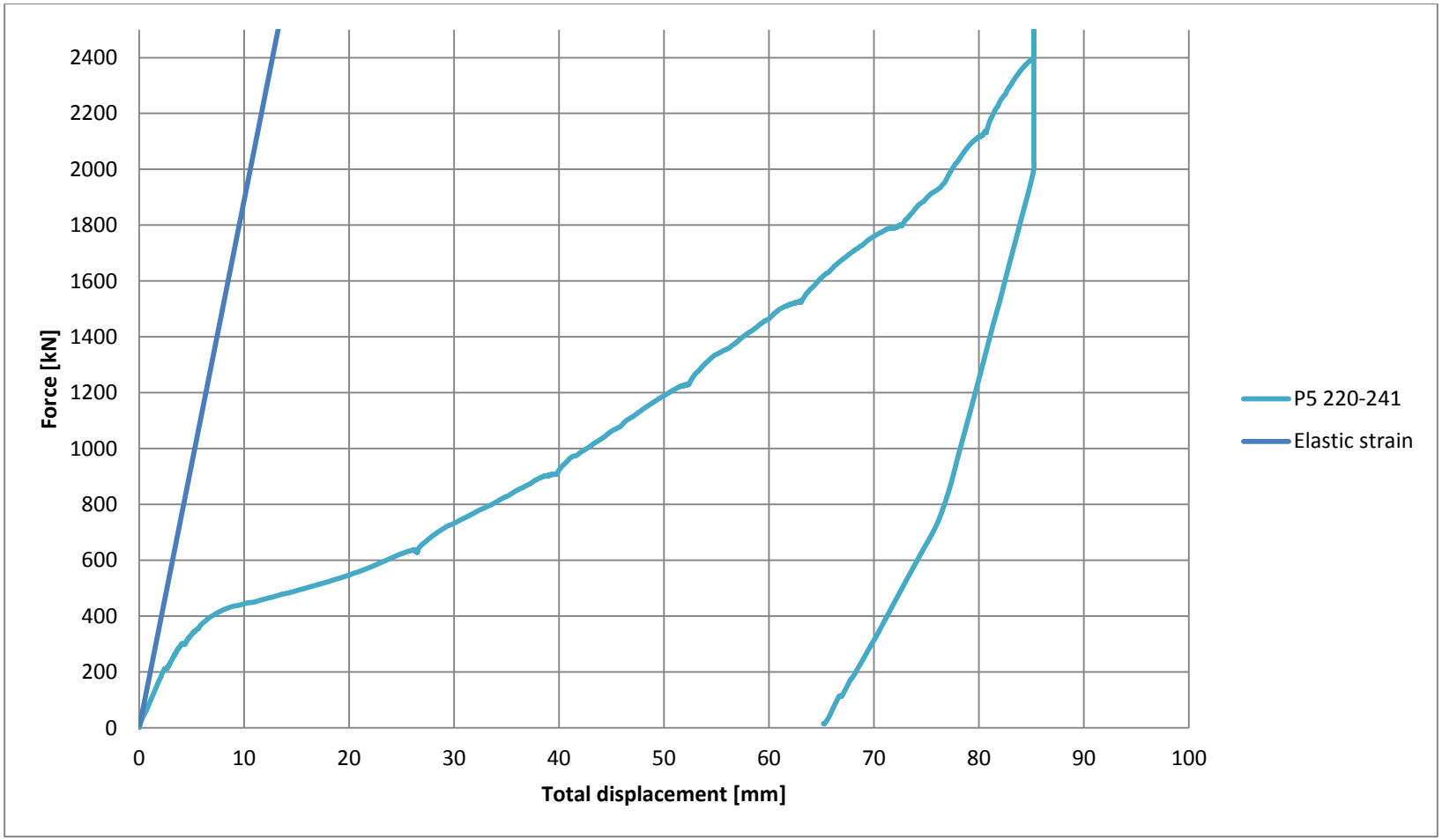

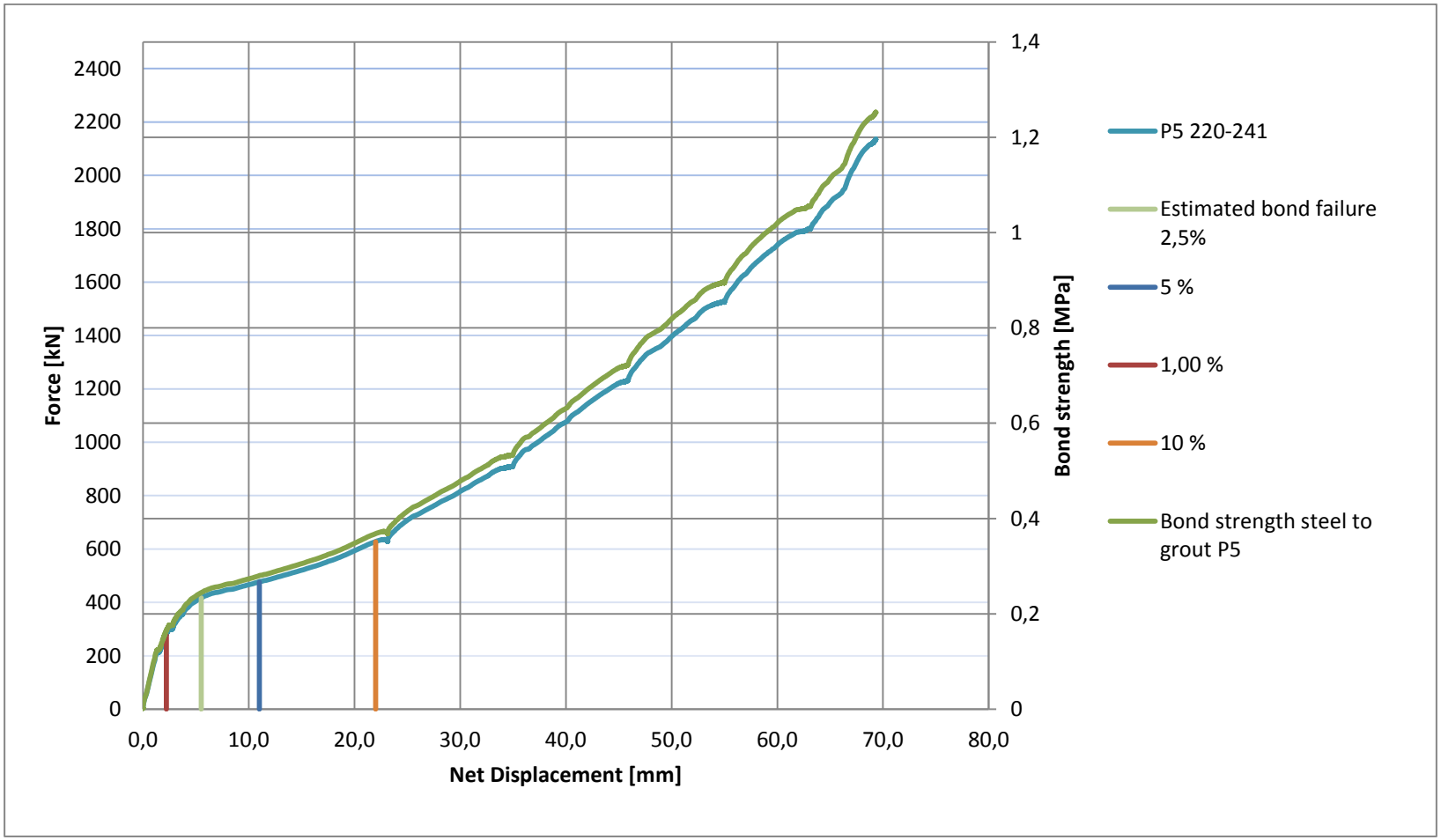
Force [kN]
2400
2200
2000
1800
1600
1400
1200
1000
800
600
400
200
0
0,0
10,0
20,0
30,0
40,0
50,0
60,0
70,0
80,0
Net Displacement [mm]
1,4
1,2
1
0,8
0,6
0,4
0,2
0
Bond strength [MPa]
P5 220-241
Estimated bond failure 2,5%
5 %
1,00 %
10 %
Bond strength steel to grout P5

APPENDIX 7: FORCE — DISPLACEMENT GRAPH P6

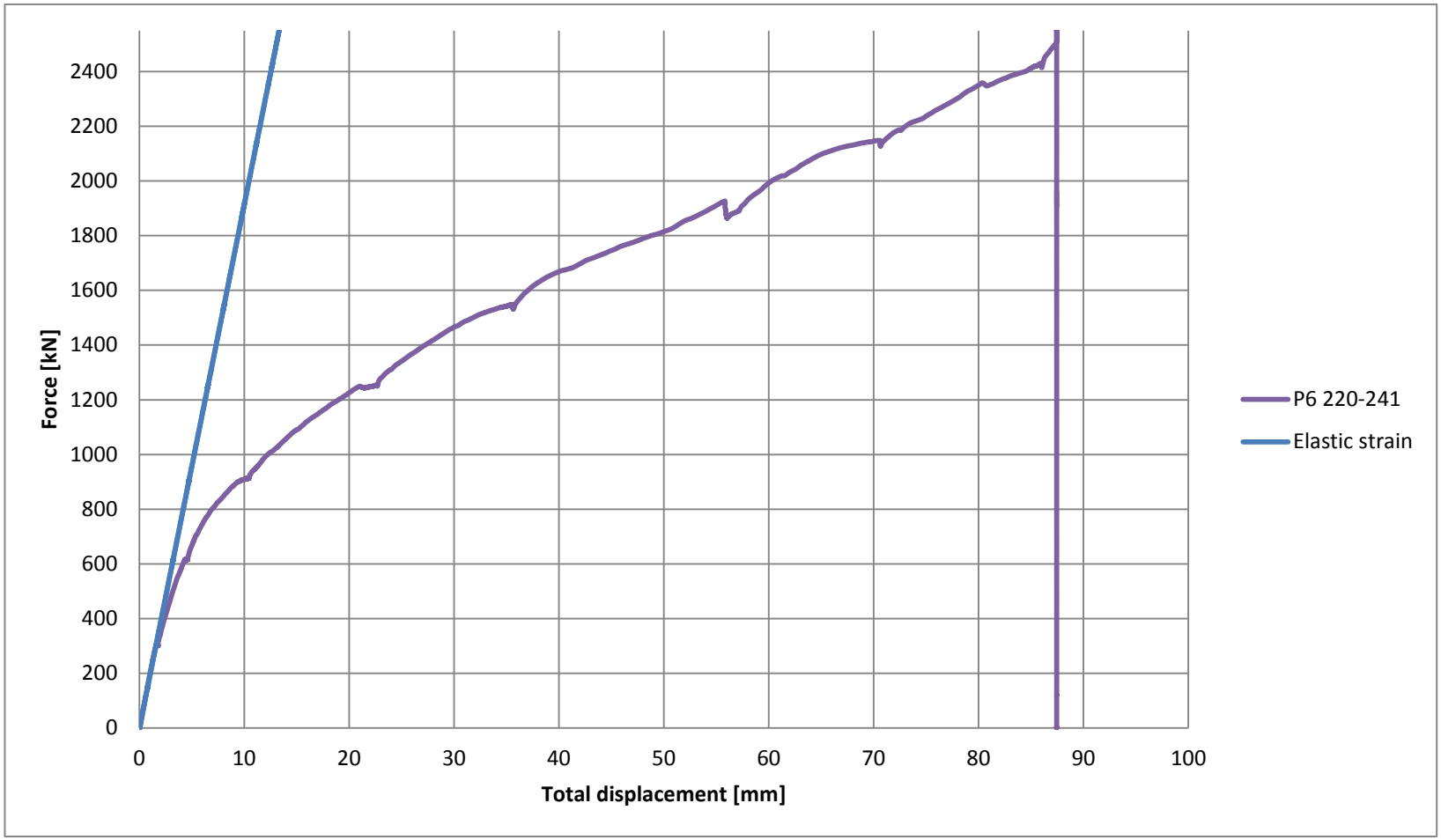

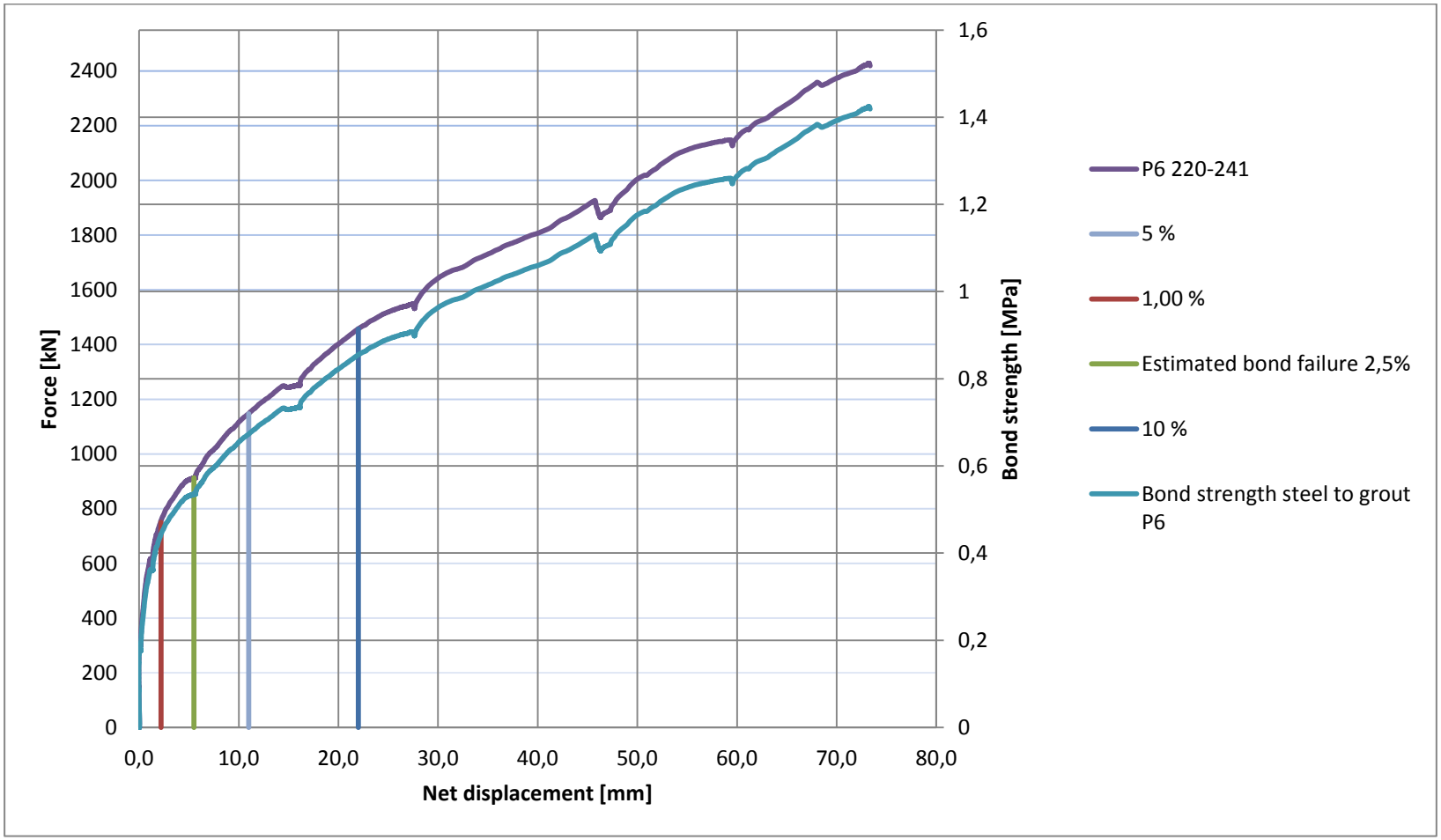
Force [kN]
2400
2200
2000
1800
1600
1400
1200
1000
800
600
400
200
0
0,0
10,0
20,0
30,0
40,0
50,0
60,0
70,0
80,0
Net displacement [mm]
1,6
1,4
1,2
1
0,8
0,6
0,4
0,2
0
Bond strength [MPa]
P6 220-241
5 %
1,00 %
Estimated bond failure 2,5%
10 %
Bond strength steel to grout P6

APPENDIX 8: FORCE — DISPLACEMENT GRAPH P7

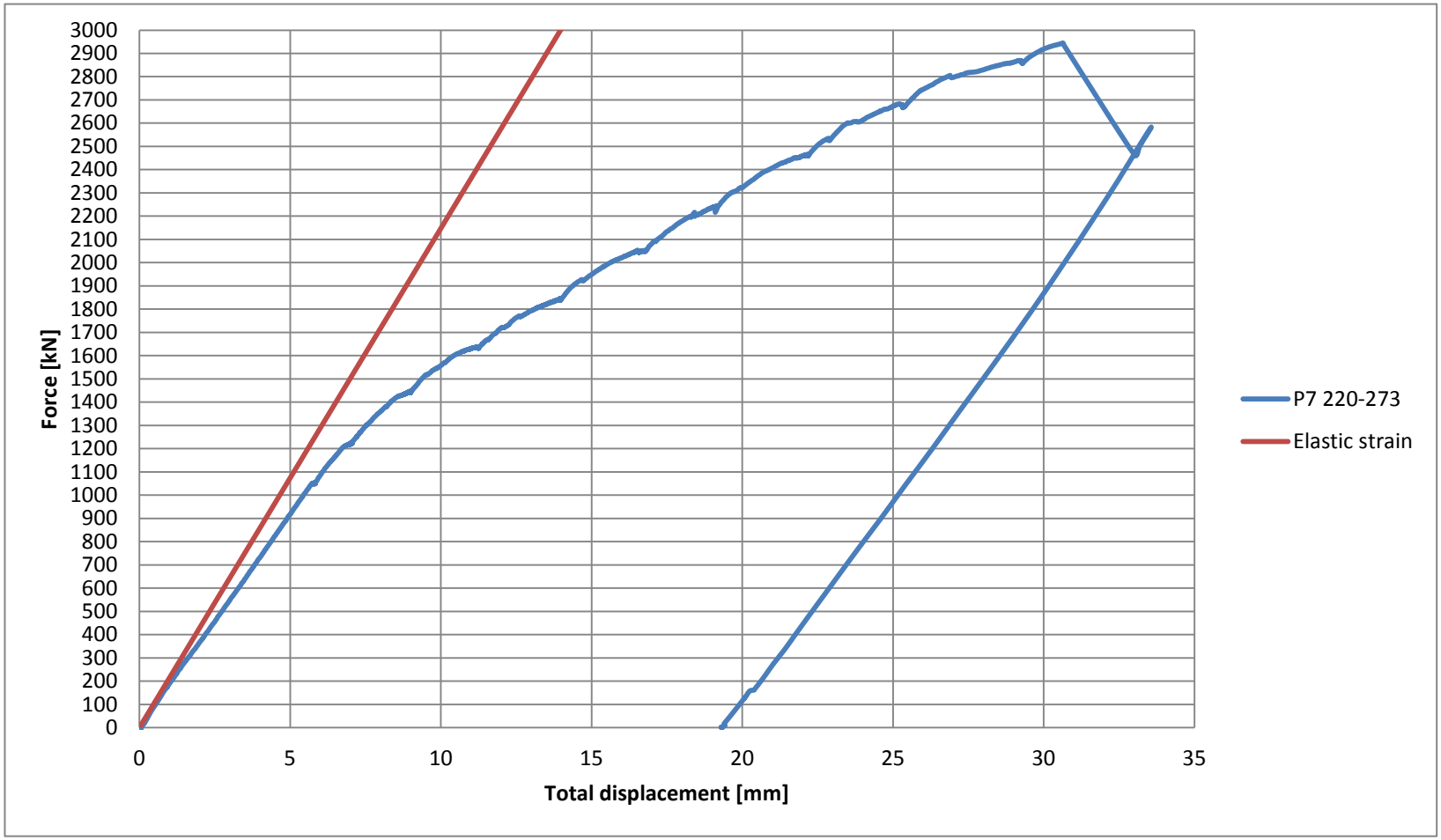

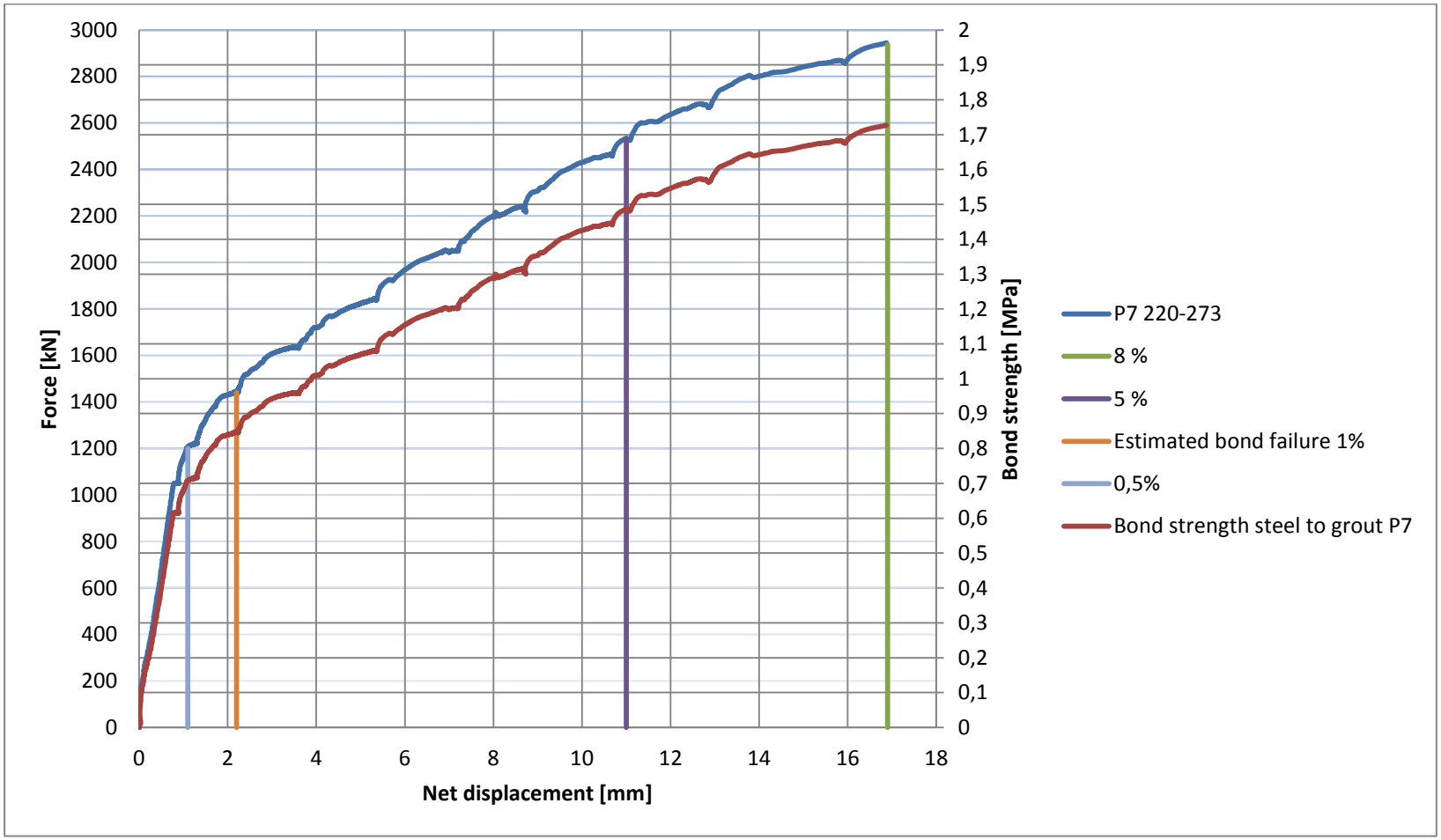
Force [kN]
3000
2800
2600
2400
2200
2000
1800
1600
1400
1200
1000
800
600
400
200
0
Bond strength [MPa]
2
1,9
1,8
1,7
1,6
1,5
1,4
1,3
1,2
1,1
1
0,9
0,8
0,7
0,6
0,5
0,4
0,3
0,2
0,1
0
0
2
4
6
8
10
12
14
16
18
Net displacement [mm]
P7 220-273
8 %
5 %
Estimated bond failure 1%
0,5%
Bond strength steel to grout P7

APPENDIX 9: FORCE — DISPLACEMENT GRAPH P8

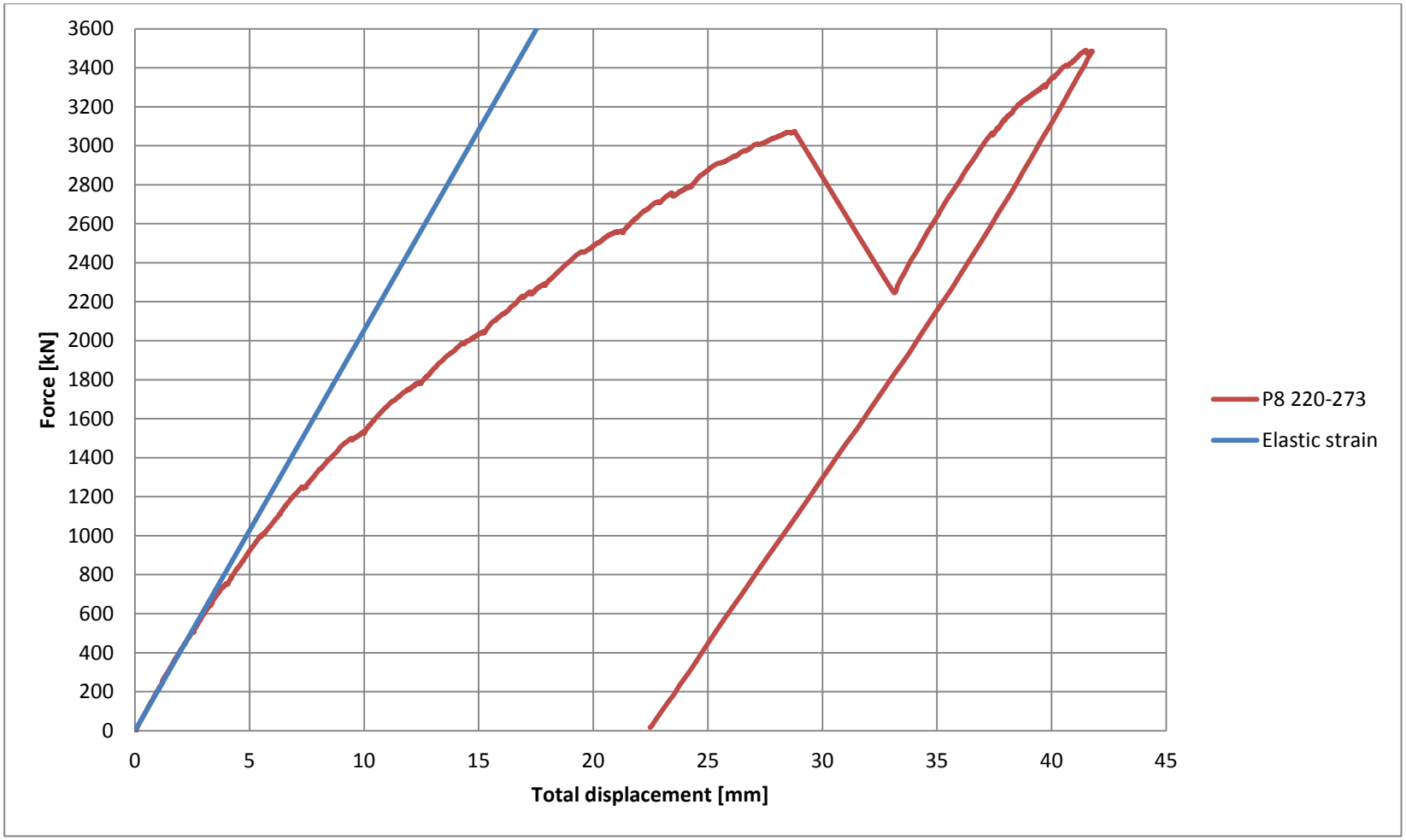

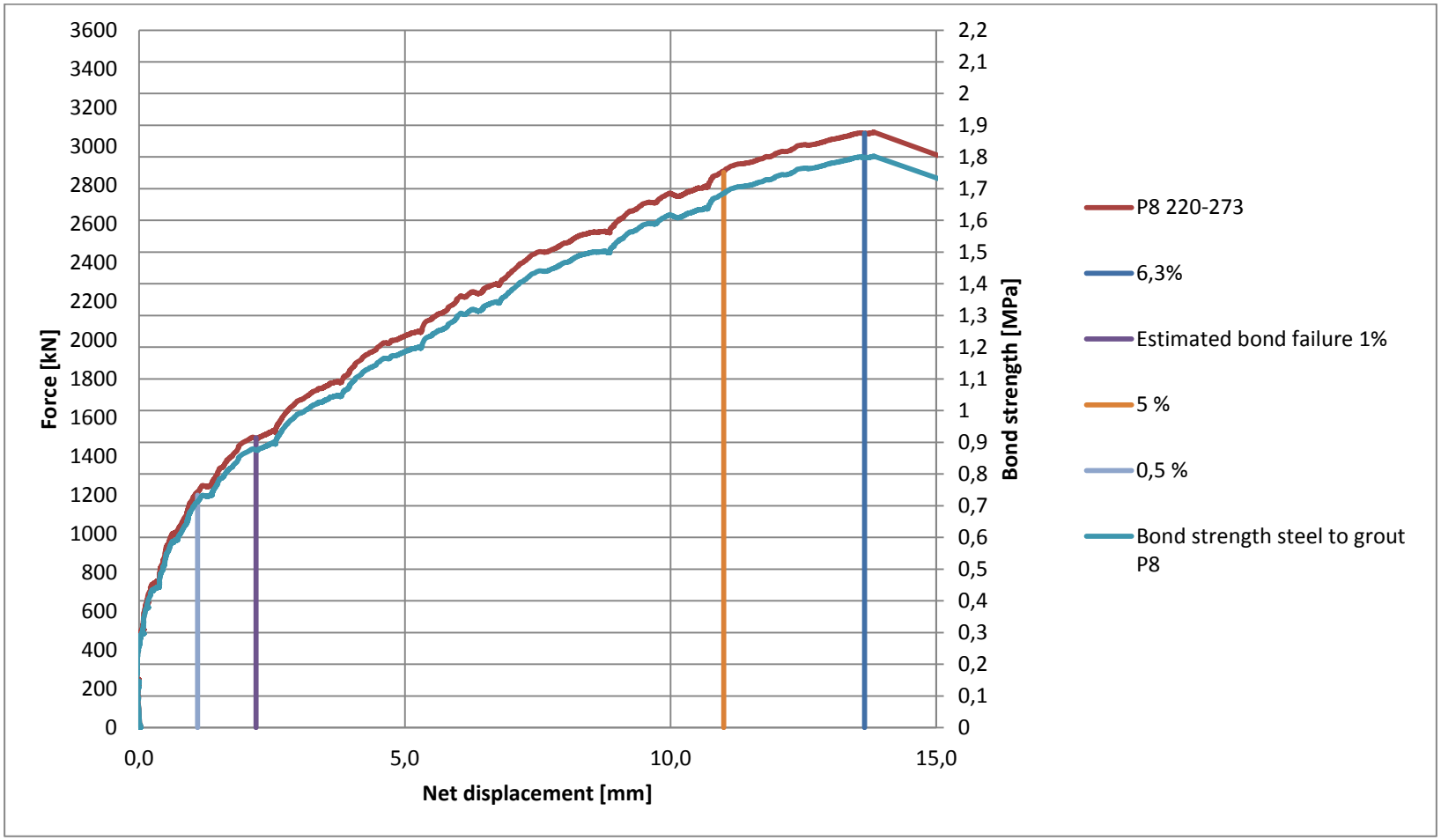
Force [kN]
3600
3400
3200
3000
2800
2600
2400
2200
2000
1800
1600
1400
1200
1000
800
600
400
200
0
Bond strength [MPa]
2,2
2,1
2
1,9
1,8
1,7
1,6
1,5
1,4
1,3
1,2
1,1
1
0,9
0,8
0,7
0,6
0,5
0,4
0,3
0,2
0,1
0
0,0
5,0
10,0
15,0
Net displacement [mm]
P8 220-273
6,3%
Estimated bond failure 1%
5 %
0,5 %
Bond strength steel to grout P8

APPENDIX 10: FORCE — DISPLACEMENT GRAPH P9

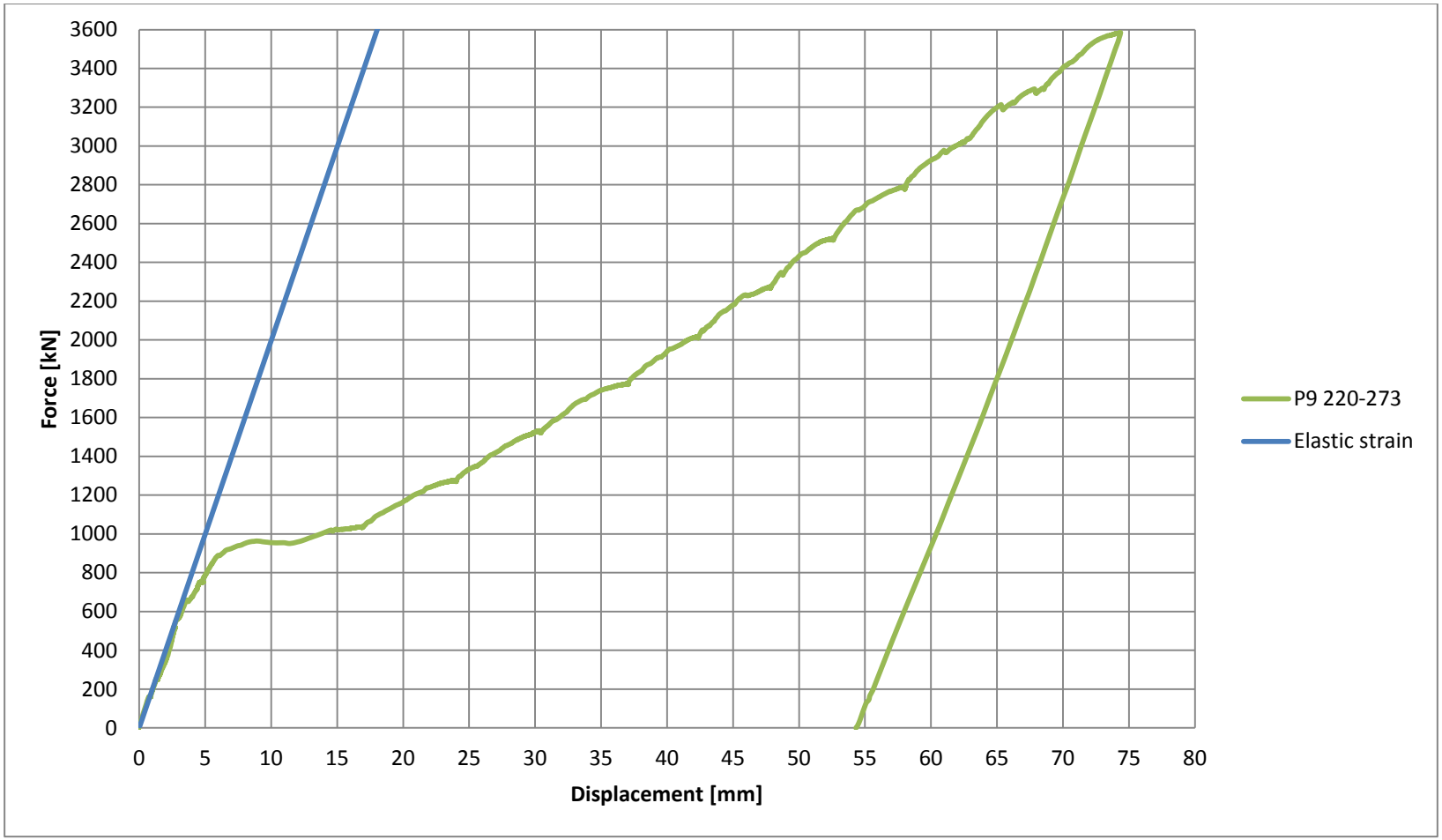

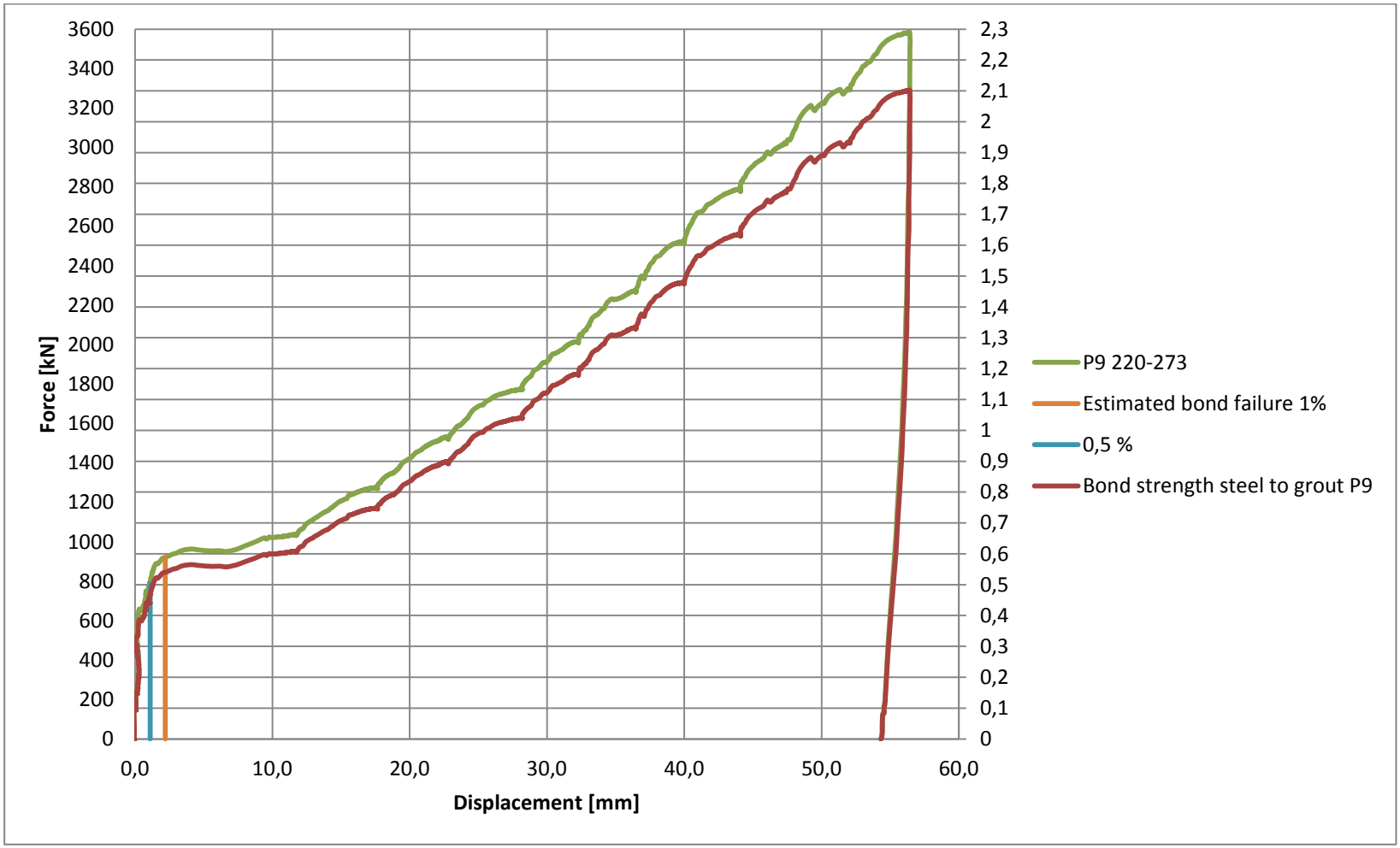
Force [kN]
3600
3400
3200
3000
2800
2600
2400
2200
2000
1800
1600
1400
1200
1000
800
600
400
200
0
2,3
2,2
2,1
2
1,9
1,8
1,7
1,6
1,5
1,4
1,3
1,2
1,1
1
0,9
0,8
0,7
0,6
0,5
0,4
0,3
0,2
0,1
0
0,0
10,0
20,0
30,0
40,0
50,0
60,0
Displacement [mm]
P9 220-273
Estimated bond failure 1%
0,5 %
Bond strength steel to grout P9

APPENDIX 11: FORCE — DISPLACEMENT GRAPH – P1—P3

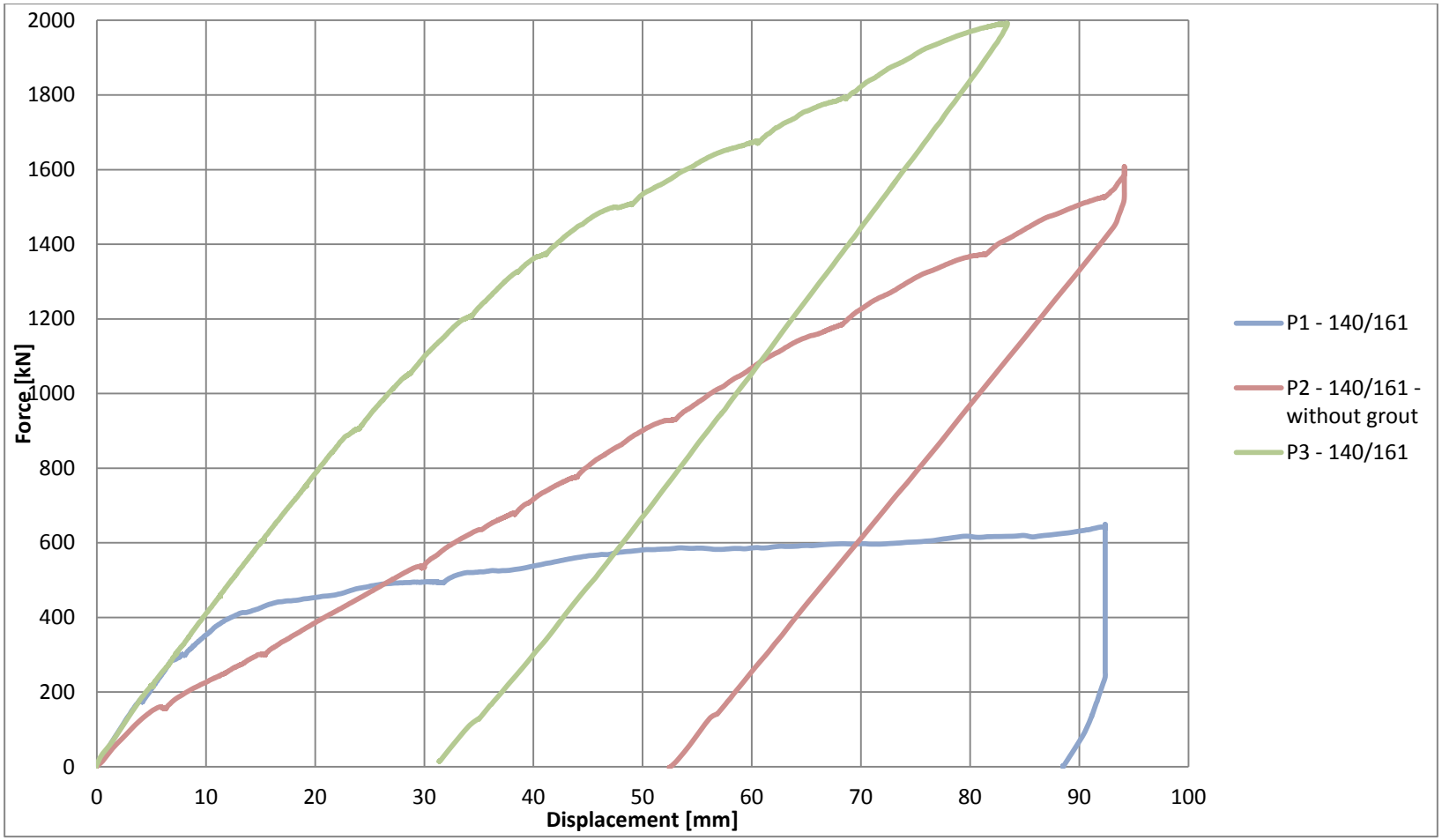

APPENDIX 12: FORCE — DISPLACEMENT GRAPH – P4—P6

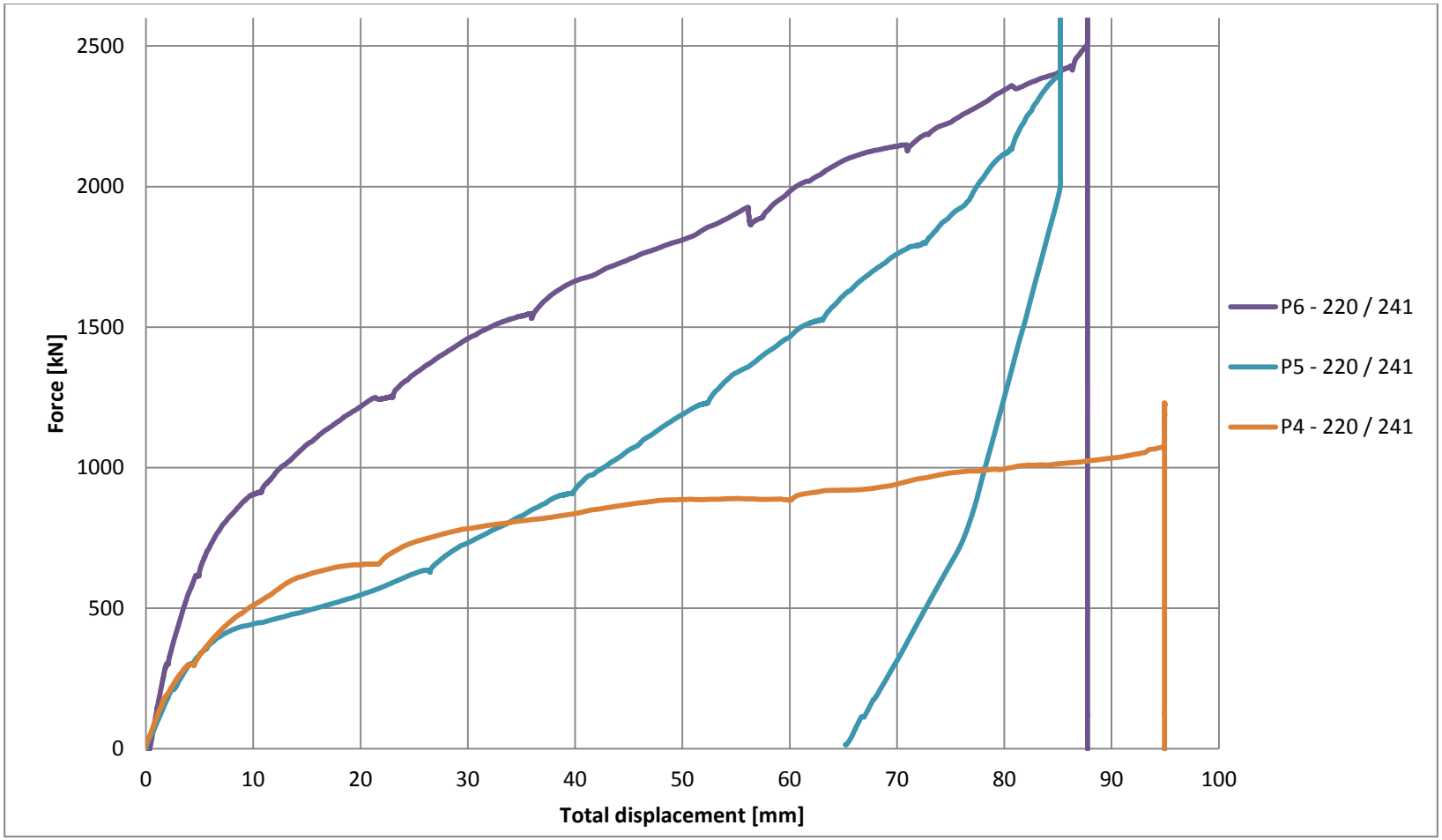

APPENDIX 13: FORCE — DISPLACEMENT GRAPH – P7—P9

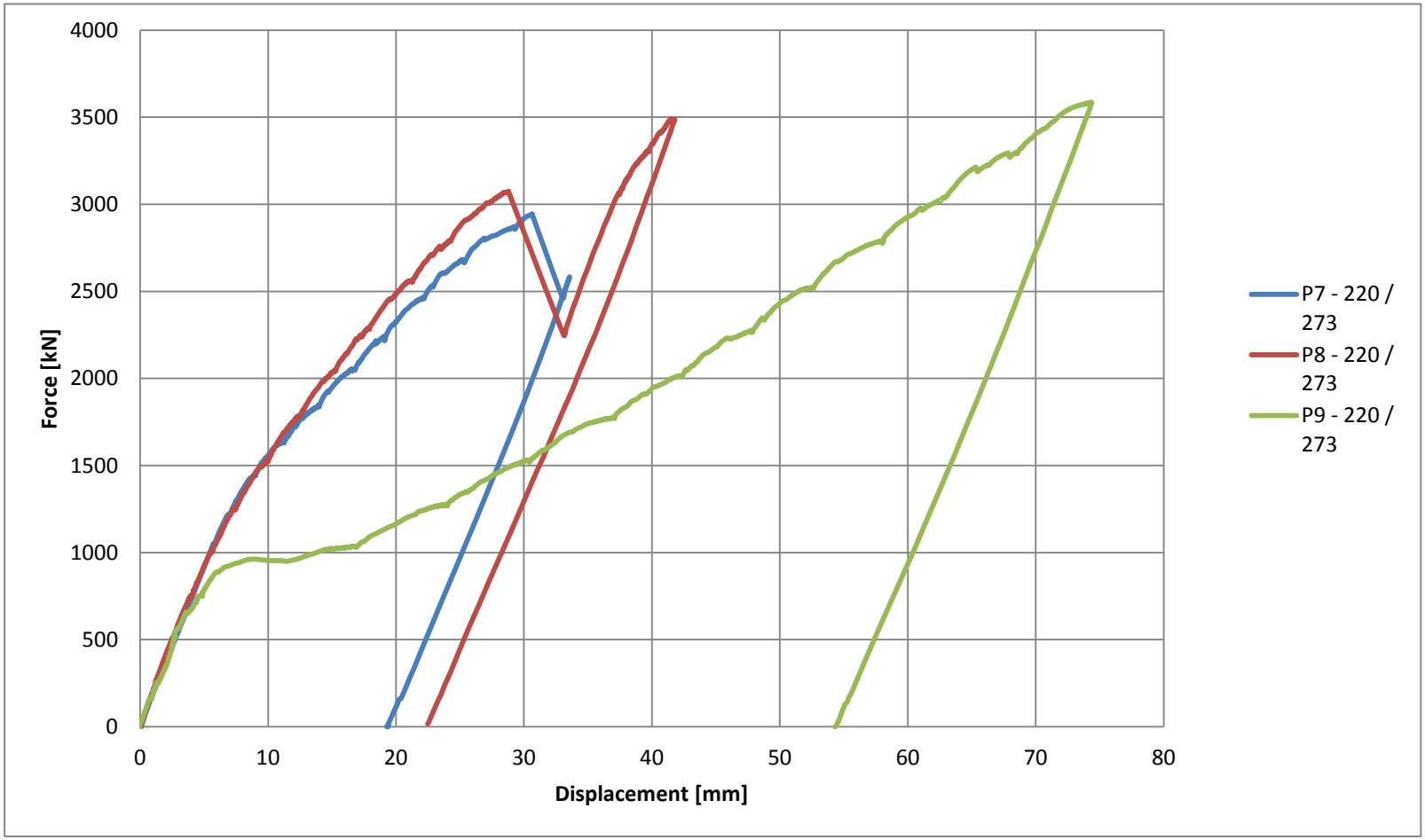

APPENDIX 14: CAPACITY AND FAILURE MODE COMPARISON

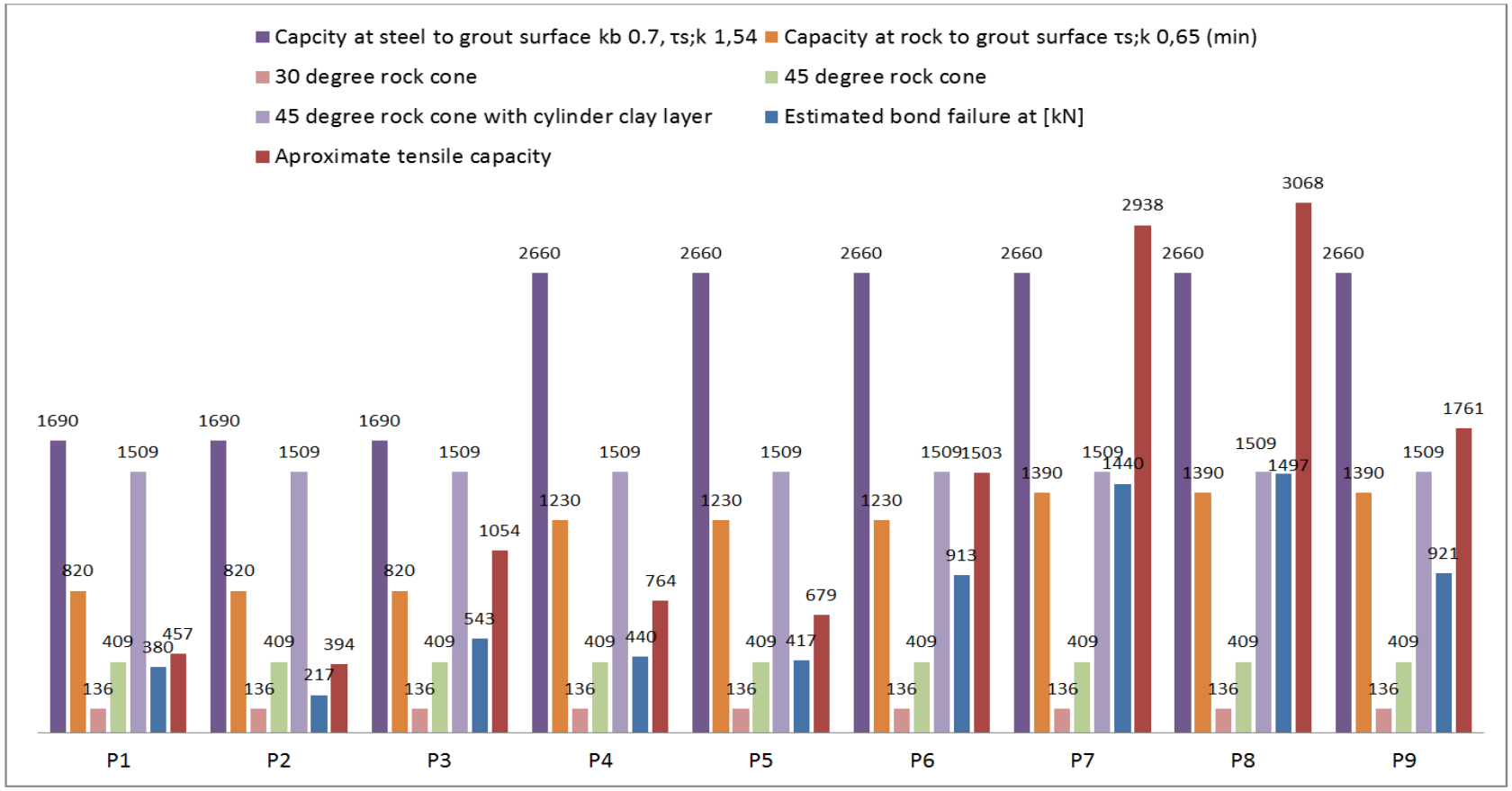

APPENDIX 15: BOND STRENGTH STEEL TO GROUT COMPARISON

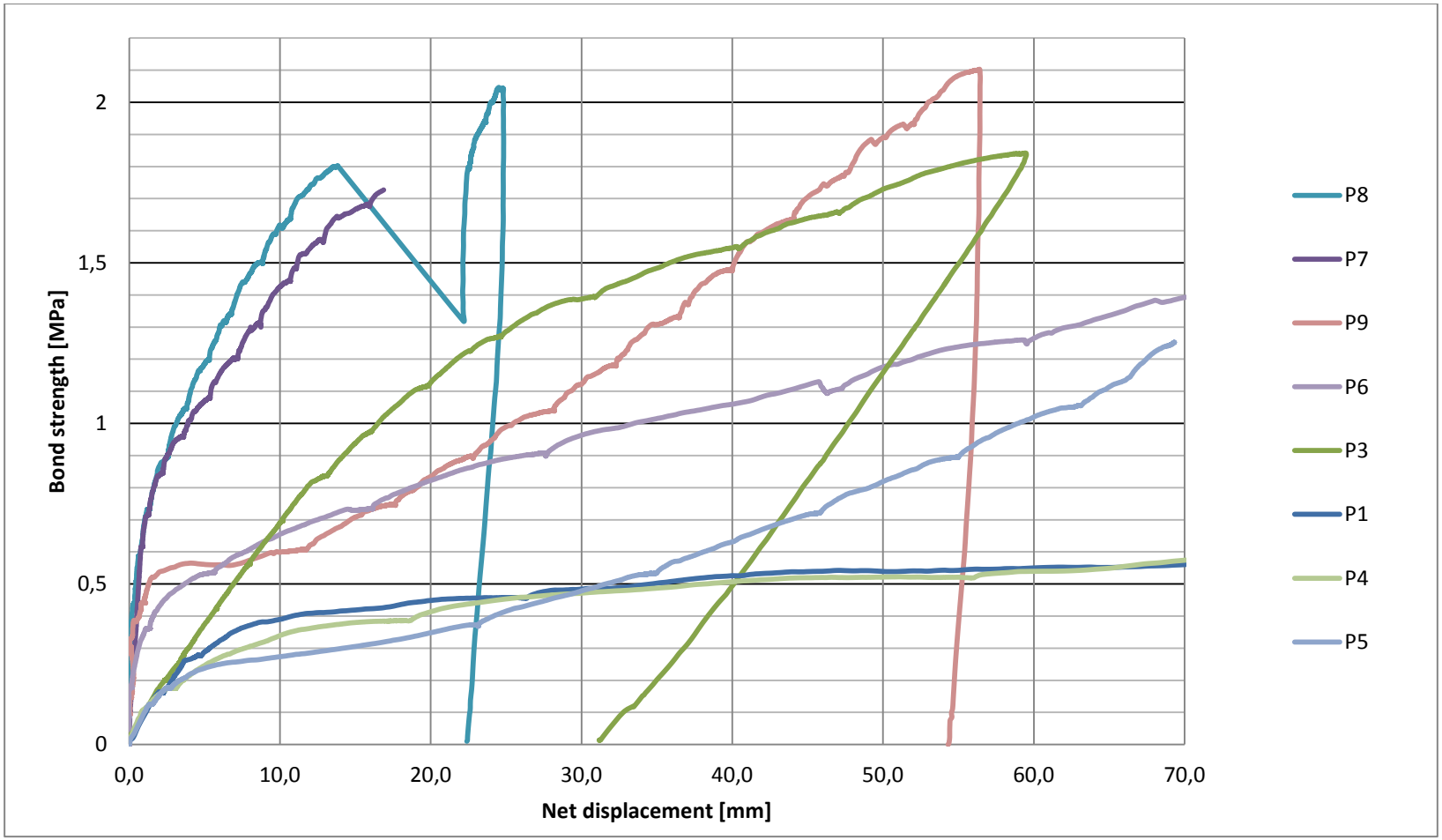

APPENDIX 16: DATA FROM THE LOADING STEPS

P1			
Force [kN]	Displacement [mm]	Elastic strain [mm]	Difference [mm]
23,00	0,51	0,25	0,25
91,14	1,92	1,00	0,92
179,11	4,31	1,97	2,34
301,83	8,15	3,31	4,83
493,83	31,82	5,42	26,40
649,00	92,38	7,13	85,25

P2 - No grouting			
Force [kN]	Displacement [mm]	Elastic strain [mm]	Difference [mm]
158,28	6,41	1,76	4,65
1608,02	94,13	17,90	76,24

P3			
Force [kN]	Displacement [mm]	Elastic strain [mm]	Difference [mm]
59,67	1,23	0,72	0,51
215,31	4,94	2,59	2,35
303,78	7,30	3,65	3,65
464,68	11,42	5,59	5,84
619,39	15,49	7,44	8,05
754,19	19,22	9,07	10,15
904,38	23,92	10,87	13,05
1059,78	28,88	12,74	16,14
1206,02	34,20	14,50	19,70
1367,29	40,48	16,43	24,05
1979,31	83,26	23,79	59,47

P4			
Force [kN]	Displacement [mm]	Elastic strain [mm]	Difference [mm]
89,63	0,76	0,42	0,35
190,69	1,93	0,89	1,05
301,72	4,53	1,41	3,13
579,79	12,73	2,70	10,03
674,55	22,12	3,14	18,97
703,58	23,23	3,28	19,96
919,69	64,40	4,28	60,12
1076,68	94,93	5,01	89,91
1228,06	Maximum force		

P5			
Force [kN]	Displacement [mm]	Elastic strain [mm]	Difference [mm]
58,07	0,63	0,31	0,32
172,80	1,94	0,91	1,02
371,72	5,96	1,97	3,99
466,34	12,48	2,47	10,01
637,52	26,52	3,37	23,14
905,90	39,24	4,79	34,45
1230,78	52,36	6,51	45,85
1525,60	63,06	8,07	54,99
1795,49	72,31	9,50	62,81
2132,62	80,67	11,29	69,39
2415,97	85,23	12,78	72,44
2596,20	Maximum force		

P6				
Force [kN]	Displacement [mm]	Calibrated displacement	Elastic strain [mm]	Difference [mm]
148,22	1,08	1,04	0,77	0,31
284,10	1,77	1,73	1,48	0,29
553,74	3,98	3,93	2,89	1,09
617,70	4,92	4,87	3,23	1,69
912,62	10,74	10,70	4,77	5,98
1104,69	15,83	15,78	5,77	10,06
1260,58	23,06	23,02	6,58	16,48
1558,26	36,32	36,28	8,14	28,19
1889,71	57,38	57,34	9,87	47,51
2145,36	70,23	70,19	11,20	59,03
2420,40	86,38	86,34	12,64	73,74
2692,12	87,76	87,72	14,06	73,70
3496,27	Maximum force			

P7				
Force [kN]	Displacement [mm]	Calibrated displacement	Elastic strain [mm]	Difference [mm]
175,72	1,32	0,92	0,82	0,10
330,17	2,19	1,78	1,54	0,25
1049,76	6,23	5,83	4,89	0,94
1224,10	7,46	7,05	5,70	1,35
1442,93	9,41	9,01	6,72	2,29
1635,70	11,68	11,27	7,62	3,66
1839,90	14,38	13,98	8,57	5,41
2050,47	17,20	16,80	9,55	7,25
2243,30	19,56	19,16	10,45	8,71
2460,39	22,59	22,18	11,46	10,72
2680,06	25,66	25,26	12,48	12,78
2868,00	29,66	29,25	13,36	15,89
2944,83	31,04	30,63	13,71	16,92

P8			
Force [kN]	Displacement [mm]	Elastic strain [mm]	Difference [mm]
246,01	1,19	1,20	-0,01
505,52	2,54	2,46	0,08
755,00	4,05	3,68	0,37
1011,34	5,64	4,92	0,72
1244,50	7,32	6,06	1,26
1534,53	10,00	7,47	2,53
1787,39	12,45	8,70	3,74
2045,09	15,23	9,96	5,27
2290,03	17,87	11,15	6,72
2562,08	21,23	12,47	8,76
2785,61	24,10	13,56	10,54
3074,55	28,78	14,97	13,81
3485,19	Maximum force		

P9			
Force [kN]	Displacement [mm]	Elastic strain [mm]	Difference [mm]
161,30	0,87	0,81	0,06
250,05	1,31	1,25	0,06
323,38	1,87	1,62	0,25
517,62	2,73	2,59	0,14
752,14	4,80	3,77	1,03
1035,62	16,84	5,19	11,65
1276,69	23,98	6,40	17,58
1531,50	30,33	7,67	22,66
1775,34	37,01	8,89	28,12
2015,16	42,24	10,10	32,15
2275,37	47,85	11,40	36,45
2525,31	52,58	12,65	39,93
2790,39	58,08	13,98	44,10
3020,78	62,41	15,13	47,28
3294,57	67,84	16,50	51,34
3585,87	74,36	17,96	56,40